Published in final edited form as:
Chem Rev. 2014 April 9; 114(7): 3919–3962. doi:10.1021/cr400415k.

Heme Enzyme Structure and Function

Thomas L. Poulos*
Departments of Molecular Biology & Biochemistry, Pharmaceutical Sciences, and Chemistry, University of California Irvine, Irvine, California 92697-3900

1. Introduction

Metalloporphyrins are widely used throughout the biosphere and of these heme (iron protoporphyrin IX, Fig. 1) is one of the most abundant and widely used. Heme shuttles electrons between proteins as in mitochondrial respiration or transports and stores O_2 as with the globins. The role of heme in more active enzymatic chemical transformation began to be appreciated just after the discovery by Mason[1] and Hayaishi[2] that O_2 O atoms can be enzymatically incorporated into organic substrates which represented the seminal discovery of oxygenases. While the enzymes used in these studies did not contain heme, it was not too long before heme-containing oxygenases also were discovered. In 1958 Klingenberg[3] and Garfinkel[4] found an unusual pigment in microsomes that when reduced in the presence of CO generated a spectrum with a peak at 450 nm instead of the expected 420 nm peak. Hence the name P450 was born. In 1964 Omura and Sato[5,6] showed that this "pigment" is actually a protein and the function of this strange heme protein became clear in a seminal study by Estabrook et al.[7] that demonstrated the involvement of the 450 nm pigment in steroid hydroxylation. Thus by the mid-1960s it was established that heme plays an active role in biology by somehow catalyzing the hydroxylation of organic substrates. While these discoveries certainly mark the beginning of modern approaches to studying heme enzyme oxygenases, the enzymatic role of heme dates much earlier to 1903 when horseradish peroxidase (HRP) was described.[8] Indeed, owing to the ease of purification and stability of the various intermediates, HRP dominated heme enzyme studies until P450 was discovered.

Heme enzymes can catalyze both reductive and oxidative chemistry but here we focus on those that catalyze oxidation reactions, and especially those for which crystal structures are available. There are two broad classes of heme enzyme oxidants: oxygenases that use O_2 to oxidize, usually oxygenate, substrates and peroxidases that use H_2O_2 to oxidize, but not normally oxygenate, substrates. Of the two oxidants molecular oxygen is the most unusual because even though the oxidation of nearly all biological molecules by O_2 is a thermodynamically favorable process, O_2 is not a reactive molecule. The reason, of course, is that there is a large kinetic barrier to these reactions owing to O_2 being a paramagnetic molecule so the reaction between a majority of biological molecules that have paired spins is a spin forbidden process. Overcoming this barrier is why Nature recruited transition metals and heme into enzyme active sites. As shown in Fig. 2, heme oxygenases bind O_2 and store the O_2 oxidizing equivalents in the iron, porphyrin, and/or amino acid side chains for further selective oxidation of substrates. Peroxidases use H_2O_2 as the oxidant and while not having the O_2 spin barrier, H_2O_2 presents its own problems. The reaction between H_2O_2 and transition metals generates toxic hydroxyl radicals in the well known Fenton chemistry[9] which would be highly destructive to enzyme active sites. As illustrated in Fig. 2, all heme oxidases are at some point in the catalytic cycle peroxidases. Molecular oxygen must first be reduced by two electrons to the peroxide level before the interesting chemistry starts:

*Corresponding author: poulos@uci.edu; 949-824-7020.

cleavage of the O-O bond. This bond can cleave either homolytically, which gives two hydroxyl radicals, or heterolytically to effectively give H_2O and a naked O atom with only 6 valence electrons. Since the release of hydroxyl radicals in the active site must, in most cases, be avoided Nature has engineered heme enzyme active sites to ensure that the heterolytic pathway dominates.

The list of heme enzymes is substantial and thus it is necessary to be selective on which to discuss in detail. It may appear that a disproportionate amount of space is devoted to peroxidases and P450s. This is true and admittedly reflects the author's own interests and area of expertise. Additionally, however, peroxidases are the most extensively studied heme enzymes and have provided fundamental insights into the chemistry and structure shared by many other enzymes. The other enzymes to be discussed were selected owing to both subtle variations on common themes and novel features that Nature selected for specific biological function.

2. Peroxidases

2.1. Introduction

Peroxidases and catalases played a critical role in the early days of enzymology[10] in part owing to the relative ease of preparing reasonable amounts of purified material. Just as important were the spectrally distinct intermediates formed during the reaction cycle which enabled Britton Chance to develop rapid reaction methods for following the formation and decay of catalase intermediates.[11,12] The following catalytic cycle initially was worked out with horseradish peroxidase (HRP).

In the first step, peroxide removes one electron from the iron and a second from the porphyrin (R in the above scheme) to generate a porphyrin π cation radical.[13] This first intermediate exhibits a green color with distinct spectral characteristic quite different from the brownish-red color of the resting enzyme (Fig. 3). In some peroxidases an amino acid side chain rather than the porphyrin ring is oxidized in Compound I. The earliest and most well known example is cytochrome c peroxdase (CCP) which forms a Trp cationic radical.[14,15] In the second step a substrate molecule delivers one electron to Compound I which reduces the porphyrin π cation radical to give the red Compound II. Finally, in the last step a second substrate reduces Fe^{4+} back to Fe^{3+}. The precise physiological role of the peroxidase determines the nature of the reducing substrate, SH, which are normally phenols and aromatic amines in HRP-like enzymes.

Based on sequence homologies, source, and crystal structures non-mammalian peroxidases are divided into 3 classes.[16] Class I are intercellular peroxidases with the most notable example being mitochondrial yeast cytochrome c peroxidase (CCP); Class II are the extracellular fungal peroxidases; Class III are the extracellular plant peroxidases such as HRP. These enzymes are single polypeptide chains of ≈30,000–40,000 daltons with a single heme group attached to the protein *via* iron ligation to a His residue. Class I peroxidases have no disulfide bonds while Class II and III peroxidases require additional stabilization which is why these peroxidases have 4–5 disulfide bonds and two calcium ion binding sites. The extracellular peroxidases also have sites of glycosylation. Crystal structures now are available for all 3 classes and not too surprisingly, the overall core helical and active site structures are well conserved (Fig. 4).

2.2. Compound I Formation

Although crystal structures provided the stereochemical details of Compound I formation, a good deal was known from elegant biochemical and spectral studies well before the first crystal structures. In 1972 Schonbaum et al.[17] demonstrated, using alkyl hydroperoxides,

that there is a quantitative release of the alcohol. This means that the peroxide O-O bond cleaves heterolytically, the alcohol departs, and what remains is an oxygen atom with only 6 valence electrons. Given the similarity in reactivity to carbenes, the electron deficient oxygen atom was given the name oxene, later modified to oxenoid.[18,19] Magnetic susceptibility[20] and Mössbauer[21] studies showed that the iron is oxidized to Fe(IV) and that the porphyrin is oxdized.[13,22] Thus the oxidizing equivalents of the oxene O atom are stored as $Fe(IV)O^{2-}$ and a porphyrin π cation radical.

The kinetics of Compound I formation are second order, stoichiometric, and irreversible with a rate constant in the range of 10^7–10^8M-sec^{-1}. It thus is interesting that Km values often are reported for H_2O_2 binding to peroxidases where the second order kinetics indicate no stable pre-reaction complex. Even so it has been argued that peroxidases do form a pre-reaction ES-type complex[23] and low temperature work[24] indeed does show saturation kinetics indicating a pre-reaction complex must form. Assuming that the solvent conditions required for the low temperature work do not alter the catalytic mechanism, then the inability to observe saturation at room temperature may simply be the result of the reaction being too fast to measure at high peroxide concentrations.

Solution of the yeast CCP structure[25] provided the structural details of peroxide activation. As shown in Fig. 4, CCP and other peroxidases have a proximal His ligand H-bonded to an Asp residue. This H-bond imparts more imidazolate character to the His which helps to lower the redox potential of the heme iron relative to the heme group in globins where the His ligand donates an H-bond to a peptide carbonyl O atom. That the H-bonding environment and charge on the proximal ligand are important for redox potential control was initially demonstrated with model heme complexes.[26,27] Subsequent mutagenesis work, primarily with CCP,[28–31] clearly showed a close correlation between ligand charge and redox potential.

The stereochemical mechanism of Compound I formation is shown in Fig. 5.[32] The distal His residue is the essential acid-base catalyst that transfers the peroxide O1 proton to the O2 oxygen thus promoting heterolytic cleavage the O-O bond. Mutagenesis studies have demonstrated that the distal His is indeed essential for Compound I formation.[33,34] The role of the distal Arg residue found in all 3 classes of non-mammalian heme peroxidase has been more challenging to unravel primarily because the kinetics of Arg mutants are more complex. Initially it was proposed that the distal Arg plays a key role in stabilizing the developing negative charge on the leaving O2 atom thus promoting heterolysis.[32] Mutagenesis work with both CCP[35] and HRP[36] showed that with distal Arg mutants Compound I formation exhibits saturation kinetics and at high peroxide concentrations the rate of Compound I formation is 2–3 orders of magnitude slower than in the wild type enzymes. Thus the distal Arg mutants slow O-O bond cleavage as predicted but it also was found that the Arg mutants alter the reactivity and stability of Compound I.[35,36] This makes sense in light of Compound I crystal structures[37,38] where the distal Arg is seen to move in to donate an H-bond to the ferryl O atom which certainly must modulate the reactivity of the ferryl center.

The one problem with the original mechanism[32] is that the distal His is too far from the peroxide O1 atom to form a strong H-bond. One possibility is that the O1 proton is removed prior to formation of the iron-O1 bond but this seems unlikely since the peroxide pKa is about 11.6. Density functional calculations[39] suggest another viable option which is for a water molecule to intervene and serve as a proton transfer conduit from the O1 atom to O2 *via* the distal His (Fig. 5). This is consistent with the Compound I crystal structures since there is a well ordered water molecule in exactly the right place to serve this function (Fig. 6).

2.3. Structure of the Compound I Ferryl Center

The stability of peroxidase Compound I has made it possible to use a variety of spectral and other biophysical tools to probe the electronic structure and especially the nature of the Fe(IV) intermediate. Of particular importance is the question on whether Compound I is best described as Fe(IV)=O or Fe(IV)-OH. Resonance Raman and EXAFS are two of the best tools for providing direct information on the iron-oxygen bond distance. Raman studies[40–42] indicate a short Fe(IV)=O double bond and EXAFS also predicts a short 1.64–1.67Å Fe(IV)=O double bond.[43–45] However, a majority of crystal structures[46–49] of various heme proteins obtain a much longer distance, 1.8–1.9Å, indicating a single Fe(IV)-OH bond. Green[50] has analyzed these data in terms of an empirical formulation called Badger's rule (Fig. 7A). Here the computed Fe-O bond distance is plotted against the computed stretching frequency and, as one might expect, a straight line is obtained. The experimental resonance Raman and a majority of EXAFS fit the empirical plot very well and only the crystal structures are outliers. The reason for this discrepancy is a now well recognized problem in crystallography which is that x-rays generate hydrated electrons that can reduce metal centers[51] and high potential centers like Fe(IV) are especially vulnerable. The problem is quite severe at high intensity synchrotron sources now routinely used.

The more routine use of single crystal spectroscopy and robotic data collection methods at synchrotron facilities has helped to resolve these discrepancies. By carefully monitoring the redox state of the Compound I or II iron using single crystal UV/Vis spectroscopy, the reduction of Fe(IV) as a function of x-ray dose can be accurately determined. Based on this information, a data collection strategy can be developed that ensures the structure of 80–90% Compound I is determined. This requires collecting x-ray intensity data for very short times using many crystals followed by merging data sets to obtain one complete data set for a low x-ray dose Compound I structure. This strategy has been used for both HRP[37] and CCP.[38] The 1.6Å HRP Compound I structure gives a Fe-O distance of 1.7Å. For CCP several structures as a function of x-ray dose were solved to 1.4Å resolution. The plot in Fig. 7B is the refined Fe-O distance as a function of x-ray dose. This plot extrapolates back to 1.72Å which is quite close to the 1.68Å distance derived from Raman studies.[41] These more recent structures now agree well with both Raman and EXAFS experiments. In previous crystal structure work what was thought to be Fe(IV)-OH was more likely Fe(III)-OH owing to x-ray induced reduction. As the plot in Fig. 7 shows, the Fe-O distance increases linearly as a function of x-ray dose as the iron steadily marches from Fe(IV) to Fe(III) and possibly even to Fe(II).

2.4. The Compound I Radical

While HRP has a porphyrin π cation radical in Compound I,[13] it was found early on that yeast CCP is unusual since the EPR properties of Compound I[52] coupled with protein chemistry work[14] indicated a Trp radical. Note that CCP has two Trp residues in the active site, Trp51 and Trp191 (Fig. 4). Given that Trp51 is directly adjacent to the peroxide binding site, this initially was thought to be the radical site[32] although ENDOR studies suggested Met instead.[53] The CCP structure was consistent with both views since at the time only the HRP[54] and CCP[55] sequences were known and HRP was predicted (correctly) to have Phe residues in the active site rather than Trp and HRP also lacks the Met residues found in the proximal heme pocket of CCP (Fig. 4). Since Phe is harder to oxidize than Trp or Met then HRP forms a porphyrin radical while CCP forms a Trp or Met radical. Early mutagenesis worked showed that Trp191[56] but not Trp51[57,58] is essential for catalysis which once again pointed to Trp. The situation finally was settled with elegant isotope substitution studies that unequivocally showed that Trp191 forms a cationic radical in Compound I.[15] This work was followed by a comprehensive analysis of the peculiar EPR properties of the Trp191 radical.[59]

The question of why HRP forms a porphyrin radical while CCP forms a Trp radical appeared to have been answered. Since HRP has the higher redox potential active site Phe residues in place of the CCP Trp residues, the porphyrin cationic radical is the more stable species while in CCP the Trp cationic radical is more stable. However, as more peroxidases were recombinantly expressed, characterized, and crystal structures solved this view no longer was adequate. Ascorbate peroxidase (APX) presented the first challenge. It was clear from the initial sequence of pea cytosolic APX[60] that APX would have the same Trp residues in the heme pocket as CCP which later was confirmed by the crystal structure.[61] It was fully anticipated that APX would produce a Trp radical but freeze quench EPR[62] and stopped flow studies[63] showed that APX Compound I has a catalase-like porphyrin radical. Thus began some detective work to figure out why. A close comparison between APX and CCP shows that APX has a monovalent cation bound about 8Å from the proximal pocket Trp (Fig. 8). Many other peroxidases have a Ca^{2+} at this site while CCP has no cation owing to the lack of appropriate ligands. It thus was hypothesized that the nearby cation would destabilize the positive charge on the Trp191 cationic radical. Moreover, it was found by cavity complementation[64,65] and computational chemistry[66,67] that the space occupied by Trp191 strongly prefers binding cationic ligands. This was experimentally tested by engineering in the APX monovalent cation site into CCP and as predicted both the Trp191 EPR signal (Fig. 8) and enzyme activity were greatly decreased.[66,68] By engineering in suitable ligands it was even possible to change the selectivity of the cation site from monovalent to Ca^{2+} and effectively decrease activity by titrating in Ca^{2+}.[69] The reverse experiment of engineering out the monovalent cation site in APX failed since the mutant undergoes a structural change resulting in a hexacoordinate heme complex most probably by the distal His dropping down to coordinate the heme iron.[70] Although APX forms a porphyrin radical, a small amount of Trp radical can be detected if Compound I is allowed to spontaneously decay.[71] The amount and lifetime of the proximal Trp radical signal in APX can be increased by converting the local electrostatic environment to that found in CCP and *Leishmania major* peroxidase (LmP). Namely, changing Leu203, Gln204, and Ser160 in APX (Fig. 8) to Met dramatically increases the amount and stability of the Trp179 radical (Fig. 8).[72] LmP also forms a very stable Trp radical and although the intensity of the EPR signal is similar to CCP the shape is quite different (Fig. 8).[73] The LmP Trp radical EPR closely resembles the D235E mutant in CCP[59] and these subtle changes in the EPR have been attributed to weak coupling between the Trp radical and the Fe^{4+}=O center while various conformational states result in a distribution of coupling from antiferromagnetic to ferromagnetic. Thus, the precise shape of the spectrum is quite sensitive to subtle differences in the local environment so it is not too surprising that the LmP radical is similar in signal strength but the details differ from that of CCP.

The story becomes somewhat more complicated in CCP since CCP is quite sensitive to which cyt c is used as a substrate. It was found that some of the cation mutants lose substantial activity when horse heart cyt c is used as the substrate but when the natural yeast cyt c is the substrate the activity is close to normal at low ionic strength but substantially decreases at high ionic strength.[74] This was attributed to a change in rate limiting step as a function of ionic strength and the conclusion that even in Compound I EPR silent mutants, a full equivalent of the Trp191 radical initially forms but because the Trp191 now is so unstable the radical rapidly migrates elsewhere, most likely Tyr residues. To follow the logic of this explanation, it is useful to refer to the generally accepted mechanism for CCP shown scheme 2.[75,76]

First and most importantly each of the two electron transfer steps requires a Trp191 radical. After the initial reduction of Trp191 there is an equilibrium between Fe^{4+} and Trp191 to give $Fe^{3+}Trp^{\bullet+}$ which is the electron acceptor for the second electron transfer step (step 3). At low ionic strength dissociation of cyt c is limiting and slow so there is plenty of time for

electron transfer (rate $\approx 6.1\times10^4 s^{-1}$)[77] to the mutants where the Trp191 radical is short-lived. However, at high ionic strength, dissociation is not limiting so the Trp191 radical lifetime comes into play and is too short to maintain high steady state activity. This notion was also supported by stopped flow studies where it was found that adding H_2O_2 to a mix of the cation CCP mutant and reduced cyt c leads to complete oxidation of cyt c but no loss of the UV/Vis spectrum associated with CCP Compound I Fe^{4+}=O.[74] This could only mean that a full equivalent of the Trp191 radical lasted long enough for full oxidation of cyt c in the preformed CCP-cyt c complex.

These results led to the idea that it might be possible to measure the lifetime of the cation mutants by a double mix stopped flow experiment outlined in Fig. 9.[78] In the first mix peroxide is added with CCP to form Compound I. In the second mix, reduced cyt c is added to Compound I. The variable is the delay time between the first and second mix. The variation in the amount of cyt c oxidized and the rate of oxidation as a function of delay time will give an estimate of the Trp191 radical lifetime. Indeed, it was found that for a series of cation mutants, the activity and the strength of the Trp191 EPR signal in Compound I correlates well with the rate and extent of cyt c oxidation in the double mixed stopped flow experiment. It was anticipated that if the Trp191 radical is sufficiently destabilized then the Compound I radical should end up on the porphyrin but this does not occur. CCP has a total of 14 Tyr residues and it is well known that the spontaneous decay of Compound I results in crosslinking *via* modification of surface Tyr residues[79] so it appears that oxidation of Tyr residues is preferred over porphyrin oxidation. The preferred Tyr radical appears to be Tyr236[80] which is close to Trp191. Thus it is interesting to note that in the double mix experiments, the Tyr236Phe CCP mutant introduced on top of the inactive cation mutant recovers activity and increases the life time of the Trp191 radical.[78] A possible explanation for these observations is that the Trp191, while thermodynamically quite destabilized in the cation mutants, can be kinetically trapped in the Tyr236Phe mutant (Fig. 9). In effect Tyr236 provides a conduit for the Trp191 radical to migrate elsewhere and by blocking this radical escape route, the lifetime of the Trp191 radical increases.

More recently the second peroxidase, *Leishsmania major* peroxidase (LmP), that also forms a stable Trp radical, has been characterized.[81,82] As was expected from sequence alignments, the LmP structure is very similar to CCP and LmP forms a stable Trp208 radical (Fig. 8).[73] What was puzzling, however, is that LmP has the same cation site near Trp208 as APX so one would think that a cationic Trp208 radical would not be very stable. Note, however, that LmP has Cys197 whose sulfur atom contacts Trp208 where CCP has Thr180. The close proximity of the Cys197 might provide additional stability to the positive charge on a Trp208 cation radical. Replacing Cys197 with Thr indeed decreases activity to ≈8% of wild type and nearly eliminates the EPR signal associated with Trp208.[73]

The CCP family of peroxidases is not the only one to form Trp radicals. Two other peroxidase, lignin peroxidase (LiP) and versatile peroxidase (VP),[83] both form short-lived Trp radicals. The initial crystal structures of LiP[84] showed a large lobe of unexplained electron density very near the Cβ of Trp171 (Fig. 10). The position and distance suggested that Cβ had been hydroxylated in an autocatalytic process where the initial turnover events resulted in Compounds I and II leading to Trp171 hydroxylation. Since hydroxylation occurs under anaerobic conditions the mechanism in Fig. 10 wherein water provides the OH group is favored.[84] Thus in the absence of a reducing substrate, both oxidizing equivalents of Compound I are utilized to oxidize Trp171. Whether or not this post-translational modification is a requirement for activity remains to be seen but Trp171 is essential for activity. Replacing Trp171 with Phe eliminates >99% of the activity toward the natural substrate, veratryl alcohol, but has little effect on other generic peroxidase substrates.[85] Veratryl alcohol is a small aromatic alcohol that is directly oxidized by LiP and then serves

as a diffusible oxidant that oxidizes lignin.[86–88] That Trp171 is critical for veratryl alcohol peroxidation and not the peroxidation of other non-natural substrates has led to the proposal that veratryl alcohol binds near Trp171 while other substrates bind near the exposed heme edge, the substrate binding site in HRP.[89] In VP Trp164, the homolog to LiP Trp174, plays the same role and is critical for activity. [90–92] Note (Fig. 10) that Trp171 is surrounded by carboxylate groups so, as in CCP, the local electrostatic environment promotes the initial formation of a cationic radical. The importance of the local environment for Trp radical stabilization was tested by engineering in the Trp and three local negative charges into the *Coprinus cinereus* peroxidase.[93] The engineered Trp radical could be detected by EPR and the veratryl alcohol peroxidation activity increased from essentially 0 to about 12% of wild type LiP. Peroxidases thus have provided considerable information on the formation, stabilization, and migration of amino acid centered radicals in proteins.

While relatively simple electrostatic considerations can explain how a protein stabilizes Trp cationic radicals, the question remains open on how other peroxidases stabilize a porphyrin radical. The only way it has been possible to observe a porphyrin radical in CCP is to mutate Trp191 to Phe.[94] As noted in the previous discussions, even in those mutants with a much destabilized Trp191 radical, Trp191 is still the preferred initial site of oxidation and then the radical rapidly migrates to other sites, probably Tyr, but not to the porphyrin. Thus the porphyrin is the oxidation site of “last resort”. Even so there must be other factors that favor formation of a porphyrin π cation radical given that the HRP porphyrin π cation radical is fairly long-lived. Computational studies suggest that the heme propionates may play an important role.[95,96] The basic idea is that a propionate with no H-bonding partners would be free to back-fill the positively charged hole of the porphyrin radical thus destabilizing a porphyrin cationic radical. Thus one might anticipate that peroxidases with strongly H-bonded propionates would form a more stable porphyrin radical. There is some experimental support for this scenario since replacing an Arg that H-bonds with a heme propionate in APX with Asn results in a very unstable porphyrin π cation radical.[72] The possible direct involvement of propionates is further underscored by the substrate complexes of both manganese peoxidase (MnP)[97] and APX.[98] In both these peroxidases the substrate, Mn^{2+} in MnP and ascorbate in APX, directly interact with a heme propionate indicating that the propionate provides an electron transfer conduit to the porphyrin ring.

One final example of how Nature handles the location and movement of oxidizing equivalents in heme enzymes are bacterial diheme peroxidases that function as cytochrome c peroxidases.[99,100] The best investigated is the diheme peroxidase from *Pseudomonas aeruginosa*. These enzymes are homodimers with about 300 residues per monomer. Each monomer contains two hemes both of which are covalently tethered to the protein *via* thioether bonds between Cys residues and the heme vinyl groups. One heme exhibits a high redox potential and is designated the high potential or HP heme and the second is the low potential LP heme.[101] Both hemes start off in the low-spin Fe^{3+} oxidation state. His and Met serve as the axial ligands for the HP heme while the LP heme has two His residues coordinating the heme iron.[102] The proposed mechanism is outlined in Fig. 11.[103] This is a traditional heme peroxidase mechanism except a porphyrin or amino acid radical is not involved. Instead, the second electron required for peroxide O-O bond cleavage derives from the HP heme. The enzyme is inactive when both hemes are in the Fe^{3+} redox state. However, electron transfer from an external donor reduces the HP heme which results in a large conformational change (Fig. 11) that displaces one of the His ligands, His171, of the LP heme thus freeing up one axial coordination position of the LP heme for peroxide binding.[104–106] In addition, Glu144 moves from the surface of the protein into the active site where it likely plays a catalytic role in cleaving the peroxide O-O bond. Based on crystal structures, mutagenesis, spectroscopic, and kinetic studies an elegant explanation has been put forward to explain the cascade of events that results in the structural change.[104]

Reduction of the HP heme is accompanied by the uptake of a proton on to a HP heme propionate which disrupts a HP heme H-bond with a peptide NH group resulting in a slight change in the position of the HP heme propionate. This leads to further changes in protein groups between the two hemes ultimately resulting in displacement of His171. This is a remarkable example of how subtle changes in a heme can be amplified resulting in large structural changes some 16Å away and is reminiscent of the T and R state transitions in hemoglobin. Clearly Nature has found interesting ways to exploit the physiochemical properties of heme to control enzyme activity and conformational dynamics.

2.5. Substrate Complexes

Most peroxidases oxidize small molecules so it was anticipated that peroxidases would have traditional substrate binding pockets. When only the CCP structure was available there was a general consensus that small molecules would bind near the exposed heme edge. This view was supported by some clever experiments wherein the available heme edge in CCP was chemically modified with phenylhydrazine thus blocking access to the exposed heme edge.[107] The activity against HRP-like aromatic alcohol substrates was severely impaired while the cyt c peroxidase activity was only moderately affected. These results support the view that there are two different sites for substrate oxidation: one for small molecules at the solvent exposed heme edge and a second for cyt c. The subsequent crystal structure of HRP complexed with substrates indeed showed that these molecules bind at the exposed heme edge.[89,108] HRP, however, is what we might call a generic peroxidase that is not specialized to oxidize a specific substrate. It now appears that those peroxidases with specialized functions have alternate substrate binding pockets. Some examples include manganese, lignin, and ascorbate peroxidase. As noted earlier, LiP (lignin peroxidase) very likely binds its favored substrate, veratryl alcohol, near Trp171 while in both MnP[97,109–111] and APX[98,112,113] the substrate binds near the heme propionate (Fig 12).

The substrate complex that has received the most attention is CCP. An excellent recent review[114] summarizes the wealth of information that has been generated over the years so here only a brief summary will be provided including some recent advances. Early on it was generally thought that CCP has two binding sites for cyt c. The complex non-Michaelis-Menten steady state kinetics[115] and other biophysical probes[116–118] strongly implicated two binding sites. This made sense since there are two centers that must be reduced in CCP, the Trp191 radical and Fe(IV). However, while CCP may have two binding sites the wealth of evidence[76,114] favors a single site for both electron transfer events which is the one observed in the crystal structure[119] (Fig. 13). Perhaps the biggest surprise in the CCP-cyt c structure is the lack of any close inter-protein ionic contacts. It was well known that formation of the complex is dependent on ionic strength and early chemical modification studies clearly implicated the ring of lysine residues surrounding the exposed heme edge of cyt c as being critically important.[120–122] The ionic strength dependence, however, did provide a hint that there is more to complex formation than simple electrostatics. The steady state activity of CCP steadily increases with ionic strength and then decreases up to about 100 mM salt.[115] This is a hallmark of nonpolar interactions providing part of the driving force for complex formation and, indeed, the crystal structure shows some very nice nonpolar interactions at the interface. The lack of specific ionic interactions still was a surprise unless one takes a more detailed look at what guides the formation of such complexes. The basic idea has been outlined in an excellent review[123] and is summarized in Fig. 14. The initial encounter complex is nearly diffusion controlled and is dominated by the negative electrostatic surface of CCP complementing the positive surface on cyt c. The probability of the initial encounter complex being the lowest energy complex required for electron transfer is low so after the initial encounter cyt c samples the surface of CCP *via* a “bind and crawl” process until it ultimately reaches the lowest energy productive orientation. It is this process, k_2 in Fig. 14,

that is most likely limiting and ionic strength dependent. In the case of CCP nonpolar interactions are important so the rate limiting step actually increases with increasing ionic strength owing to the well know salting-in effect that promotes nonpolar interactions. At very high ionic strength the nonpolar interactions are not sufficient to balance the loss of favorable electrostatic interactions so the activity decreases.

More recently the structure of a CCP-like ET system has been determined which is the complex formed between *Leishmania major* peroxidase (LmP) and its cyt c.[124] Fig. 13 provides a comparison between the LmP and yeast CCP systems. The complexes are very similar. Although relative to the peroxidase the cyt c rotates by about 40° and translates about 4Å, the ET path in both systems is the same. The cyt c heme contacts the same position in both peroxidases thus providing a short through sigma-bond ET path leading to the Trp radical. The main difference is that the side chains attached to this ET peptide path are more polar in LmP than in CCP (Fig. 13). Whether or not this is relevant to ET remains to be seen. Another important difference is that LmP has one very strong ion pair formed at the interface and a second weaker one at the periphery while, of course, CCP has none. The importance of the Asp211(LmP)-Arg24(cyt c) ion pair was demonstrated *via* mutagenesis. This correlates well with the ionic strength dependence since in LmP the rate steadily decreases as the ionic strength increases[125] indicating that electrostatics dominates complex formation. The large differences in the details at the interfaces is due to differences in the peroxidases. Larger side chains protruding from the surface of CCP prevents very tight packing at the interface so as a result only 550$Å^2$ of surface area is buried in the CCP complex compared to 1,180$Å^2$ in LmP complex. This tighter packing effectively seals off the Asp211-Arg24 ion pair which is probably why this interaction is so important and strong.

2.6. Prostaglandin Synthases

There are several reviews on structure-function relationships in prostaglandin endoperoxidase synthase (PGHS)[126–131] so here we focus on those structural and mechanistic features that most closely relate PGHS to the peroxidases previously covered.

PGHS enzymes are involved in prostanoid biosynthesis, a large group of hormonally active eicosanoids, and PGHS enzymes are important targets for anti-inflammatory drugs like aspirin and ibuprofen. PGHS isozymes 1 and 2 catalyze the committed steps in two sequential reactions starting with the primary precursor, arachidonic acid (Fig. 15). PGHS is a homodimeric 140 kDa membrane protein and Fig. 15 shows the structure of PGHS-1 in a complex with arachidonic acid.[132] In order to obtain this structure of a productive complex yet prevent enzyme turnover, the heme was replaced with Co(III) protoporphyrin IX. The peroxidase active site is similar to other peroxidases with His388 serving as the proximal heme ligand while His207 serves as the acid-base catalytic group required for heterolytic fission of the peroxide O-O bond in the distal pocket. Gln203, however, replaces the distal Arg found in other peroxidases. PGHS operates like a traditional heme peroxidase in forming Compound I (Fig. 15) and the first step in the reaction is the formation of Compound I consisting of Fe(IV)=O and a porphyrin radical. Fatty acid peroxides work better than more soluble peroxides and the physiologically relevant peroxide is most likely PGG2 (Fig. 15).[133,134] This creates an interesting structural problem since the large PGG2 must dock into the PGHS distal pocket. However, the heme pocket in PGHS is more open to solvent than in traditional heme peroxidases and modeling studies indicate that PGG2 can fit into the pocket with the alkyl end interacting with active site hydrophobic groups and the carboxyl end with basic amino acids.[135] As long as there is sufficient reducing substrate the peroxidase reaction (Fig. 15) can cycle independent of the cyclooxygenase cycle since the

enzyme retains peroxidase activity in the presence of non-steroidal anti-inflammatory compounds[136] that block the cyclooxygenase substrate binding site.

Once Compound I forms the porphyrin radical oxidizes the nearby Tyr385 to give a Tyr385 radical.[126,137] The crystal structure shows that the substrate, arachidonic acid, directly contacts Tyr385 which explains the specific removal of the arachidonic acid 13ProS hydrogen atom by the Tyr385 radical to generate the substrate radical. More recently it has become apparent that Tyr504 can also be oxidized and may serve as a secondary site for storing oxidizing equivalents.[131] Generation of the arachidonic acid radical is then followed by a series of reactions with two O_2 molecules to give the final products, PGG_2 and PGH_2. In order for the reaction cycle to continue, Tyr385 must be oxidized once again which requires the peroxidase cycle. As shown in Fig. 15 the conversion of PGG2 to PGH2 requires electrons with one of the intermediates being the PGG2 radical. This species could, in theory, oxidize Tyr385 thus providing an alternate route for regeneration of the Tyr385 radical although the weight of the evidence indicates that the cyclooxygenase reaction requires the peroxidase activity.[131] Determining exactly what happens during turnover is challenging since PGHS does not exhibit normal enzyme kinetics. For example, in the cyclooxygenase reaction activity increases, reaches a maximum, and then declines to zero without consuming all substrates.[136] The initial increase in activity is due to the production of the PGG2 hydroperoxide which can serve as a substrate in Compound I formation while the decrease in activity is mostly due to protein and/or heme damage.[138] In sharp contrast the peroxidase activity starts high and steadily decreases to zero but again substrates are not all consumed. This is the result of a self-inactivation which is due to the ferryl center and not the Tyr radical.[139] Despite these complications the branched-chain mechanism shown in Fig. 15D ties together the current state of knowledge on PGHS catalysis.

3. Cytochrome P450

3.1. Introduction

The range and number of P450s throughout the biosphere is truly remarkable and as such cytochrome P450 represents one of the largest enzyme families. Thus far about 18,000 P450s have been identified[140] but this is likely to have increased by the time this review is published. Humans have 57 P450s, *Arabadopsis* 273, the honeybee 48, and the list goes on and on (see http://drnelson.uthsc.edu/CytochromeP450.html for continual updates). As of June 2013 the PDB lists 416 entries with the name P450 in the structure title and of these about 64 are unique P450s, the rest being mutants and inhibitor/substrate complexes. In order to keep track of this mass of information an important P450 nomenclature has been developed. P450s are designated as CYPxyz where CYP=**CY**tochrome **P**450 and xyz is a code relating the CYP to a family, sub-family, and isoform.

The most well known function of human P450s is in xenobiotic detoxification. Drugs and other xenobiotics find their way into the liver where various P450s hydroxylate the xenobiotic which renders these molecules more soluble and susceptible to further modification for easier elimination. Of the drug metabolizing P450s CYP3A4 is perhaps the most important since this single P450 is responsible for metabolizing about half of all currently used drugs. In addition to these catabolic functions, P450s also play a critical role in the biosynthesis of important compounds with steroids topping the list. While eliminating insoluble hydrocarbons is desirable, the oxidative chemistry of P450s has a downside. P450s also can form epoxides which are highly electrophilic and thus macromolecular nucleophiles such as DNA are susceptible to covalent modification. Aromatic epoxides have the ability to intercalate into double stranded DNA where they can modify the genetic material with deleterious downstream consequences. A classic example is aflatoxin which is activated by P450 oxidation resulting in selective modification of the P53 tumor supressor gene.[141]

While P450s were first demonstrated in liver, detailed structure function studies were limited since P450s are anchored to the membrane *via* an N-terminal hydrophobic tail which presented problems with purification and recombinant expression. As a result, most of the early mechanistic and biophysical work centered on soluble P450s and *Pseudomonas putida* P450cam (CYP101) was the first to be described and well characterized [142] which included sequencing[143–145] and structure determination.[146,147] P450cam catalyzes the regio- and stereo-selective hydroxylation of camphor to 5-*exo*-hydroxycamphor which is the first step in the utilization of camphor as a carbon source.

3.2. Structure

P450s are single polypeptides ranging from 40–55 kDa and the overall fold in all P450s whose structures are known is basically the same (Fig. 16). An important difference between membrane bound and soluble P450s is a nonpolar N-terminal extension that anchors particulate P450s to the membrane but this appears to have little effect on the core structure. The very long I helix runs over the surface of the heme and contributes groups that interact with both the substrate and dioxygen. There is some variation on the exact positioning of the I helix and local helical distortions near the O_2 binding site in various P450s. The local structure around the Cys ligand, however, is much more highly conserved. The Cys ligand is situated at the C-terminal end of the L helix where the Cys sulfur accepts an H-bond from a peptide NH group. This type of H-bonding is very common in iron-Cys proteins and is required for modulating the iron redox potential.[148–150] Without such H-bonds the redox potential would be too low for physiological reductants.

P450s also are quite flexible as they must be in order to allow substrates to enter and products to leave. In general there are two extreme forms of a P450: substrate-bound (closed) and substrate-free (open). The primary motions involve large movements of the F and G helices in addition to the F/G loop connecting these helices. In some open structures the F/G loop is not visible in electron density maps indicating that this region can become highly disordered in the open form. Some examples of open/closed structures is provided in Fig. 17. The largest range of motion so far observed is in P4502B4.[151,152] In the initial crystal structure there were two P4502B4 molecules in the asymmetric unit with a His from the F/G loop in one molecule penetrating into the heme pocket of the second molecule to coordinate the heme. In the open form the substrate pocket fills with solvent molecules which are displaced in a presumably entropically favored process when substrate binds. The dynamics of the open/closed switch has been most thoroughly examined in P450cam.[153] A series of structures of P450cam with a substrate tethered to a long linker traps the substrate access channel in various stages along the open/close path.[154] This information coupled with principal component analysis leads to a picture of distinct conformational states between the fully open and closed forms. More recently a double labeling EPR experiment, double electron–electron resonance or DEER, approach has been used to study the effects of substrate binding on conformation.[155] This method involves selective labeling of engineered Cys residues and clearly shows that P450cam shifts from the open state in the absence of substrate to the closed form when substrate binds.

In the closed substrate-bound form the active site volume can vary substantially. Examples of some substrate complexes are provided in Fig. 18. P450cam and P4503A4 represent two extremes on binding pocket volume, 246$Å^3$ for P450cam and 1,020$Å^3$ for P4503A4. One common feature is that the atom to be hydroxylated is usually within 4–5Å to the iron. Thus in Compound I the ferryl O atom will directly interact with the correct carbon atom for regio- and stereo-selective hydroxylation. The main outlier thus far has been P450BM3.[156] P450BM3 is a fatty acid hydroxylase and the crystal structures show that the fatty acid is too far from the iron for hydroxylation.[157] NMR studies indicate that upon reduction, the

substrate moves closer to the iron.[158] Another peculiar feature of P450BM3 is the temperature dependence of the UV/Vis spectrum. When P450s shift from low-spin to high-spin the Soret maximum shifts from about 420nm to 390nm which provides a very convenient method for determining substrate spectral dissociation constants. P450BM3, however, in the substrate-bound form shifts from a high-spin spectrum at room temperature to low-spin at reduced temperatures.[159] This raises the possibility that in frozen crystals the substrate is "locked" in a conformation far from the iron so the heme remains low-spin but perhaps at room temperature the substrate moves, displaces the water ligand, and shifts to high-spin. In the cryogenic crystal structure of the substrate-bound complex there is a water about 3.5Å from the iron[160] and there certainly is sufficient room for direct coordination to the heme iron although 3.5Å is too long a distance between the water and iron for the water to be considered a low-spin ligand. This is a problem that could be resolved by single crystal spectroscopy and room temperature crystal structures but at present these inconsistencies are unresolved.

3.4. Electron Transfer

3.4.1. Overview—As shown by the overall catalytic cycle of P450 (Fig. 19), electrons derived from other redox proteins are required. At one time it was thought that P450 electron transfer (ET) systems could be neatly divided into two classes. One is the mammalian P450 systems which utilize a single P450 reductase that contains both FAD and FMN. The second is the bacterial systems like P450cam which has a FAD and Fe_2S_2 ferredoxin where the order of electron transfer (ET) is NADH-to-FAD-to-Fe_2S_2-to-P450. Thanks to the increasing number of genome sequences and modern recombinant protein expression technology, we now know that P450 ET systems are more diverse and can involve various combinations of flavin and iron-sulfur proteins.[161] As with any biological ET system, the two redox partners must recognize one another *via* complementary surfaces to enable the donor and acceptor redox partners to properly align with respect to distance and the intervening protein matrix.[162,163]

To date there are three crystal structures of P450 redox complexes. The first structure to be solved was that of P450BM3 complexed with the FMN domain of the reductase[164], the second was the P450scc (CYP11A1)-adrenodoxin complex,[165] and the third was the P450cam-Pdx complex.[166] As expected the redox partner docks on the proximal side (Cys ligand side) of the heme which is the closest approach of the heme to the surface.

3.4.2. P450BM3—Next to P450cam P450BM3 has been one of the most heavily investigated P450s. Part of the reason is that P450BM3 was the first catalytically self-sufficient P450 to be discovered[167] since the FAD/FMN reductase is fused to the C-terminal end of heme domain. Without the complication of co-expressing redox partners and an exceptionally high turnover rate P450BM3 has served as an ideal target for biotechnological applications and directed evolution studies.[168] In addition, P450BM3 has proven to be particularly resilient to mutagenesis thus allowing many mutants to be generated and analyzed in detail.[169] The reductase part of P450BM3 is very similar to mammalian P450 reductase whose structure is known (Fig. 20B).[170] Note that the FMN and FAD are directly contacting one another so in order for the FMN to deliver an electron to the P450 heme there must be a substantial reorientation of the FMN module for it to properly dock to P450. Such required flexibility is very likely why obtaining crystals of full length P450BM3 has not yet been achieved.

What did prove successful was a version of P450BM3 missing the FAD domain. The heme-FMN construct was used for crystallization but only one of the two molecules in the asymmetric unit has the FMN domain in place.[164] Moreover, the linker connecting the C-

terminal end of the P450 module with the N-terminal end of the FMN module had been proteolyzed. The length of the linker is known to be quite important for P450BM3 function[171] and molecular modeling indicated that the structure of the complex is consistent with structural restraints of linker length. In order to experimentally test the functional relevance of the model, fluorescence probes were introduced at key positions at the protein-protein interface (Fig. 20).[172] Binding and kinetic studies showed that Leu104 and Gln387 which were converted to Cys and modified with Cys-specific fluorescent probes are indeed critical residues.[173] In a related study the electron transfer pathway was investigated by attaching photoactive (4-bromomethyl-4′-methylbipyridine)[bis(bipyridine)]-ruthenium(II) to engineered Cys residues in the heme domain of P450BM3 (Fig. 20C). Photoexcitation of Ru(II) enables the rate of heme reduction to be measured (Fig. 20). Attaching the Ru compound to Cys387 gave a rate of heme iron reduction of about $4.6x10^5$ s^{-1} while attaching the Ru compound to Cys62 gave no detectable iron reduction even though the distance to the heme iron is nearly the same in both. This was taken as evidence that P450BM3 has a preferred electron transfer path *via* a continuous peptide bond connection from Gln387 to the heme ligand, Cys400. Also note that Gln387 in the heme domain directly contacts the FMN (Fig. 20C). Thus intraprotein electron transfer would require only one through space jump from FMN to Gln387.

As with mammalian P450s, ET in P450BM3 is generally thought to require some significant conformational gymnastics. The P450 reductase structure (Fig. 20B) shows that the FMN and FAD are in direct contact. If the P450BM3-FMN complex is a representative example of what mammalian P450 redox complexes will look like, then the FMN module of P450 reductase must undergo a substantial rearrangement in order to correctly dock to the P450. Some clever engineering of P450 reductase supports this view. Mutants designed to increase the distance between the flavins severely impairs FAD to FMN ET but not the ability of the FMN to reduce P450.[174] Engineering in an S-S bond between the FMN and FAD domains nearly eliminates the ability of P450 reductase to support P450 catalysis but reduction of the S-S bond restores activity.[175] Clearly P450 reductase as seen in the crystal structure with the flavins so close is not the active species and the FMN module must be free to move.

3.4.3. CYP11A-Adx—CYP11A catalyzes the conversion of cholesterol to pregnenolone, the first step in steroid biosynthesis (Fig. 21). The redox partner is adrenodoxin (Adx), a Fe_2S_2 ferredoxin. The crystal structure of the complex was solved by fusing adrenodoxin to the N-terminal end of CYP11A1.[165] Although a good part of the Adx was disordered and not visible in electron density maps, the interface with CYP11A1 was well defined (Fig. 21). The interface is dominated by electrostatic interactions and those residues involved are consistent with mutagenesis and chemical modifications studies.[176–178] A comparison between the free enzyme[179] and the enzyme complexed with Adx are essentially identical so Adx binding does not result in any significant structural change.

3.4.4. P450cam-Pdx—An interesting feature of P450 ET systems is that with P450cam there is a strict requirement for one and only one redox partner while others are more promiscuous. The FAD/FMN P450 reductase in microsomes services a large number of P450s and the actinomycete P450eryF, which is involved in erythromycin biosynthesis, can be supported by spinach ferredoxin and ferredoxin reductase.[180] In sharp contrast P450cam exhibits a strict requirement for its own redox partner, the Fe_2S_2 protein putidaredoxin or Pdx.[181–183] Such specificity has led to the idea that Pdx exerts an effector role by inducing structural changes in P450cam required for activity. Prior to the recent crystal structure of the P450cam-Pdx complex, the Pochapsky lab has led the way in using NMR and computational methods to develop a model of the P450cam-Pdx complex (Fig. 22)[184] which is supported by mutagenesis data[185–189] and has guided experiments on ET in P450cam.

A wealth of spectral data shows that when Pdx binds on the proximal side of the heme spectral changes ensue that are associated with the opposite distal substrate binding pocket with some examples provided in Fig. 22. These changes include resonance Raman,[190] infrared,[189,191] and NMR.[192–194] A tour de force set of NMR studies[195,196] showed that Pdx binding results in changes well removed from the expected Pdx binding site including the B ′, C, F, and G helices (Fig. 22). The B′ helix provides key contacts with the substrate while large movements of the F and G helices are the main features of the open/close transition.[153] Perhaps the most puzzling results are that oxidized Pdx binding to oxy-P450cam decreases the stability of the oxy complex 150-fold[197] while oxidized Pdx shifts oxidized P450cam to the low-spin state[198] which is an inactive complex since low-spin P450cam cannot be reduced by Pdx. The binding of reduced Pdx to oxy-P450cam results in the immediate formation of product at a rate that is orders of magnitude faster than the spontaneous decay oxy-P450cam with or without oxidized Pdx.[197,199] These sorts of changes are normally associated with a *destabilization* of the substrate binding pocket which many would conclude is just the opposite of what is required for a highly coupled and efficient P450.

The first crystallographic picture of what Pdx might be doing came from a particular mutant of P450cam, L358P, which mimics the effects of Pdx binding. That is, the L358P mutant exhibits spectral features similar to those induced by Pdx binding (Fig 22).[193] The crystal structure of the CO complex of the L358P provided a structural basis for these effects.[200] In wild type P450cam the binding of CO results in very few changes other than a slight repositioning of the substrate to make room for CO.[201] However, in the CO complex of the L358P mutant the I helix adopts the conformation observed in the wild type oxy complex. Thus the I helix opens up allowing the catalytic waters to move into place. The reason appears to be a “push” from the larger Pro358 side chain on the proximal surface of the heme which transmits movements to the distal pocket resulting in the deoxy to oxy conformational switch of the I helix. Another similarity between the L358P and the effects of Pdx is that like Pdx, the L358P oxy-complex is much less stable than the wild type oxy-P450cam and substrate hydroxylation in L358P can be supported by artificial reductants.[193] These observations have led to the idea that Pdx binding transmits changes to the distal pocket that lowers the activation energy barrier in the deoxy to oxy I helix transition and thus Pdx plays an effector role by helping to arm the catalytic machinery required for proton delivery and oxygen activation. It is possible that without proton transfer there can be no electron transfer so the effector role of Pdx is to stabilize the correct conformation for proton coupled electron transfer.

Obtaining the P450cam-Pdx crystal structure has been a long sought goal and recently a crosslinking approach has been used to trap the complex resulting in a 2.2 and 2.09Å crystal structure of the oxidized and reduced P450cam-Pdx complex, respectively.[166] This structure was followed by determination of the P450cam-Pdx NMR structure which agrees well with the crystal structures.[202] In the oxidized state P450cam adopts the open conformation with no substrate bound and a water molecule coordinated to the heme iron giving a low-spin complex which is consistent with earlier studies where both UV/Vis and resonance Raman studies showed that Pdx shifts P450cam to the low-spin form[198] which probably means substrate dissociates. This, of course, cannot be the active form since substrate is absent and Pdx cannot reduce low-spin P450cam. However, under turnover conditions where Pdx is in excess, reduced and/or oxy-P450cam will dominate. Thus the functionally relevant complex related to the effector role of Pdx is between the reduced proteins and not between the two oxidized proteins. The 2.09Å structure of the dithionite reduced complex still shows P450cam in the open conformation but substrate or product is bound. These crystals have 4 molecules in the asymmetric unit and 3 of the 4 have product bound and the remaining molecule has substrate bound. It appears that ET, O_2 activation, and hydroxylation occurred during data collection suggesting that the crystalline complex is active.

Interactions at the interface are consistent with NMR studies[196] and a wealth of mutagenesis data.[184,187,189,203–207] Pdx_{Asp38} interacts with $P450cam_{Arg112}$ (Fig. 23) which requires little movement in either protein in the vicinity of the ion pair. However, interactions involving Pdx_{Trp106}, which has been known for some time to be a critical residue,[182] require substantial motion (Fig. 23). Pdx_{Trp106} forms nonbonded contacts with $P450cam_{Ala113}$ and H-bonds with $P450cam_{Arg108}$ and $P450cam_{Asn116}$ all of which necessitates movement of the C helix up toward Pdx by about 2–3Å. This motion of the C helix is coupled to movements in the B′, I, F, and G helices, all of which are involved with substrate access or direct contacts with both substrates, camphor and O_2. This motion results in a large movement of the F and G helices and the F/G loop which effectively opens the active site to bulk solvent. This open conformation is basically the same as observed by Lee et al.[153] The main difference is that in the structure solved by Lee et al.[153] the B′ helix is disordered while in a complex with Pdx the entire P450cam is highly ordered and the key interactions between camphor and the local environment remain, by-and-large, unchanged from the closed conformation. The key driving force in the closed to open switch appears to be Pdx_{Trp106} which could not form tight interactions with P450cam without the structural switch.

How these changes are coupled to activity is illustrated in Fig. 23D and focuses on the I helix which forms part of the O_2 binding pocket. The switch in the I helix in going from the closed to open state requires that the H-bond between Thr252 and Gly248 be weakened which opens up the I helix. The transition to the oxy conformation is along the same trajectory and the opening of the I helix in the oxy-complex is about midway between the extremes of the open and closed state. As noted earlier, this opening is required to enable the catalytic waters to move into place for proton transfer to dioxygen.[208,209] It thus has been postulated[166] that the oxy conformer is along the same reaction coordinate as the closed-to-open transition and that Pdx favors binding to the open form of P450cam. It is important to note that the oxy-P450cam crystal structures probably do not represent the final “active” species for the following reason. As noted earlier, Pdx binding perturbs the oxy-P450cam spectrum and results in a 150-fold destabilization of the oxy complex.[197] It is very unlikely that this unstable form of oxy-P450cam was trapped in the crystal so what we see in the oxy-P450cam crystal structures is a snapshot prior to Pdx binding and further activation. Based on the P450cam-Pdx structure, it appears that this next step along the reaction coordinate when Pdx binds involves a further opening of the active site. In addition, Pdx alters the electronic properties of the Cys ligand.[197,198] The perturbation of the oxy-P450cam spectrum when Pdx binds has been attributed to a less electron rich Cys sulfur ligand when Pdx binds which promotes electron transfer from Pdx thus making it easier to reduce the heme iron. In the P450cam-Pdx structure there is a 0.2–0.3Å shortening of a peptide NH-sulfur H-bond which would be consistent with a change in the electronic properties of the sulfur ligand.

If this view is correct it predicts that those P450s that are less specific with respect to redox partner may not require the conformational gymnastics observed in P450cam. In other words, less specific P450s require less “help” from the redox partner in achieving the correct conformation for proton coupled electron transfer in O_2 activation. Unfortunately there is only one other oxy-P450 structure known: P450eryF.[210] Here O_2 binding causes no change in structure outside of solvent and P450eryF catalysis can be supported by non-native redox partners.[180] In addition, P450eryF has an Ala in place of the Thr252 found in P450cam so the I helix in P450eryF already is partially open. This, of course, is insufficient information to draw any sweeping conclusions but now there is a structural underpinning on the effector role of Pdx that can serve as a basis for designing additional experiments to test the interplay between redox partner binding, O_2 activation, and conformational states. The implications of the open form of P450cam possibly being the true active species is considered in the next section on mechanism.

3.5 Catalytic Mechanism

3.5.1. Introduction—The overall catalytic cycle of P450 is illustrated in Fig. 19. In the resting state the heme is hexacoordinate and low-spin. When substrate binds the axial aqua ligand and other water molecules occupying the active site pocket are displaced. This shifts the heme to high-spin but also increases the redox potential. This shift in redox potential ensures that electrons are transferred to only the substrate-bound enzyme. The electron donor is another protein, usually containing a flavin or FeS cofactor, whose redox potential is such that electron transfer is thermodynamically favored to the higher potential substrate-bound P450. This avoids the wasteful consumption of NADH/NADPH derived reducing equivalents being funneled into the substrate-free enzyme and released as peroxide or water. The non-productive formation of peroxide and/or water is usually referred to as uncoupling. Reduction of the heme iron by the redox partner enables O_2 to bind to the Fe^{2+} iron giving the oxy complex which is usually depicted as the ferric-superoxide complex (3 in Fig. 19). The second electron transfer event gives the peroxy intermediate which is protonated resulting in heterolytic cleavage of the O-O bond thus generating the active hydroxylating agent, Compound I. In the highly specialized P450s the substrate is held in position for precise regio- and stereo-selective interaction with the ferryl O atom in order to give the proper product. The process of “uncoupling” is when peroxide or water is released from the active site without giving product. The degree of uncoupling is most often measured by determining the ratio of NADPH/NADH consumed to product formed: a 100% coupled system consumes one NADH/NADPH per product molecule formed.

The proposed mechanism clearly parallels what we know about peroxidases and, indeed, the terminology (ie Compound I) and the requirement for protonation of the distal O atom are built on what had been learned from peroxidases. The problem with P450s, however, is that the intermediates shown in Fig. 19 were only inferred and not proven for quite some time. Now, however, most of the intermediates have been trapped and spectroscopically characterized. The first breakthrough was the use of cryogenic annealing methods coupled with EPR and ENDOR spectroscopy.[211] In this approach γ radiation is used to reduce frozen oxy-P450 followed by annealing to allow the reaction to proceed. In P450cam the first species observed is the hydroperoxy intermediate, Fe(III)-OOH^{1-}. After this only product is observed but not the dihydroperoxy, Fe(III)-OOH_2, presumably because as soon as the second proton is added to the distal O atom the O-O bond cleaves giving Compound I which immediately leads to product.

3.5.2. Compound I—What was most illusive is the trapping of Compound I. With the substrate present Compound I has only a fleeting existence so the only hope of observing Compound I was to use peracids to oxidize the Fe(III) substrate-free enzyme to Compound I. Stopped flow studies using *m*-chloroperbenzoic acid (*m*-CPBA) revealed a spectral intermediate very similar to what was expected for Compound I in both P450cam[212,213] and the thermophilic P450, CYP119[214]. The yields were low thus requiring singular value decomposition analysis to extract out the Compound I spectrum. While these studies strongly suggested that Compound I can be formed in P450, it still was not known if this species is active in substrate hydroxylation. This issue has been clarified with recent studies where the CYP119 Compound I yield was substantially increased thus enabling both Mössbauer and EPR spectroscopy to be used which unambiguously proved that the *m*-CPBA generated species is indeed Fe(IV).[215,216] Most importantly double mix stopped flow experiments showed that the *m*-CPBA generated Compound I is competent in substrate hydroxylation similar to the natural O_2-driven reaction.[215] Thus we no longer need to assume that a peroxidase-like Compound I intermediate is the active hydroxylating species in P450.

3.5.3. O_2 Activation—What remains a problem is the mechanism by which O_2 is activated. Again by analogy with peroxidases, the distal O atom must be protonated to ensure heterolytic cleavage of the O-O bond in order to give the ferryl Compound I species. This is where the analogy ends. A major difference between peroxidases and P450 is that in peroxidases the substrate, H_2O_2, enters the active site with protons while O_2 does not. The job of the peroxidase then is to properly redistribute the peroxide protons to promote O-O bond heterolysis which is the primary function of the distal His residue. With P450s the source of protons is solvent and there is no obvious traditional acid-base amino acid like His to assist with the proton shuttle process. As a result unraveling how P450s properly deliver protons has been a challenge. Once again most of what we understand derives from P450cam.

The crystal structure of oxy-P450cam provided the first structural insights into how water gets into the act of O_2 activation.[208,209] Fig. 24 provides a comparison between the resting ferric and oxy structures. In the resting state the Thr252 side chain OH donates an H-bond to the carbonyl O atom of Gly248. Gly248 thus cannot participate in a normal helical H-bond so the Thr252-Gly248 interactions result in a local disruption and widening of the I helix groove. When O_2 binds the Thr252-Gly248 H-bond breaks thus further widening the I helix groove which enables water to move into the active site and establish an H-bonding network with local protein groups. Another change involves the peptide group of Asp251. In the resting ferric state the peptide carbonyl has an odd conformation and is pointing nearly perpendicular to the I helix axis. However, when O_2 binds and the helix opens up, the Asp251 carbonyl flips into a normal helix H-bonding pattern. One of the new water molecules that moves into the active site directly H-bonds with O_2 and is thought to be the source of protons. Insights into why this structural change occurs when O_2 binds derives from the ferric-cyanide complex.[217] Cyanide induces the same structural change as O_2 but neither NO[218] nor CO[201] result in any significant I helical changes. Why? The one feature that O_2 and CN^- have in common is that the distal atom not linked to the iron carries a negative charge since the oxy complex is best described as ferric-superoxide, Fe(III)-OO^-. The I helix must open up to enable a water to move in and "solvate" *via* H-bonding the negatively charged ligand. A re-examination of the older T252A mutant structure which was solved well before the oxy complexes[219] provides some additional insights into I helix changes. Mutating Thr252 to Ala eliminates the Thr252-Gly248 H-bond and the I helix opens up just as it does in the oxy complex which allows the "catalytic" water to move in (Fig. 24). Thus simply breaking the Thr252-Gly248 H-bond is sufficient for the I helix to adopt the oxy-conformation.

Even before the oxy structures the close proximity of Thr252 to dioxygen implicated this residue in catalysis and was an early target for mutagenesis. The T252A mutant exhibited a major drop in the rate of product formation but not NADH oxidation.[188,220] This means that the T252A mutant is highly uncoupled most likely because the normal proton delivery system has been disrupted. The crystal structure of the T252A-oxy complex[209] is very similar to the wild type oxy structure so the waters required for dioxygen activation are in place. Thus the H-bonding interactions involving Thr252 are critical. The side chain Thr252 OH can be either an H-bond donor or acceptor. Its close proximity to the distal dioxygen O atom suggests that Thr252 should be an H-bond donor. However, an important *in vitro* mutagenesis study where Thr252 was replaced with methoxy-Thr showed that the enzyme retains about 30% activity but just as importantly remains fully coupled.[221] When the side chain OH is methoxylated it no longer can serve as an H-bond donor thereby suggesting that in the wild type enzyme Thr252 is an H-bond acceptor. Unfortunately in crystal structures one cannot normally resolve H atoms but the H-bond donor-acceptor relationship can be inferred as shown in Fig. 25. The key is the red catalytic water in Fig. 25. If we assume that this water donates an H-bond to dioxygen then the rest of the H-bonding donor acceptor

relationships fall into place. If this scenario is correct then there are two H-bond acceptors, Thr252 and Gly248, within about 3.0Å of the distal dioxygen O atom which should strongly promote protonation of dioxygen. Thr252 then serves as an H-bond acceptor to the hydroperoxy intermediate which also promotes the addition of the second proton.[209]

The other noteworthy residue that was targeted for mutagenesis is Asp251. The D251N mutant exhibits a two order of magnitude decrease in activity but remains highly coupled.[222] Such a mutant that remains coupled but exhibits much lower activity can provide considerable insight into mechanism and especially the rate limiting step. For example, the mutant exhibits a kinetic isotope effect of about 10 compared to 1.7 for wild type indicating that proton shuttling is altered in the mutant.[223] In addition, since the rate limiting step involving proton transfer has been slowed it was possible to capture a new intermediate, most likely the peroxy intermediate.[224] The crystal structure of the D251N mutant oxy complex provides a structural rationale for the decrease in activity.[209] In the oxy complex of this mutant the H-bond between Thr252 and Gly248 remains intact and the I helix does not undergo the structural change required for the catalytic waters to enter the active site. Thus proper proton delivery is substantially slowed which accounts for both the decrease in activity and kinetic isotope effects. Further support for the importance of water and protons derives from studies on Gly248 mutants.[225]

Two proposals have been put forward on the role of Asp251: one where Asp251 directly participates in the delivery of protons to dioxygen and the second is a structural role in the O_2-induced I helix structural change. A slightly modified version of the initial model proposed by Gerber and Sligar[222] is outlined in Fig. 26A. Here Asp251 serves the role of shuttling protons from bulk solvent to O_2 *via* a water molecule. The main problem with this model is Asp251 is tied up in salt bridges with Arg186 and Lys178 (Fig. 26C) and breaking these ion pairs so Asp251 could rotate into position would be energetically quite costly.[226]

The high energetic cost of moving Asp251 plus the D251N oxy-P450cam structure gave rise to a “mechanical” model.[209] In this model the Asp251 ion pairs constrain the I helix to open when O_2 binds in such a way that allows catalytic waters to enter the active site. In the D251N mutant the I helix is not so constrained and thus there is insufficient room for the catalytic waters to enter and activity is lost. Given that Asp251 is highly conserved one would think that its role in catalysis would be the same in most P450s. If so then recent work with P450cin places into question the mechanical model. Asp241 in P450cin corresponds to Asp251 in P450cam and the D241N mutant in P450cin shows that Asp241 also is essential for activity[227] but is not tied down by ion pairs and should be free to rotate into the active site. A way out of this apparent conundrum is if the open conformation of P450cam observed in P450cam-Pdx structure represents the active conformational state. In a complex with Pdx the Asp251 ion pairs are broken thus leaving Asp251 free to rotate into the active site. In fact, one of the favored rotamers would place Asp251 in an ideal position to H-bond with one of the active site waters found on the oxy-P450cam structure which, in turn, H-bonds with dioxygen (Fig. 26B). Thus Asp251 very likely does participate in the proton relay network as originally proposed[222] and computational approaches have shown that such a function of Asp251 is energetically feasible once the salt bridges to Asp251 are broken.[228] The main modification to the Gerber-Sligar model is to remove Arg186 and Lys178 from the mechanism and have Asp251 rotate in and out of the active site so it can shuttle protons from bulk solvent to dioxygen. This, of course, requires that the active form of P450cam is closer to the open conformation observed in the P450cam-Pdx crystal structure.[166] This also provides an explanation for an effector role of Pdx since Pdx favors binding to the open form of P450cam which, unlike the closed form, has Asp251 available for catalysis.

3.5.4. Substrate Hydroxylation—The generally accepted mechanism for substrate hydroxylation is the radical rebound mechanism initially proposed by Groves.[229] In this mechanism Compound I abstracts an H atom from the substrate leaving a carbon radical followed by radical recombination to give the C-OH product. However, it also is possible to obtain a cationic intermediate or to have a concerted mechanism. To differentiate between the possible mechanisms of C-OH bond formation, cyclopropyl radical clocks have been developed[230–232] (reviewed in[233]). Knowing the rate of ring opening in a strained ring of a substrate, such as cyclopropyl, together with product analysis, can provide information on the mechanism of C-OH bond formation. For example, formation of a radical α to the ring could result in ring opening thus generating predictable products. A concerted mechanism, however, would not allow ring opening. Generally these experiments support the radical rebound process[234] although experiments with different P450s and other substrates indicate a cationic intermediate rather than a radical.[235] Another complication is that ultrafast radical clocks are not consistent with a radical mechanism.[236] Density functional calculation (DFT) calculations[237,238] have provided important insights that help to clarify some of the complications in the interpretation of radical clock experiments. The key result is that the process of C-OH bond formation is dependent on spin state of the ferryl center. In the low spin state there is no energetic barrier to radical recombination so the reaction is effectively concerted. In sharp contrast, there is a substantial barrier in the high spin state so here the reaction proceeds in the more traditional stepwise fashion. This difference between a concerted and stepwise process, both of which use Fe(IV)O, can give different product profiles as well as deceptively short estimates of radical lifetimes. While not totally resolving some of the complexities surrounding the radical clock experiments, the concerted vs. stepwise mechanisms using the traditional Fe(IV)O Compound I intermediate with the added feature of spin state does provide a picture of substrate hydroxylation consistent with much of the experimental data.

3.6. P450 Fold but Non-P450 Chemistry

3.6.1 P450nor—There now are a few examples of enzymes that exhibit the P450 fold but do not catalyze P450 chemistry. The best known of these is P450nor from the fungus *Fusarium oxysporum* that catalyzes the NADPH/NADH supported reduction of NO to N_2O.[239–242] The heme iron does not go through a redox cycle but remains Fe^{3+} throughout the catalytic cycle so its main function is to coordinate one of the two NO molecules required to generate N_2O. P450nor exhibits the typical P450 fold.[243] NADH binds to an open P450nor active site channel and delivers both reducing equivalents to the bound NO molecules but so far it has not been possible to obtain a structure of the P450nor-NADH complex. However, a cluster of positive charges near the B′ helix region looks to provide an ideal place for binding the negatively charge phosphate esters of NADH/NADPH.

3.6.2 P450BSβ—Another example is P450BSβ, a peroxidase from *Bacillius subtilis*.[244] This enzyme catalyzes the hydroxylation of fatty acids but uses H_2O_2 as the oxidant and the iron remains Fe^{3+}. As shown in Fig. 27, P450BSβ exhibits the typical P450 fold. Unlike another fatty acid oxidase, P450BM3, where the carboxyl end of the fatty acid extends out of the active site, in P450BSβ the carboxyl end enters the active site and ion pairs with Arg242 in the I helix. This has led to the interesting proposal that the substrate carboxyl group serves the same acid-base catalytic function as the distal His in peroxidases and the resulting Compound I hydroxylates the substrate similar to other P450s. Thus we have a possible example of substrate assisted catalysis.

3.6.3. Prostacyclin Synthase—Prostacylin (PGI2, Fig. 28) is a member of the potent bioactive eiscosanoid family of signaling molecules derived from fatty acids. PGI2 inhibits platelet aggregation, is an important vasodilator[245], and is used commercially as a

pulmonary hypertension drug known as epoprostenol. The formation of PGI2 is part of the complex arachidonic acid metabolic machinery but the immediate precursor is prostaglandin H2 (PGH2) which is converted to PGI2 by prostaglandin synthase (PGIS) in a non-redox isomerization reaction (Fig. 28). PGIS exhibits the classic P450 fold[246] but does not catalyze classic P450 chemistry (Fig. 28). The mechanism proposed by Hecker and Ullrich[247] is outlined in Fig. 28A. The PGIS heme coordinates specifically to one of the PGH2 oxygen atoms resulting in homolytic cleavage of the O-O bond and oxidation of the iron from Fe^{3+} to Fe^{4+}. This initiates the isomerization reaction resulting in the formation of PGI2. The structure of PGIS complexed with the substrate analog, U51605 (Fig. 28B), provided some interesting insights into an unusual mechanism for controlling the reaction. U51605 is very similar to PGH2 except nitrogen replaces oxygen resulting in tight coordination of one N atom to the heme iron thus providing a snaphot of the enzyme-substrate complex. In going from the substrate-free to -bound complex the heme itself shifts about 2Å (Fig. 28B). In the ligand/substrate-free state steric crowding around the heme iron would prevent other ligands from coordinating to the heme iron. Only when the correct substrate binds will the heme shift thus allowing coordination of the substrate resulting in the radical mediated isomerization reaction. The role of heme motion is, therefore, to prevent the substrate-free structure from interaction with other non-substrate ligands that could potentially initiate destructive radical chemistry.[247] One way to envision the heme switch process is a simple equilibrium between the substrate-free and -bound forms (Fig. 29). In the substrate-free state the water coordinated to the heme iron H-bonds with neighboring residues, Asn277 and the carbonyl oxygen of Val273. When the heme slides out one heme propionate now can interact with Arg339 and Gln94. As with many protein equilibria, weak interactions, in this case H-bonds, are lost in one state but formed in the next state. In the absence of substrate the substrate-free form dominates but in the presence of substrate the substrate-bound form is captured thus shifting the equilibrium toward the substrate-bound state.

3.6.4. Allene Oxide Synthase (AOS)—AOS is a plant enzyme that converts alkyl hydroperoxides to allene oxides.[248] Initial purification and characterization showed that AOS is a P450 enzyme (CYP74A)[249] and the subsequent crystal structure of *Arabidopsis*[250] and *Parthenium argentatum*[251] AOS demonstrated that, as expected, AOS has the P450 fold. The reaction mechanism shown in Fig. 30 is based on biochemical studies reviewed in[248] and the AOS crystal structures. The enzyme promotes homolytic cleavage[252] of the substrate peroxide O-O bond giving the ferryl Fe(IV)-OH with no porphyrin radical, or Compound II. The fate of the enzyme generated substrate radical can go one of two ways illustrated in Fig. 30. In CYP74A (AOS) the radical reduces Fe(IV)-OH leaving a carbocation followed by removal of a proton to give the final allene oxide product.[248] Importantly, in CYP74B both substrate O atoms are retained in the product[252] so CYP74B undergoes a P450-like radical rebound mechanism. This mechanism where the radical forms on C13 is most consistent with the crystal structures since C13 would be positioned close to the ferryl O atom (Fig. 30).

4. Nitric Oxide Synthase

4.1. Introduction

Nitric oxide synthase catalyzes the oxidation of the simple amino acid, L-arginine, to L-citrulline and nitric oxide (NO).

NO is an important signaling molecule in the cardiovascular, immune, and nervous systems.[253,254] NO binding to the heme of guanyl cyclase activates the enzyme which converts GTP to cyclic GMP, the final signaling molecule leading to various physiological effects.[255] When the first NOS sequences became available it was clear that the C-terminal half of the molecule closely resembles cytochrome P450 reductase,[256] the diflavin protein

that transfers electrons to the P450 heme. It later was shown that the N-terminal half of the molecule binds heme and the reduction in the presence of CO gives the 450 nm absorption band characteristic of P450s[257–259] although there is no sequence homology with P450s. The architecture of NOS is thus similar to P450BM3 wherein the C-terminus of the heme domain is linked to the N-terminus of the diflavin reductase thus providing a catalytically self sufficient oxygenase. Ca^{2+}-calmodulin activates NOS by binding to the linker segment connecting the heme and reductase domains.[260] Regulation is at the level of electron transfer and it appears that calmodulin binding favors a conformation where electron flow from the flavins to heme is most efficient. NOS dimerizes through the heme domains and the FMN from subunit A of the NOS homodimer transfers electrons to the heme of subunit B.[261] An unusual feature of NOS is the requirement for the cofactor, tetrahydrobiopterin or BH4.[262]

4.2. NOS Structure

Mammals produce 3 NOS isoforms: endothelial NOS (eNOS, cardiovascular system), neuronal NOS (nNOS, nervous system), and inducible NOS (iNOS, immune system). The crystal structures of the heme domain for all 3 isoforms have been determined.[263–266] Despite the similarity in spectral properties and the same Cys heme ligation, the architecture of NOS is totally different than P450s (Fig. 31). Rather than having helices define the substrate entry channel as in P450s, the heme is surrounded by more rigid beta structure. In addition, the heme is relatively exposed to solvent without the need for large open/close motions as in P450s. Thus the substrate can easily diffuse into the active site and, more importantly, the product, NO, can easily depart.

As in P450s the substrate is held in place such that the atom to be hydroxylated is positioned close to the heme iron. While nonpolar P450 substrates are anchored in place *via* nonpolar interactions, the more polar L-arginine H-bonds with neighboring protein groups and one heme propionate. The local architecture around the Cys ligand is quite different than in P450s although like P450s the Cys accepts an H-bond from a nearby NH group (Fig. 31). In P450s this is a peptide NH group while in NOS it is the indole NH of a Trp residue. The essential cofactor, BH4, is positioned at the dimer interface where it H-bonds with the same heme propionate that H-bonds with the substrate. Unlike other pterin-containing enzymes where BH4 undergoes a two electron redox cycle and must dissociate from the enzyme for reduction, in NOS BH4 is permanently bound and serves as an one-electron donor in the O_2 activation process,[267–269] a topic to be discussed in the next section.

4.3. Mechanism

NOS catalysis proceeds in two steps. The first step, conversion of L-arginine to N^{ω}-L-hydroxyarginine (L-NHA), is generally thought to proceed as a traditional P450 reaction. The main difference is that BH4 serves as the source of the electron required to reduce the oxy complex to the peroxy level[267–269] to form a cationic pterin radical.[270] Presumably the radical is reduced back to BH4 by the flavin reductase.

The second step of the reaction, the oxidation of L-NHA to L-citrulline and NO, has been more challenging to unravel. However, data from several sources are consistent with one of two mechanisms shown in Fig. 32. Early questions centered on whether or not the traditional compound I oxyferryl or a peroxy species is the active oxidant. The stoichiometry of this second step, however, requires only one electron which is inconsistent with a compound I mechanism so mechanistic proposals have centered on a peroxy/superoxy species as the active oxidant. In both mechanisms shown in Fig. 32 the first question to address is which L-NHA hydrogen atom is abstracted from the iron-linked oxidant. In theory either the OH or NH can donate an H atom. However, two NHA analogues, N-*tert*-butyloxy-L-arginine and N-(3-methyl-2-butenyl)oxy-L-arginine that have no H atom attached to the oxygen, are

substrates[271] thus favoring the N-radical mechanism (Fig. 32). Crystal structures[272,273] and ENDOR[274] studies are consistent with the NH group of L-NHA being close enough to interact with the proximal O atom directly linked to the iron (Fig. 32). This has the added effect of preventing heterolytic cleavage of the O-O bond. The ferric-peroxy intermediate shown in Fig. 32 also is known to be the first observed intermediate after cryo-reduction of the oxy complex.[275]

In the non BH4 radical mechanism the proximal O atom of the oxy complex abstracts an H atom from L-NHA to give the hydroperoxy species.[271] The cyclic intermediate collapses to give products. In the BH4 radical mechanism the oxy complex does not abstract the L-NHA H atom but instead BH4 reduces the oxy complex to the peroxy intermediate followed by formation of the cyclic intermediate. This intermediate collapses to give NO^- and L-citrulline. A BH4 radical does indeed form during the oxidation of L-NHA but at the end of the reaction cycle the radical is reduced back to BH4.[268] What remains unknown is how the BH4 radical is reduced. Forming NO^- as shown in Fig. 32 balances the electron count but the precise mechanism of back electron transfer to the BH4 radical remains an open question.

4.4. Calmodulin Regulation of NOS Activity

The constitutive NOS isoforms, eNOS and nNOS, are regulated by Ca^{2+}-calmodulin (CaM)[260] by controlling NOS at the level of electron transfer. Binding of CaM to the linker peptide connecting the heme and FMN domains triggers a structural change that enables electrons to flow from FMN to heme (Fig. 33). The structure of the nNOS reductase domain[276] and the iNOS FMN domain in a complex with calmodulin[277] have been determined (Fig. 34). The reductase domain closely resembles P450 reductase[170] especially in the positioning of the FMN and FAD which form direct nonbonded contacts in both structures. This means that the FMN domain must swing away from the FAD domain in order to properly dock to the heme domain for electron transfer and somehow CaM binding to the linker connecting the heme and FMN domains triggers this movement. The FMN-CaM structure provides some important insights into the CaM induced changes and has identified key differences between iNOS, which binds CaM more tightly, and the constitutive isoforms, eNOS and nNOS.

A simple diagnostic for the conformational change is FMN fluorescence.[278,279] When CaM binds FMN fluorescence dramatically increases (Fig. 35) which has been attributed to greater solvent exposure of the FMN as it breaks away from the FAD module. A particular mutant of nNOS reductase where Gly810 was deleted has shed further light on the CaM induced changes.[280] This mutant was designed to flip the redox potentials of the FMN semiquinone and hydroquinone (Fig. 36A). Like P450 reductase, it is the fully reduced FMN hydroquinone (Fig 36A) that is the electron donor to the heme since the hydroquinone exhibits a lower potential than the semiquinone. In P450BM3, however, it is the one electron reduced red anionic semiquinone that has the lower potential.[281] In P450BM3 the FMN loop region is missing this Gly residue (Fig 32C) which enables the peptide NH of Asn537 (Fig. 36C) to donate an H-bond to N5 of FMN which should help stabilize the red anionic semiquinone. By removing Gly810 from the FMN module in nNOS, it was reasoned that the FMN binding loop would resemble that of P450BM3 and indeed, the redox potentials of the semiquinone and hydroquinone flipped.[280] Moreover, CaM has little effect on fluorescence (Fig. 36B) indicating that in the mutant the connection between the FMN and FAD modules has been loosened. This explanation seems reasonable since the Asn811-Glu1392 H-bond between the FMN and FAD modules is very likely lost in the ΔGly810 mutant (Fig. 36D).

A more sophisticated analysis of FMN fluorescence lifetimes as a function of CaM presents a more complex picture.[282] In the absence of CaM the FMN in holo-nNOS exhibits complex

lifetime kinetics with three lifetimes of 90ps, 0.9ns, and 4ns with the 90ps state accounting for about 70% of the amplitude. In the presence of CaM, the 0.9 and 4ns states increase at the expense of the 90ps state. In the ΔGly810 only 5% of the lifetime data can be accounted for by the 90ps state supporting the previous conclusions that this mutant favors the more open state even in the absence of CaM. Such complex kinetics argue for an ensemble of CaM-sensitive conformational states rather than simple two open/closed states in rapid equilibrium.

Since the main role of CaM is to promote FMN-to-heme electron transfer, it is highly desirable to study this ET event alone. This becomes complicated since electrons must flow from NADPH to FAD and then to FMN so isolating the FMN-to-heme ET reaction is difficult. This has been partially overcome by removing the FAD domain altogether. This approach worked well with P450BM3 where laser flash photolysis methods enabled a detailed study of just the FMN-to-heme ET reaction.[172] P450BM3 has the great advantage that it is the one electron reduced FMN semiquinone that delivers an electron to heme. As a result, it is straightforward to use laser photoreduction methods to generate the one electron reduced FMN semiquinone. The situation is not so simple with NOS since it is the fully 2 electron reduced hydroquinone, $FMNH_2$, that is the ET donor to heme. The trick then becomes one of how to generate $FMNH_2$ using laser-induced one electron reductants. Feng et al. have worked this out using the method outlined in Fig. 37.[283,284] The FMNH• Fe(II)-CO is formed using steady light illumination of the heme-FMN NOS construct in the presence of deazariboflavin, a sacrificial electron donor like semicarbazide, and CO. The light induced reduction of deazariboflavin generates the semiquinone radical, a powerful reductant, that reduces the iron which, in the presence of CO, forms Fe(II)-CO while the FMN is reduced to the semiquinone. This is followed by a 450 nm laser flash which dissociates the CO. The free Fe(II) has a low enough redox potential to reduce the FMN semiquinone which leads to the following reversible intramolecular electron transfer

This enables the measurement of the desired rate constant from $FMNH_2$ to Fe(III). The rate increases from $22s^{-1}$ in the absence of CaM to $262s^{-1}$ in the presence of CaM.[284] This approach also can be useful in estimating electron transfer distances[285] which agree well with the 18.1Å distance between the $FMNH^{\cdot}$ semiquinone and Fe(III) estimated from EPR methods.[286]

To piece all of this together, of course, requires the structure of holo-NOS which has yet to be achieved. Cryo-electron microscopy[287] has been used to generate low resolution structures of CaM-free and -bound eNOS. Structures are derived by fitting crystal structures of the individual modules into the EM data. The heme domain fits well but the reductase domain, especially in the absence of CaM, exhibits substantial mobility. Even so the EM data are consistent with mutagenesis data that suggest a positive patch (Fig. 38) on the backside of the heme for FMN module docking.[288] “Eye-ball” docking of the nNOS FMN module to this region of the heme domain in nNOS gives a FMN edge-to-iron distance of about 18Å which is basically the same as the distance obtained from EPR.[286] One possible problem with this view is the involvement of BH4 in electron transfer. As noted in the last section, the transfer of an electron from BH4 to oxy-P450cam is required for activity and presumably the missing BH4 electron is replenished from the reductase FMN. This would mean the electron transfer from the FMN would have to pass through the heme to the BH4 radical rather than the FMN domain docking to some other site where the FMN-BH4 distance would be shorter. This may not be much of a problem since the BH4 is H-bonded to a heme propionate thus providing a fairly tight electron transfer circuit even if the FMN-BH4 distance is quite long. Very recently deuterium exchange and mass spec methods[289] have been used to map out which regions of the FMN and heme domains interact and is the most detailed picture to date of a NOS electron transfer complex. The region of the heme

domain predicted to interact with the FMN domain is the same as that illustrated in Fig. 38. An added level of detail is that CaM also is predicted to interact with the heme domain and so CaM not only promotes the required change to reorient the FMN domain but also provides contacts with the heme domain.

5. Chloroperoxidase

Although the biological role of chloroperoxidase (CPO) from the slime mold *Caldariomyces fumago* is to catalyze the chlorination of organic compounds,[290–292] CPO is one of the most versatile heme enzymes owing to its ability to catalyze P450, peroxidase, and catalase type reactions (Fig. 39). For many years CPO was the only known peroxidase that exhibits P450-like spectral properties owing to a Cys residue serving as one axial heme ligand exactly as in P450 and NOS. However, similar enzymes now have been found in other organisms.[293]

CPO has been described as a peroxidase-P450 hybrid although the overall structure of CPO has no similarity to either peroxidases or P450s. The main similarity with P450 and NOS is that the Cys ligand accepts an H-bond from a nearby NH group. However, the distal pocket is much more peroxidase-like in that the distal pocket is polar and provides an acid-base catalytic group that promotes heterolysis of the peroxide O-O bond. With CPO, however, this group is a Glu (Fig. 39) rather than His. As a result, the optimal pH for CPO activity is near 3.[294] Like peroxidases CPO forms Compound I[295] and the mechanism of Compound I formation is basically the same as traditional heme peroxidases except the active sight Glu replaces the distal His.[296,297] Since the biological function of CPO is to chlorinate compounds, the Compound I oxidizing equivalents are used to convert Cl^- ions into a chlorinating agent such as HOCl. Whether or not the chlorination reaction takes place in the active site has been actively debated but the weight of evidence favors a non-enzymatic process that occurs outside the active site.[298]

CPO also exhibits P450-like behavior and can catalyze the oxidation of a variety of molecules (reviewed in[299]). Of particular note is the ability of CPO to catalyze enantio-selective reactions such as epoxidations.[300] As shown in Fig. 39, CPO has a small opening above the distal pocket bracketed by Phe residues that provides the docking site for small organic substrates including its natural substrate, cyclopentanedione.[301] Modeling studies[296] indicate that the asymmetry of the active site nicely explains the known enantio-selective epoxidation reactions catalyzed by CPO. CPO, however, also operates as a traditional peroxidase and the pattern is for large substrates that cannot gain access to the active site to undergo peroxidase-like H atom abstraction at the molecular surface.[302]

6. Differences Between Peroxidases and P450

6.1. Introduction

Since the reactive intermediate in both P450s and peroxidases is called Compound I, it is sometimes assumed that this is the same species in both enzymes. However, peroxidases do not catalyze the insertion of oxygen into C-H bonds while P450s do not catalyze peroxidase-like electron transfer reactions. One view holds that part of the difference is due to steric hindrance in peroxidases which prevents the close approach of substrate to the Fe(IV)=O center while P450s have substrate binding pockets directly adjacent to the reactive ferryl intermediate. The problem with this scenario is that if the reactivity of Fe(IV)=O were basically the same in both enzymes, then one might expect the peroxidase Compound I to attack nearby amino acid residues or exhibit a fleeting existence owing to such high reactivity. Neither of these is true which means that the reactivity of the Fe(IV)=O intermediate is profoundly different in peroxidases and P450s. Clearly the protein environment tunes Fe(IV)=O reactivity.

6.2. Distal Pocket Differences

We first focus on the distal side of the heme. In peroxidases the distal pocket is polar owing to the active site Arg and His while in P450s the pocket is considerably more nonpolar. While the job of both enzymes is to heterolytically cleave the O-O bond, they do so by substantially different mechanisms. As noted earlier, peroxidases utilize a His for acid base catalysis to redistribute the protons that are part of the H_2O_2 substrate. P450s, however, utilize an H-bonded water network to shuttle protons from bulk solvent to dioxygen. The structure of peroxidase Compound I also shows that the ferryl O atom is surrounded by H-bond donors one of which is the distal pocket Arg.[37,38] This suggests that the ferryl O atom is acidic and not protonated which is further supported by the short Fe(IV)=O bond.

EXAFS work on CPO Compound II indicates a 1.82Å Fe(IV)-O bond while Raman data shows an isotope dependent Fe-OH stretch,[303] both consistent with a protonated ferryl O atom (Fig. 40). This has important implications for the traditional oxygen rebound mechanism of P450s.[304,305] If the ferryl O atom abstracts an H atom from the substrate, then the strength of the ferryl O-H bond must be large enough to overcome the barrier of breaking the substrate C-H. The higher the pKa and the higher the redox potential the stronger the O-H bond. This relationship can be quantitated by the following equation.[306]

$$\text{strength of O}-\text{H bond} = 1.37\Delta \text{pK}_{\text{OH}} + 23.06\Delta \text{E}_{\text{ox}} + 57.2 \pm 2 \quad (1)$$

Using reasonable estimates of the Compound II redox potential, the pKa needs to be about 8.2 to have sufficient O-H bond energy to overcome the barrier of breaking the substrate C-H bond.[303] By contrast the pKa of the peroxidase Compound II ferryl O atom in HRP is less than 3.5[307] and thus cannot as effectively insert into a C-H bond.

6.3. The Proximal Ligand

If only adjustments around the distal pocket are required to convert a peroxidase into a P450, consider the energetic cost. If pKa is indeed correlated with reactivity,[303] the peroxidase ferryl O atom pKa would need to increase from about 3.5 to 8.2, an approximate 6.4kcal/mol change. This adjustment should be within reach of distal local electrostatic effects. If the ferryl O atom in peroxidases carries a negative charge, then the more polar P450-like substrate pocket would favor a higher pKa. However, the Fe-O bond distance also is a key parameter and the short bond found in peroxidase Compound I favors the lower pKa. The next most obvious place to look for what controls ferryl reactivity is the proximal ligand, His in peroxidase and Cys in P450s. It was recognized early on that the P450 Cys ligand could provide an extra electron “push” effect[308] that transfers electron density to the iron thus promoting O-O bond cleavage and modulate the reactivity of Compound I. Mutagenesis is one obvious approach to probe the role of the proximal ligand. Would replacing the proximal His ligand convert a peroxidase into a P450? Unfortunately, results from such mutagenesis experiments have proven difficult to interpret. The first problem is steric. Cys is too short to properly substitute for His and cannot effectively reach the heme iron without considerable conformational adjustments. The first attempt at replacing the His ligand in peroxidase with Cys resulted in the oxidation of Cys to cysteic acid with one of the cysteic acid oxygen atoms coordinated to the heme iron.[28] A second attempt which involved the introduction of one additional mutation resulted in the successful replacement of His with Cys that was able to coordinate the heme iron[309] although this mutant has not been enzymatically characterized. Another problem, however, is second sphere effects owing to the local environment. In P450s the Cys ligand has nearby H-bond donors which is a universal property of iron-sulfur proteins and helps to attenuate and increase the redox potential of the iron.[148] In sharp contrast, the His ligand in peroxidases donates an H-bond

to a buried Asp which decreases the redox potential and thus the second sphere environments are nearly opposite in peroxidases and P450s. To properly model the P450 ligand environment thus requires much more than a simple swapping of ligands.

Here is where density functional and QM/MM calculation have provided important insights. In general the various calculations support the stronger “push” effect of the Cys ligand compared to His in peroxidases as being a key factor in understanding the differences in Compound I reactivity. In P450 Compound I models substantial spin density is localized on the sulfur ligand rather than the porphyrin and the S-Fe bond distance increases.[310–312] However, QM/MM approaches indicate that the surrounding protein environment, especially H-bonding to the Cys sulfur, moves the spin density back to the porphyrin and decreases the length of the S-Fe bond by as much as 0.1Å.[312] This enhances the strong push of the Cys relative to His and favors a mixing of the two Compound I resonance forms (Fig. 41) relative to peroxidases.[313] As a result P450s are not very good electron acceptors compared to peroxidases. At the simplest level the difference in peroxidase and P450 Compound I reactivity comes down to three factors: 1) the strong push of the Cys ligand in P450 decreases the ability of Compound I to serve as an electron acceptor; 2) the Cys push helps to increase the Fe-O bond length which contributes to increasing the pKa of the ferryl O atom in Compound II thus increasing the H atom abstraction ability of Compound I and; 3) the greater polarity of the peroxidase distal pocket compared to P450 lowers the proton affinity of the ferryl O atom in peroxidases relative to P450s.

7. Heme Oxygenase

7.1. Introduction

The degradation of heme proteins results in the release of toxic free heme and thus it is imperative not to allow its accumulation. Hemoglobin is the main source of heme and approximately 6–8 gms of hemoglobin are degraded daily thus releasing about 300mg of heme per day. Since free heme is not re-utilized, it must be degraded and the iron released and stored for further use. The enzyme responsible for heme degradation is heme oxygenase or HO[314,315] which was first described in the late 1960s.[316,317] The final product of HO-mediated heme degradation is biliverdin (Fig. 42) which is converted to bilirubin by bilirubin reductase.[316] Mammals contain two isoforms, HO-1 and HO-2, that are differentially regulated and have different biological roles. The primary function of HO-1 is in heme catabolism while HO-2 has been postulated to generate CO as a messenger molecule[318–320] and possibly plays other important roles. For example, HO-2 is involved with the calcium dependent potassium channels which are inhibited by hypoxia and thus are O_2 sensitive.[321] Mammalian HO is anchored to microsomal membranes *via* a C-terminal membrane segment and the soluble active enzyme can be released by mild proteolysis.[322] Mechanistic studies on HO were greatly facilitated by the cloning and expression of the truncated form of human HO-1 lacking the C-terminal membrane anchor[323] and the discovery of bacterial HOs[324–326].

7.2. Structure

Human HO-1 was the first heme oxygenase structure reported in 1999.[327] Since then there have been several other proteins called heme oxygenases whose structures have been solved but here we confine the discussion to those HOs that are structurally related to human HO-1. These include a small handful of bacterial HOs[328–330] rat HO[331], and human HO-2.[332] The overall fold of these HOs is unique and not shared with other known protein structures. The heme is sandwiched between the proximal and distal helices (Fig. 43) with His serving as an axial heme ligand. The distal helix consists of a Gly-rich segment just over the heme whose flexibility is likely to be important for function. Unlike other heme enzymes discussed thus

far the heme itself is the substrate for HO and as a result active site flexibility is likely required for substrate binding and product release. Most HOs are selective for oxidation of the *α-meso* heme carbon (Fig. 42) although *P. aeruginosa* HO oxidizes the *δ-meso* position (Fig. 43).[333] A comparison between the bacterial and human HOs provides a fairly simply picture on what structural features control which carbon is oxidized (Fig. 43). In HO-1 a cluster of basic side chains, Arg179, Arg183, and Lys18 interact with the heme propionates. In *P. aeruginosa* the only basic side chains available for propionate interactions are Lys132 and Arg154 which requires about a 100° rotation of the heme relative to its position in HO-1. This places the *δ-meso* carbon in the bacterial HO in the same position as the HO-1 *α-meso* carbon. In both HOs the *meso* carbon to be hydroxylated is pointing toward the back of the active site pocket and exhibits far less steric crowding than the remaining 3 *meso* carbons and thus is the only one available for reaction.

7.3. Mechanism

The mechanism of HO has been covered in some recent reviews[334–336] and here we provide the main highlights. Much of the early attention focused on the first step of the reaction (Fig. 42) which is the formation of α-*meso*-hydroxyheme. P450 reductase serves as the biologically relevant source of electrons to reduce the heme iron thus enabling O_2 to bind. The first question to be addressed was whether or not HO proceeds like P450 to form Fe(IV)=O which then serves as the active oxidant. Since HO uses His as an axial ligand and in light of our earlier discussion on the differences in reactivity between Fe(IV)=O in peroxidase and P450 and the role that the distal ligand plays, it is unlikely that Fe(IV)=O in HO could serve as the oxidant. Moreover, the ferryl O atom is simply too far from the α-*meso* heme carbon without some very unlikely distortions of the heme ring. The key experiments showing that Fe(IV)=O is not involved utilized artificial oxidants. Akyl and acyl hydroperoxides form Fe(IV)=O but do not support HO catalysis while H_2O_2 does support catalysis.[337,338] A second key experiment showed that addition of ethylhydroperoxide to HO results in ethoxylation of the α-*meso* heme carbon.[339] Finally, it was shown that HO Compound I formed with *m*-chlorperbenzoic acid could not hydroxylate the heme.[340] These results led to the mechanism shown in Fig. 42. The crystal structure of the oxy complex of a bacterial HO[341] supports this mechanism since the Fe-O-O angle of 110° is substantially more acute than in other heme proteins thus placing the distal O atom about 3.6Å from the *α-meso* heme carbon and presumably the hydroperoxy intermediate is similar. Cryo-reduction methods enabled trapping and EPR/ENDOR characterization of the hydroperoxy intermediate thus proving that this species immediately precedes formation of product.[342–344] The mechanism in Fig. 42 suggests a concerted reaction that forms a tetrahedral intermediate in the transition state which is consistent with kinetic isotope effects.[342,345] However, computational studies suggest that the more energetically feasible path is homolytic cleavage of the O-O bond resulting in the addition of the $HO^{\cdot}$ radical to the α-*meso* carbon.[346,347]

As in P450 and peroxidase, HO must properly deliver protons to dioxygen once bound to the heme in order to promote cleavage of the O-O bond. Initially it was thought that an Asp residue in the distal pocket of human HO-1 might be the key catalytic group but this residue is not conserved and is unlikely to be a key player in the O_2 activation process.[334,335] One current view holds that the intricate H-bonded network of water in the active site found in all high resolution HO structures is the key to proper proton delivery to the iron-linked dioxygen.[336] The precise nature of the amino acids at the active site thus is less important than the H-bonded water network. What remains an open question is whether or not the hydroxylation reaction is a concerted process or proceeds *via* heterolytic cleavage of the O-O bond.

The next step in the reaction is conversion of α-*meso* hydroxyheme to verdoheme. There has been a minor controversy on whether or not Fe^{3+} must first be reduced to Fe^{2+} *via* an external electron donor.[348,349] There is complete agreement that Fe^{2+} is required to bind O_2 but since one of the resonance structures of α-*meso*-hydroxyheme has Fe^{2+} and a radical (Fig. 42) an external source of electrons may not be required. Indeed, a g = 2.004 has been observed when O_2 is added to an anaerobic solution of HO-1-α-*meso* hydroxyheme which has been attributed to a porphyrin radical.[348] It does appear, however, that prior reduction of Fe^{3+} is not strictly required for the conversion of α-*meso*-hydroxyheme to verdoheme.[350,351] The situation may be quite different under more *in vivo*-like turnover conditions where there is an abundance of reducing power available. Different mechanisms developed for both views thus may be equally valid depending on experimental conditions. Despite the controversy, the role of the protein may be minimal since the conversion of hydroxyheme to verdoheme is a spontaneous process in the presence of O_2.[352]

The final step, verdoheme to biliverdin, has proven to be the most difficult to unravel. An early observation that limits possible mechanisms is that the two oxygen atoms in the biliverdin product derive from two different O_2 molecules.[353] In addition, verdoheme can be converted to biliverdin by either H_2O_2 or O_2 and it is conceivable that both processes operate *in vivo* but here we consider the O_2 pathway. A recent combination of crystallography and QM/MM calculations have provided the most recent details (Fig. 42).[354] Cleavage of the O-O bond results in the addition of the distal O atom to the porphyrin ring leaving behind a Compound I-type intermediate that is subject to attack by an active site water/hydroxide. This initiates the process of ring opening followed by electron transfer to give the final biliverdin product. Essential to this mechanism is a cluster of highly ordered active site water molecules that were visualized in the crystal structure of the HO verdoheme-azide complex as a reasonable mimic for the verdoheme-oxy complex.[354] These waters provide the proton relay network required to enable the critical step of hydroxide attack.

8. Indoleamine 2,3-Dioxygenase (IDO) and Tryptophan 2,3-Dioxygenase (TDO)

8.1. Introduction

IDO and TDO are soluble heme enzymes that catalyze the conversion of L-Trp to N-formylkynurenine (Fig. 44), the first step in L-Trp metabolism *via* the kynurenine pathway. Studies with these enzymes date back to the 1930s[355] and for some time the naming of these enzymes as tryptophan pyrrolase or tryptophan peroxidase-oxidase[355–358] caused some confusion but eventually these were recognized as dioxygenases. In the past few years IDO and TDO have been recognized as important players in various cancers.[359] Tryptophan has long been known to be involved in maintaining a strong immune response[360] and as a result, tumor cells that catabolize tryptophan generate a local immunosupressive environment. Therefore, IDO and TDO have emerged as potential therapeutic targets. A comprehensive review on structure-function relationships up to 1996 appeared in Chemical Reviews[361] and a more recent update was published in 2011[362] so here we briefly summarize the most recent findings.

8.2. Structure and Mechanism

It was only in the past few years that recombinant expression systems were developed for TDO and IDO which subsequently resulted in the determination of crystal structures. To date the crystal structures of human IDO[363], *Xanthomonas campestris* TDO[364] and, *Ralstonia metallidurans* TDO[365] have been determined. We focus attention on the *X. campestris* TDO structure since this is in a complex with the substrate, L-Trp (Fig. 45). As

might be expected a comparison between the human IDO and bacterial TDO structures reveals striking similarities. The overall helical fold forming the heme pocket is conserved although human IDO has an extra domain missing in the bacterial TDO structure (Fig. 44A). This is very likely due to the difference in oligomeric structure. TDO is a functional homo-tetramer[365] while IDO is a monomer[366] and the missing domain in TDO relative to IDO is taken up by another TDO subunit.

The active sites are very similar with the important exception that Ser167 in IDO is His55 in TDO. The substrate is held in place by H-bonds between the substrate carboxylate and Arg117 while the substrate α-amino group interacts with the heme propionate. Conservation of Arg117 in IDO (Arg231) suggests that the binding mode of L-Trp in IDO is very similar. These crystal structures are at least in part consistent with early views on the IDO/TDO mechanism[367] (Fig. 44B). In this mechanism a base catalyst that abstracts the substrate N1 proton is required to activate the substrate for attack on the distal O_2 O atom. The reaction proceeds to product by either a Criegee rearrangement or through the dioxetane intermediate. This view received support when it was found that derivatives of L-Trp that have the N1 position blocked (ie 1-methyl-L-Trp) are competitive inhibitors.[368] Although His55 in IDO is ideally situated to serve as the expected base catalyst, this residue is Ser in the TDO structure (Fig. 43). Moreover, mutation of His55 to Ala decreases but does not abolish activity[364,369] suggesting that a protein base may not be required. Similar conclusions have been made from a thorough investigation of various active site mutations.[370] These observations together with resonance Raman data[371] indicating strong H-bonding and/or steric interactions between the substrate and ligand in IDO led to a modification of the of the original protein base catalyzed mechanism.[364,371] The main difference here is that the O_2 oxygen atom linked to the iron abstracts the N1 proton rather than a protein base. This proposal was followed by a DFT[372] study which seriously challenged these mechanisms since the simultaneous attack on the indole by the distal O_2 O atom and N1 proton abstraction has a very high energy barrier owing to a highly distorted transition state. Thus a novel mechanism was proposed where the N1 proton is not removed, the distal O_2 O atom attacks the indole ring, and the O-O bond cleaves heterolytically followed by addition of the proximal O_2 O atom (Fig. 44C). The DFT[372] work illustrated the energetic feasibility of forming a ferryl-type intermediate but at the time there was no experimental support.

Three key experiments consistent with the DFT work look to have settled the question and put the final nail in the coffin on both the base catalyzed and concerted oxygen insertion mechanism. First, it was found that 1-methyl L-Trp, although a poor substrate, is still a substrate demonstrating that the N1 proton is not essential.[373] This may at first appear to contradict earlier work where 1-methyl L-Trp was found to be a competitive inhibitor.[368] However, Cady and Sono[368] tested various Trp analogs as inhibitors of the normal reaction using L-Trp as a substrate. Since the 1-methyl derivative is a poor substrate it might well behave as a competitive inhibitor for L-Trp but still be a substrate so there really is no inconsistency between the two studies. Second was the discovery that TDO can form a relatively stable ferryl intermediate.[374] Resonance Raman studies identified a 799cm^{-1} band for the Fe-O bond stretch which, by using Badger's rule,[50] translates into a bond distance of 1.65Å clearly indicating Fe(IV)=O species. Optical spectroscopy was most consistent with a Compound II-like intermediate rather than Compound I.[374] Third, Basran et al.[375] showed that an intermediate could be trapped and analyzed by mass spectrometry that was consistent with having only one O_2-derived oxygen atom inserted into the intermediate. These results show that initially only one O atom is transferred to the substrate while the second remains bound to the heme iron. Pooling these results together with additional QM/MM calculations[376] leads to the mechanism shown in Fig. 44C. The first step is the electrophilic addition of the superoxide form of the dioxygen complex to the C2-C3 double bond of L-

Trp and homolytic cleavage of the O-O bond. A proton from the α-amino N atom of L-Trp then is transferred to the epoxide O atom together with the nucleophilic attack of the ferryl O atom results in ring opening.

9.0 MauG

Nature often requires cofactors of specialized function that are generated by post translational modification of amino acids. One such cofactor is called tryptophan tryptophylquinone (TTQ) and is formed by oxidation and covalent linkage of two nearby tryptophan residues (Fig. 46). TTQ is found in the bacterial enzyme methyl amine dehydrogenase (MADH) where it directly participates in the oxidative deamination of amines to an aldehyde and ammonia.[377] The enzyme responsible for the post translational synthesis of TQQ is MauG (for recent reviews see[378,379]). MauG bears striking structural but little functional homology to the diheme peroxidases discussed in section 2.4.[380] Like these peroxidases MauG has two c-type hemes, one of which is high-spin and the other low-spin. TTQ forms in the presence of O_2 and di-ferrous MauG (both hemes reduced) or by reaction of di-ferric MauG with H_2O_2.[381] In both cases both hemes are oxidized to Fe^{4+} with the high-spin heme forming the traditional oxyferryl species.[382] This is quite different than in diheme peroxidases which do not react with O_2 and the low-spin heme cycles between Fe^{2+}/Fe^{3+} rather than Fe^{3+}/Fe^{4+} as in MauG. This is due to the traditional Met ligand found in c-type cytochromes and diheme peroxidases being replaced with Tyr in MauG. The additional negative charge on the Tyr phenolate oxygen lowers the heme redox potential[383] thus providing additional stabilization of the extra positive charge on Fe^{4+}.

Why ferrous MauG is able to react with O_2 but not diheme peroxidases is not clear given that the active site structures of MauG and the peroxidases around the high-spin heme O_2 binding site are so similar. However, unlike diheme peroxidases the two hemes in MauG behave as a single redox unit.[382,384] In diheme peroxidases each heme can be in different redox states thus giving mixed valency while the MauG hemes cannot. This is no doubt due the Tyr ligand in the low spin heme which brings the two heme redox potentials closer to equivalency. The two hemes also share both charge and spin *via* Trp93[385] which is situated between the two hemes (Fig. 47). However, this Trp alone cannot be responsible for the close electronic communication between the two hemes since this Trp is conserved in diheme peroxidases. Once again the key difference points to the Tyr (MauG) vs Met (peroxidase) ligand of the low spin heme that adjusts the redox properties to more closely match that of the high spin heme thus providing an easier mixing of electronic properties through Trp93. What remains to be explained is how such unique heme communication is connected to O_2 activation. Throughout this review the general theme has been that the local acid-base catalytic machinery controls the mechanism of O-O bond cleavage. MauG may provide an example where longer range tuning of the heme electronic properties helps to control the O_2 activation process. One final mechanistic question is how oxidizing equivalents are shuttled between MADH and MuG. As shown in Fig. 46, Trp199 of MauG is situated about midway between the low-spin heme and the TQQ cofactor of MADH in the MauG-MADH complex at a distance of about 7Å from each. Trp199 mutants have little effect on the spectroscopic or heme reactivity properties of MauG but TQQ biosynthesis is eliminated[384] clearly implicating Trp199 in electron transfer. Overall MauG provides a fascinating example of how a seemingly subtle change in a heme ligand can result in dramatic changes in functional properties. The O_2 activation process and the hexacoordinate low spin Fe^{4+} heme are unique to MauG and further exploration of these properties promises to provide important new insights into the diversity of heme enzyme function.

9.0 Concluding Remarks

As with many areas of research within the biochemical sciences, progress in understanding heme enzyme structure and function is directly related to technological advances. At the heart of these advances is the relative ease of obtaining entire genome sequences. Powerful bioinformatics tools enable one to search a vast array of information on potentially new and interesting enzymes. A classic example covered in this review is cytochrome c peroxidase. For decades yeast CCP was the only known peroxidase to utilize cytochrome c as a substrate which, even in the early days, seemed odd given that Nature tends to reuse something that has proven successful. We now know that yeast CCP is not so unique and both closely and distantly related organisms have the same enzyme. As is often the case, we can learn just as much or more by studying the next few examples of the same enzyme since this teaches what structural features are most important and conserved for function. In the heme enzyme field nowhere has this had a bigger impact than in P450s. There are now in the range of 18,000 different P450s and the end is not in sight. In addition to providing more targets for structure function studies, this has opened up studying new and unexpected biological functions of P450s. This wealth of genomic data also has decreased the time and effort required to obtain pure protein. For those primarily interested in enzyme structure and function the days of actually cloning a gene from its original host are coming to an end since now the biochemist need only have the gene of interest synthesized and inserted into an expression plasmid.

Advances in protein crystallography also have played a major role. While the debate on the wisdom of diverting so much NIH funding to the so-called protein structure initiatives goes on,[386] it is doubtful that the rapid development and automation of synchrotron beamlines and highly sophisticated user-friendly software would be at their current levels without the push provided by these large scale projects. This has opened up crystal structure determination to a wider audience and one can effectively solve a structure without having much of a clue on how it all works. While the purist might bemoan this type of development, there now are sufficient checks and balance within the PDB to help maintain quality. High powered x-rays, however, come at a price since it now is more fully appreciated that x-ray induced reducing equivalents readily changes the redox state of metal centers in addition to causing crystal damage. Indeed, it is very likely that nearly any Fe(III) heme protein where data were collected at a synchrotron is probably not Fe(III) but Fe(II). This is not much of an issue in the initial structure determination but certainly will cause a problem in deriving mechanistic insights. The increasing use of robotics and single crystal spectroscopy has helped to resolve some of these problems but requires many well diffracting crystals and complicated composite data collection protocols. A potentially exciting advance is the free electron lasers now in the early stages of applications at various synchrotron sources. The promise of this technology is to provide structures with essentially zero x-ray damage as well as providing snapshots of very short lived intermediates. While the future is somewhat uncertain on the ability of this technology to deliver high resolution structures, there is considerable optimism and excitement.

A particularly attractive feature in studying heme enzymes has been the confluence of spectroscopy, theory, model chemistry, enzymology, and crystallography. As noted in the Introduction, heme enzymes were of fundamental importance in the early development of modern enzymology owing to the many spectroscopic tools that can be used and this continues to be the case. In addition, model heme chemistry has been critical in understanding heme enzyme mechanisms especially by bringing some rather fanciful ideas back to the realties of chemistry and physics. Indeed, there have been few areas of enzymology where the research on models and enzymes has been so closely tied and interdependent and again it comes down to the many spectroscopic probes that can be used

to study both. Although spectroscopy has always been central to heme enzyme research, it only has been in recent years that a better appreciation has developed for the importance of correlating crystal structures with spectroscopy. At one time the crystal structure was the final word and any inconsistency between crystal structures and solution studies were considered shortcomings of the solution work. To the betterment of the field, this no longer is the case. One of the best recent examples discussed in this review is the inconsistency between spectroscopy and crystallography on the nature of the Compound I ferryl center[50] which prompted crystallographers to do the "correct" experiment[37,38] and reconcile the inconsistencies. Although these and other advances are impressive, there is much more to be learned. Nagging questions remain such as the relationship between redox partner binding and P450 O_2 activation chemistry, how drug metabolizing P450s adapt to so many different substrates, how a porphyrin radical is stabilized in one peroxidase but not another, and, of course, the biological role of heme enzymes. This last problem is likely to become particularly interesting as the genomic data base continues to swell and new enzymes are discovered. Indeed, heme enzymes can be found in the most unexpected places. Why, for example, does a virus encode a P450?[387] With the increasing ease of generating substantial protein for biochemical and structural studies we are in the odd position of having the cart before the horse since we can work out structure, spectroscopy, and other biochemical details before we know much about biological function. As a result we need to learn how to let the structural work guide us toward biological function. Given the rapid generation of new structures, the powerful informatics tools now available, and the important assumption that Nature is not too deceptive, the future is bright assuming there is sufficient research support for work on fundamental structural problems where clear cut biological and/or health related significance is unclear.

Acknowledgments

Work in the Poulos lab was supported primarily by NIH. I am indebted to Drs. Dipanwita Batabyal, Michael Green, Paul Ortiz de Montellano, Ah-Lim Tsai, and Carrie Wilmot for helpful suggestions and comments and a special thanks to Dr. Huiying Li. Also acknowledged are past and current lab members including B. Bhaskar, Chris Bonagura, Silvia Delker, Jeff Holden, Joumana Jamal, Victoria Jasion, Mack Flinspach, Yarrow Madrona, Yergalem Mehrranena, CS Raman, David Schuller, Sarvind Tripathi, Irina Sevrioukova, and Tiffany Yano.

References

1. Mason HS, Fowlks WL, Petersin E. J Am Chem Soc. 1955; 77:2914.
2. Hayaishi O, Katagari M, Rothberg S. J Am Chem Soc. 1955; 77:5450.
3. Klingenberg M. Arch Biochem Biophys. 1958; 75:376. [PubMed: 13534720]
4. Garfinkel D. Arch Biochem Biophys. 1958; 77:493. [PubMed: 13584011]
5. Omura T, Sato R. J Biol Chem. 1964; 239:2379. [PubMed: 14209972]
6. Omura T, Sato R. J Biol Chem. 1964; 239:2370. [PubMed: 14209971]
7. Estabrook RW, Cooper DY, Rosenthal O. Biochem Z. 1963; 338:741. [PubMed: 14087340]
8. Bach A, Chodat R. Ber. 1903; 36:600.
9. Fenton HJH. J Chem Soc, Trans. 1894; 65:899.
10. Dunford, HB. Peroxidases & Catalases: Biochemistry, Biophysics, Biotechnology, and Physiology. 2. Wiley; 2010.
11. Chance B. Acta Chem Scand. 1947; 1:236.
12. Chance B. J Biol Chem. 1949; 179:1341. [PubMed: 18134594]
13. Dolphin D, Forman A, Borg DC, Fajer J, Felton RH. Proc Natl Acad Sci U S A. 1971; 68:614. [PubMed: 5276770]
14. Coulson AF, Yonetani T. Biochem Biophys Res Commun. 1972; 49:391. [PubMed: 4344886]
15. Sivaraja M, Goodin DB, Smith M, Hoffman BM. Science. 1989; 245:738. [PubMed: 2549632]
16. Welinder KG. Current Opin Struc Biol. 1992; 2:388.

17. Schonbaum GR, Lo S. J Biol Chem. 1972; 247:3353. [PubMed: 5063682]
18. Hamilton, G. Chemical models and mechanisms for oxygenases. Hayaishi, O., editor. Academic Press; New York: 1974.
19. Hamilton GA. J Am Chem Soc. 1964; 86:3391.
20. Iizuka T, Kotani M, Yonetani T. J Biol Chem. 1971; 246:4731. [PubMed: 4327326]
21. Lang G, Spartalian K, Yonetani T. Biochim Biophys Acta. 1976; 451:250. [PubMed: 188453]
22. Fajer J, Borg DC, Forman A, Dolphin D, Felton RH. J Am Chem Soc. 1970; 92:3451. [PubMed: 5422767]
23. Jones P, Dunford HB. J Theor Biol. 1977; 69:457. [PubMed: 607017]
24. Baek HK, Van Wart HE. Biochemistry. 1989; 28:5714. [PubMed: 2775733]
25. Poulos TL, Freer ST, Alden RA, Edwards SL, Skogland U, Takio K, Eriksson B, Xuong N, Yonetani T, Kraut J. J Biol Chem. 1980; 255:575. [PubMed: 6243281]
26. Chang CK, Traylor TG. J Am Chem Soc. 1973; 95:8477. [PubMed: 4797935]
27. Valentine JS, Sheridan RP, Allen LC, Kahn PC. Proc Natl Acad Sci U S A. 1979; 76:1009. [PubMed: 220604]
28. Choudhury K, Sundaramoorthy M, Hickman A, Yonetani T, Woehl E, Dunn MF, Poulos TL. J Biol Chem. 1994; 269:20239. [PubMed: 8051115]
29. Hirst J, Wilcox SK, Ai J, Moenne-Loccoz P, Loehr TM, Goodin DB. Biochemistry. 2001; 40:1274. [PubMed: 11170453]
30. Hirst J, Wilcox SK, Williams PA, Blankenship J, McRee DE, Goodin DB. Biochemistry. 2001; 40:1265. [PubMed: 11170452]
31. Poulos TL. J Biol Inorg Chem. 1996; 1:356.
32. Poulos TL, Kraut J. J Biol Chem. 1980; 255:8199. [PubMed: 6251047]
33. Erman JE, Vitello LB, Miller MA, Shaw A, Brown KA, Kraut J. Biochemistry. 1993; 32:9798. [PubMed: 8396972]
34. Howes BD, Rodriguez-Lopez JN, Smith AT, Smulevich G. Biochemistry. 1997; 36:1532. [PubMed: 9063902]
35. Vitello LB, Erman JE, Miller MA, Wang J, Kraut J. Biochemistry. 1993; 32:9807. [PubMed: 8396973]
36. Rodriguez-Lopez JN, Smith AT, Thorneley RN. J Biol Chem. 1996; 271:4023. [PubMed: 8626735]
37. Berglund GI, Carlsson GH, Smith AT, Szoke H, Henriksen A, Hajdu J. Nature. 2002; 417:463. [PubMed: 12024218]
38. Meharenna YT, Doukov T, Li H, Soltis SM, Poulos TL. Biochemistry. 2010; 49:2984. [PubMed: 20230048]
39. Vidossich P, Fiorin G, Alfonso-Prieto M, Derat E, Shaik S, Rovira C. J Phys Chem B. 2010; 114:5161. [PubMed: 20345187]
40. Hashimoto S, Tatsuno Y, Kitagawa T. Proc Jpn Acad. 1984; 60:345.
41. Reczek CM, Sitter AJ, Terner J. J Molec Struc. 1989; 214:27.
42. Sitter AJ, Reczek CM, Terner J. Biochim Biophys Acta. 1985; 828:229. [PubMed: 3986209]
43. Chance B, Powers L, Ching Y, Poulos T, Schonbaum GR, Yamazaki I, Paul KG. Arch Biochem Biophys. 1984; 235:596. [PubMed: 6097192]
44. Chance M, Powers L, Poulos TL, Chance B. Biochemistry. 1986; 25:1266. [PubMed: 3008825]
45. Pennerhahn JE, Eble KS, Mcmurry TJ, Renner M, Balch AL, Groves JT, Dawson JH, Hodgson KO. J Am Chem Soc. 1986; 108:7819. [PubMed: 22283292]
46. Bonagura CA, Bhaskar B, Shimizu H, Li H, Sundaramoorthy M, McRee D, Goodin DB, Poulos TL. Biochemistry. 2003; 42:5600. [PubMed: 12741816]
47. Fulop V, Phizackerley RP, Soltis SM, Clifton IJ, Wakatsuki S, Erman J, Hajdu J, Edwards SL. Structure. 1994; 2:201. [PubMed: 8069633]
48. Hersleth HP, Dalhus B, HGCKAK. J Biol Inorg Chem. 2002; 7:299. [PubMed: 11935353]

49. Murshudov GN, Grebenko AI, Brannigan JA, Antson AA, Barynin VV, Dodson GG, Dauter Z, Wilson KS, Melik-Adamyan WR. Acta Crystallogr D Biol Crystallogr. 2002; 58:1972. [PubMed: 12454454]
50. Green MT. J Am Chem Soc. 2006; 128:1902. [PubMed: 16464091]
51. Hersleth HP, Hsiao YW, Ryde U, Gorbitz CH, Andersson KK. Chem Biodivers. 2008; 5:2067. [PubMed: 18972498]
52. Yonetani T, Schleyer H, Eherenberg A. J Biol Chem. 1966; 241:3240. [PubMed: 4287913]
53. Hoffman BM, Roberts JE, Brown TG, Kang CH, Margoliash E. Proc Nat Acad Sci U S A. 1979; 76:6132.
54. Welinder KG. Eur J Biochem. 1979; 96:483. [PubMed: 38113]
55. Takio K, Titani K, Ericsson LH, Yonetani T. Arch Biochem Biophys. 1980; 203:615. [PubMed: 6257176]
56. Mauro JM, Fishel LA, Hazzard JT, Meyer TE, Tollin G, Cusanovich MA, Kraut J. Biochemistry. 1988; 27:6243. [PubMed: 2851317]
57. Fishel LA, Villafranca JE, Mauro JM, Kraut J. Biochemistry. 1987; 27:351. [PubMed: 3030406]
58. Goodin DB, Mauk AG, Smith M. J Biol Chem. 1987; 262:7719. [PubMed: 3034903]
59. Houseman ALP, Doan PE, Goodin DB, Hoffman BM. Biochemistry. 1993; 32:4430. [PubMed: 8386547]
60. Mittler R, Zilinskas BA. FEBS Lett. 1991; 289:257. [PubMed: 1915856]
61. Patterson WR, Poulos TL. Biochemistry. 1995; 34:4331. [PubMed: 7703247]
62. Patterson WR, Poulos TL, Goodin DB. Biochemistry. 1995; 34:4342. [PubMed: 7703248]
63. Marquez LA, Quitoriano M, Zilinskas BA, Dunford HB. FEBS Lett. 1996; 389:153. [PubMed: 8766820]
64. Fitzgerald MM, Churchill MJ, McRee DE, Goodin DB. Biochemistry. 1994; 33:3807. [PubMed: 8142383]
65. Miller MA, Han GW, Kraut J. Proc Natl Acad Sci USA. 1994; 91:11118. [PubMed: 7972020]
66. Bonagura CA, Sundaramoorthy M, Pappa HS, Patterson WR, Poulos TL. Biochemistry. 1996; 35:6107. [PubMed: 8634253]
67. Jensen GM, Bunte SW, Warshel A, Goodin DB. J Phys Chem B. 1998; 102:8221.
68. Bonagura CA, Sundaramoorthy M, Bhaskar B, Poulos TL. Biochemistry. 1999; 38:5538. [PubMed: 10220341]
69. Bonagura CA, Bhaskar B, Sundaramoorthy M, Poulos TL. J Biol Chem. 1999; 274:37827. [PubMed: 10608846]
70. Cheek J, Mandelman D, Poulos TL, Dawson JH. J Biol Inorg Chem. 1999; 4:64. [PubMed: 10499104]
71. Hiner AN, Martinez JI, Arnao MB, Acosta M, Turner DD, Lloyd Raven E, Rodriguez-Lopez JN. Eur J Biochem. 2001; 268:3091. [PubMed: 11358529]
72. Barrows TP, Poulos TL. Biochemistry. 2005; 44:14062. [PubMed: 16245922]
73. Jasion VS, Polanco JA, Meharenna YT, Li H, Poulos TL. J Biol Chem. 2011
74. Bhaskar B, Bonagura CA, Li H, Poulos TL. Biochemistry. 2002; 41:2684. [PubMed: 11851415]
75. Miller MA. Biochemistry. 1996; 35:15791. [PubMed: 8961942]
76. Millett F, Miller MA, Geren L, Durham B. J Bioenerg Biomembr. 1995; 27:341. [PubMed: 8847347]
77. Liu RQ, Hahm S, Miller M, Durham B, Millett F. Biochemistry. 1995; 34:973. [PubMed: 7827055]
78. Barrows TP, Bhaskar B, Poulos TL. Biochemistry. 2004; 43:8826. [PubMed: 15236591]
79. Spangler BD, Erman JE. Biochim Biophys Acta. 1986; 872:155. [PubMed: 3015215]
80. Musah RA, Goodin DB. Biochemistry. 1997; 36:11665. [PubMed: 9305956]
81. Adak S, Datta AK. Biochem J. 2005; 390:465. [PubMed: 15850459]
82. Yadav RK, Dolai S, Pal S, Adak S. Biochim Biophys Acta. 2008; 1784:863. [PubMed: 18342641]

83. Ruiz-Duenas FJ, Camarero S, Perez-Boada M, Martinez MJ, Martinez AT. Biochem Soc Trans. 2001; 29:116. [PubMed: 11356138]
84. Blodig W, Doyle WA, Smith AT, Winterhalter K, Choinowski T, Piontek K. Biochemistry. 1998; 37:8832. [PubMed: 9636023]
85. Doyle WA, Blodig W, Veitch NC, Piontek K, Smith AT. Biochemistry. 1998; 37:15097. [PubMed: 9790672]
86. Kirk TK, Farrell RL. Annu Rev Microbiol. 1987; 41:465. [PubMed: 3318677]
87. Renganathan V, Miki K, Gold MH. Arch Biochem Biophys. 1985; 241:304. [PubMed: 4026322]
88. Wariishi H, Huang J, Dunford HB, Gold MH. J Biol Chem. 1991; 266:20694. [PubMed: 1939119]
89. Henriksen A, Schuller DJ, Meno K, Welinder KG, Smith AT, Gajhede M. Biochemistry. 1998; 37:8054. [PubMed: 9609699]
90. Ruiz-Duenas FJ, Morales M, Mate MJ, Romero A, Martinez MJ, Smith AT, Martinez AT. Biochemistry. 2008; 47:1685. [PubMed: 18201105]
91. Ruiz-Duenas FJ, Pogni R, Morales M, Giansanti S, Mate MJ, Romero A, Martinez MJ, Basosi R, Martinez AT. J Biol Chem. 2009; 284:7986. [PubMed: 19158088]
92. Pogni R, Baratto MC, Teutloff C, Giansanti S, Ruiz-Duenas FJ, Choinowski T, Piontek K, Martinez AT, Lendzian F, Basosi R. J Biol Chem. 2006; 281:9517. [PubMed: 16443605]
93. Smith AT, Doyle WA, Dorlet P, Ivancich A. Proc Natl Acad Sci U S A. 2009; 106:16084. [PubMed: 19805263]
94. Erman JE, Vitello LB, Mauro JM, Kraut J. Biochemistry. 1989; 28:7992. [PubMed: 2557891]
95. Guallar V, Baik MH, Lippard SJ, Friesner RA. Proc Natl Acad Sci USA. 2003; 100:6998. [PubMed: 12771375]
96. Guallar V, Olsen B. J Inorg Biochem. 2006; 100:755. [PubMed: 16513175]
97. Sundaramoorthy M, Gold MH, Poulos TL. J Inorg Biochem. 2010; 104:683. [PubMed: 20356630]
98. Sharp KH, Mewies M, Moody PC, Raven EL. Nat Struct Biol. 2003; 10:303. [PubMed: 12640445]
99. Ellfolk N, Soininen R. Acta Chem Scand. 1970; 24:2126. [PubMed: 5485031]
100. Soininen R, Sojonen H, Ellfolk N. Acta Chem Scand. 1970; 24:2314. [PubMed: 5485037]
101. Ellfolk N, Ronnberg M, Aasa R, Andreasson LE, Vanngard T. Biochim Biophys Acta. 1983; 743:23. [PubMed: 6297595]
102. Fulop V, Ridout CJ, Greenwood C, Hajdu J. Structure. 1995; 3:1225. [PubMed: 8591033]
103. Foote N, Turner R, Brittain T, Greenwood C. Biochem J. 1992; 283(Pt 3):839. [PubMed: 1317165]
104. Echalier A, Brittain T, Wright J, Boycheva S, Mortuza GB, Fulop V, Watmough NJ. Biochemistry. 2008; 47:1947. [PubMed: 18217775]
105. Echalier A, Goodhew CF, Pettigrew GW, Fulop V. Structure. 2006; 14:107. [PubMed: 16407070]
106. Shimizu H, Schuller DJ, Lanzilotta WN, Sundaramoorthy M, Arciero DM, Hooper AB, Poulos TL. Biochemistry. 2001; 40:13483. [PubMed: 11695895]
107. DePillis GD, Sishta BP, Mauk AG, Ortiz de Montellano PR. J Biol Chem. 1991; 266:19334. [PubMed: 1655784]
108. Henriksen A, Smith AT, Gajhede M. J Biol Chem. 1999; 274:35005. [PubMed: 10574977]
109. Sundaramoorthy M, Kishi K, Gold MH, Poulos TL. J Biol Chem. 1994; 269:32759. [PubMed: 7806497]
110. Sundaramoorthy M, Kishi K, Gold MH, Poulos TL. J Biol Chem. 1997; 272:17574. [PubMed: 9211904]
111. Sundaramoorthy M, Youngs HL, Gold MH, Poulos TL. Biochemistry. 2005; 44:6463. [PubMed: 15850380]
112. Bursey EH, Poulos TL. Biochemistry. 2000; 39:7374. [PubMed: 10858284]
113. Mandelman D, Jamal J, Poulos TL. Biochemistry. 1998; 37:17610. [PubMed: 9860877]
114. Volkov AN, Nicholls P, Worrall JA. Biochim Biophys Acta. 2011; 1807:1482. [PubMed: 21820401]
115. Kang CH, Ferguson-Miller S, Margoliash E. J Biol Chem. 1977; 252:919. [PubMed: 14138]

116. Mauk MR, Ferrer JC, Mauk AG. Biochemistry. 1994; 33:12609. [PubMed: 7918486]
117. Stemp ED, Hoffman BM. Biochemistry. 1993; 32:10848. [PubMed: 8399235]
118. Zhou JS, Hoffman BM. Science. 1994; 265:1693. [PubMed: 8085152]
119. Pelletier H, Kraut J. Science. 1992; 258:1748. [PubMed: 1334573]
120. Kang CH, Brautigan DL, Osheroff N, Margoliash E. J Biol Chem. 1978; 253:6502. [PubMed: 210187]
121. Ferguson-Miller S, Brautigan DL, Margoliash E. J Biol Chem. 1978; 253:149. [PubMed: 201616]
122. Brautigan DL, Ferguson-Miller S, Tarr GE, Margoliash E. J Biol Chem. 1978; 253:140. [PubMed: 201615]
123. Ubbink M. FEBS Lett. 2009; 583:1060. [PubMed: 19275897]
124. Jasion VS, Doukov T, Pineda SH, Li H, Poulos TL. Proc Natl Acad Sci U S A. 2012; 109:18390. [PubMed: 23100535]
125. Jasion VS, Poulos TL. Biochemistry. 2012; 51:2453. [PubMed: 22372542]
126. Dietz R, Nastainczyk W, Ruf HH. Eur J Biochem. 1988; 171:321. [PubMed: 3123232]
127. Garavito RM, Mulichak AM. Annu Rev Biophys Biomol Struct. 2003; 32:183. [PubMed: 12574066]
128. Kurumbail RG, Kiefer JR, Marnett LJ. Curr Opin Struct Biol. 2001; 11:752. [PubMed: 11751058]
129. Rouzer CA, Marnett LJ. Chem Rev. 2003; 103:2239. [PubMed: 12797830]
130. Smith WL, DeWitt DL, Garavito RM. Annu Rev Biochem. 2000; 69:145. [PubMed: 10966456]
131. Tsai AL, Kulmacz RJ. Arch Biochem Biophys. 2010; 493:103. [PubMed: 19728984]
132. Malkowski MG, Ginell SL, Smith WL, Garavito RM. Science. 2000; 289:1933. [PubMed: 10988074]
133. Landino LM, Crews BC, Gierse JK, Hauser SD, Marnett LJ. J Biol Chem. 1997; 272:21565. [PubMed: 9261177]
134. Lu G, Tsai AL, Van Wart HE, Kulmacz RJ. J Biol Chem. 1999; 274:16162. [PubMed: 10347169]
135. Picot D, Loll PJ, Garavito RM. Nature. 1994; 367:243. [PubMed: 8121489]
136. Mizuno K, Yamamoto S, Lands WE. Prostaglandins. 1982; 23:743. [PubMed: 6812164]
137. Tsai A, Kulmacz RJ, Palmer G. J Biol Chem. 1995; 270:10503. [PubMed: 7737984]
138. Kulmacz RJ. Biochem Biophys Res Commun. 2005; 338:25. [PubMed: 16115608]
139. Wu G, Rogge CE, Wang JS, Kulmacz RJ, Palmer G, Tsai AL. Biochemistry. 2007; 46:534. [PubMed: 17209563]
140. Guengerich FP, Munro AW. J Biol Chem. 2013; 288:17063. [PubMed: 23632015]
141. Smela ME, Currier SS, Bailey EA, Essigmann JM. Carcinogenesis. 2001; 22:535. [PubMed: 11285186]
142. Katagiri M, Ganguli BN, Gunsalus IC. J Biol Chem. 1968; 243:3543. [PubMed: 4297783]
143. You IS, Ghosal D, Gunsalus IC. J Bacteriol. 1988; 170:5409. [PubMed: 2848005]
144. Haniu M, Armes LG, Yasunobu KT, Shastry BA, Gunsalus IC. J Biol Chem. 1982; 257:12664. [PubMed: 7130171]
145. Haniu M, Tanaka M, Yasunobu KT, Gunsalus IC. J Biol Chem. 1982; 257:12657. [PubMed: 6752138]
146. Poulos TL, Finzel BC, Gunsalus IC, Wagner GC, Kraut J. J Biol Chem. 1985; 260:16122. [PubMed: 4066706]
147. Poulos TL, Finzel BC, Howard AJ. J Mol Biol. 1987; 195:687. [PubMed: 3656428]
148. Adman E, Watenpaugh KD, Jensen LH. Proc Natl Acad Sci U S A. 1975; 72:4854. [PubMed: 1061073]
149. Langen R, Jensen GM, Jacob U, Stephens PJ, Warshel A. J Biol Chem. 1992; 267:25625. [PubMed: 1464583]
150. Ueyama N, Yamada Y, Okamura Ta T, Kimura S, Nakamura A. Inorg Chem. 1996; 35:6473. [PubMed: 11666795]
151. Scott EE, He YA, Wester MR, White MA, Chin CC, Halpert JR, Johnson EF, Stout CD. Proc Natl Acad Sci U S A. 2003; 100:13196. [PubMed: 14563924]

152. Scott EE, White MA, He YA, Johnson EF, Stout CD, Halpert JR. J Biol Chem. 2004; 279:27294. [PubMed: 15100217]
153. Lee YT, Wilson RF, Rupniewski I, Goodin DB. Biochemistry. 2010; 49:3412. [PubMed: 20297780]
154. Lee YT, Glazer EC, Wilson RF, Stout CD, Goodin DB. Biochemistry. 2010; 50:693. [PubMed: 21171581]
155. Stoll S, Lee YT, Zhang M, Wilson RF, Britt RD, Goodin DB. Proc Natl Acad Sci U S A. 2012; 109:12888. [PubMed: 22826259]
156. Narhi LO, Wen LP, Fulco AJ. Mol Cell Biochem. 1988; 79:63. [PubMed: 3131661]
157. Li HY, Poulos TL. Nat Struct Biol. 1997; 4:140. [PubMed: 9033595]
158. Modi S, Sutcliffe MJ, Primrose WU, Lian LY, Roberts GC. Nat Struct Biol. 1996; 3:414. [PubMed: 8612070]
159. Jovanovic T, Farid R, Friesner RA, McDermott AE. J Am Chem Soc. 2005; 127:13548. [PubMed: 16190718]
160. Haines DC, Tomchick DR, Machius M, Peterson JA. Biochemistry. 2001; 40:13456. [PubMed: 11695892]
161. Hannemann F, Bichet A, Ewen KM, Bernhardt R. Biochim Biophys Acta. 2007; 1770:330. [PubMed: 16978787]
162. Gray HB, Winkler JR. Annu Rev Biochem. 1996; 65:537. [PubMed: 8811189]
163. Gray HB, Winkler JR. Biochim Biophys Acta. 2010; 1797:1563. [PubMed: 20460102]
164. Sevrioukova IF, Li H, Zhang H, Peterson JA, Poulos TL. Proc Natl Acad Sci U S A. 1999; 96:1863. [PubMed: 10051560]
165. Strushkevich N, MacKenzie F, Cherkesova T, Grabovec I, Usanov S, Park HW. Proc Natl Acad Sci U S A. 2011; 108:10139. [PubMed: 21636783]
166. Tripathi S, Li H, Poulos TL. Science. 2013; 340:1227. [PubMed: 23744947]
167. Wen LP, Fulco AJ. J Biol Chem. 1987; 262:6676. [PubMed: 3106359]
168. Jung ST, Lauchli R, Arnold FH. Curr Opin Biotechnol. 2011; 22:809. [PubMed: 21411308]
169. Whitehouse CJ, Bell SG, Wong LL. Chem Soc Rev. 2012; 41:1218. [PubMed: 22008827]
170. Wang M, Roberts DL, Paschke R, Shea TM, Masters BS, Kim JJ. Proc Natl Acad Sci U S A. 1997; 94:8411. [PubMed: 9237990]
171. Govindaraj S, Poulos TL. Protein Sci. 1996; 5:1389. [PubMed: 8819171]
172. Sevrioukova IF, Hazzard JT, Tollin G, Poulos TL. J Biol Chem. 1999; 274:36097. [PubMed: 10593892]
173. Sevrioukova IF, Immoos CE, Poulos TL, Farmer P. Israel J Chem. 2000; 40:47.
174. Hamdane D, Xia C, Im SC, Zhang H, Kim JJP, Waskell L. J Biol Chem. 2009; 284:11374. [PubMed: 19171935]
175. Xia C, Hamdane D, Shen AL, Choi V, Kasper CB, Pearl NM, Zhang H, Im SC, Waskell L, Kim JJP. J Biol Chem. 2011; 286:16246. [PubMed: 21345800]
176. Adamovich TB, Pikuleva IA, Chashchin VL, Usanov SA. Biochim Biophys Acta. 1989; 996:247. [PubMed: 2502182]
177. Coghlan VM, Vickery LE. J Biol Chem. 1991; 266:18606. [PubMed: 1917982]
178. Wada A, Waterman MR. J Biol Chem. 1992; 267:22877. [PubMed: 1429635]
179. Mast N, Annalora AJ, Lodowski DT, Palczewski K, Stout CD, Pikuleva IA. J Biol Chem. 2011; 286:5607. [PubMed: 21159775]
180. Andersen JF, Hutchinson CR. J Bacteriol. 1992; 174:725. [PubMed: 1732208]
181. Lipscomb JD, Sligar SG, Namtvedt MJ, Gunsalus IC. J Biol Chem. 1976; 251:1116. [PubMed: 2601]
182. Sligar SG, Debrunner PG, Lipscomb JD, Namtvedt MJ, Gunsalus IC. Proc Natl Acad Sci U S A. 1974; 71:3906. [PubMed: 4530269]
183. Tyson CA, Lipscomb JD, Gunsalus IC. J Biol Chem. 1972; 247:5777. [PubMed: 4341491]
184. Pochapsky TC, Lyons TA, Kazanis S, Arakaki T, Ratnaswamy G. Biochimie. 1996; 78:723. [PubMed: 9010601]

185. Geren L, Tuls J, O'Brien P, Millett F, Peterson JA. J Biol Chem. 1986; 261:15491. [PubMed: 3096990]
186. Kuznetsov VY, Poulos TL, Sevrioukova IF. Biochemistry. 2006; 45:11934. [PubMed: 17002293]
187. Unno M, Shimada H, Toba Y, Makino R, Ishimura Y. J Biol Chem. 1996; 271:17869. [PubMed: 8663375]
188. Imai M, Shimada H, Watanabe Y, Matsushimahibiya Y, Makino R, Koga H, Horiuchi T, Ishimura Y. Proc Nat Acad Sci U S A. 1989; 86:7823.
189. Shimada H, Nagano S, Hori H, Ishimura Y. J Inorg Biochem. 2001; 83:255. [PubMed: 11293545]
190. Unno M, Christian JF, Sjodin T, Benson DE, Macdonald ID, Sligar SG, Champion PM. J Biol Chem. 2002; 277:2547. [PubMed: 11706033]
191. Nagano S, Shimada H, Tarumi A, Hishiki T, Kimata-Ariga Y, Egawa T, Suematsu M, Park SY, Adachi S, Shiro Y, Ishimura Y. Biochemistry. 2003; 42:14507. [PubMed: 14661963]
192. Tosha T, Yoshioka S, Takahashi S, Ishimori K, Shimada H, Morishima I. J Biol Chem. 2003; 278:39809. [PubMed: 12842870]
193. Tosha T, Yoshioka S, Ishimori K, Morishima I. J Biol Chem. 2004; 279:42836. [PubMed: 15269211]
194. Shiro Y, Iizuka T, Makino R, Ishimura Y, Morishima I. J Am Chem Soc. 1989; 111:7707.
195. Pochapsky SS, Pochapsky TC, Wei JW. Biochemistry. 2003; 42:5649. [PubMed: 12741821]
196. Zhang W, Pochapsky SS, Pochapsky TC, Jain NU. J Molec Biol. 2008; 384:349. [PubMed: 18835276]
197. Glascock MC, Ballou DP, Dawson JH. J Biol Chem. 2005; 280:42134. [PubMed: 16115886]
198. Unno M, Christian JF, Benson DE, Gerber NC, Sligar SG, Champion PM. J Am Chem Soc. 1997; 119:6614.
199. Brewer CB, Peterson JA. Arch Biochem Biophys. 1986; 249:515. [PubMed: 3753015]
200. Nagano S, Tosha T, Ishimori K, Morishima I, Poulos TL. J Biol Chem. 2004; 279:42844. [PubMed: 15269210]
201. Raag R, Poulos TL. Biochemistry. 1989; 28:7586. [PubMed: 2611203]
202. Hiruma, Y.; Hass, MA.; Kikui, Y.; Liu, WM.; Olmez, B.; Skinner, SP.; Blok, A.; Kloosterman, A.; Koteishi, H.; Lohr, F.; Schwalbe, H.; Nojiri, M.; Ubbink, M. J Mol Biol. 2013. http://www.ncbi.nlm.nih.gov/pubmed/23856620
203. Davies MD, Qin L, Beck JL, Suslick KS, Koga H, Horiuchi T, Sligar SG. J Am Chem Soc. 1990; 112:7396.
204. Davies MD, Sligar SG. Biochemistry. 1992; 31:11383. [PubMed: 1445875]
205. Holden M, Mayhew M, Bunk D, Roitberg A, Vilker V. J Biol Chem. 1997; 272:21720. [PubMed: 9268300]
206. Koga H, Sagara Y, Yaoi T, Tsujimura M, Nakamura K, Sekimizu K, Makino R, Shimada H, Ishimura Y, Yura K, et al. FEBS Lett. 1993; 331:109. [PubMed: 8405387]
207. Stayton PS, Sligar SG. Biochemistry. 1991; 30:1845. [PubMed: 1993199]
208. Schlichting I, Berendzen J, Chu K, Stock AM, Maves SA, Benson DE, Sweet RM, Ringe D, Petsko GA, Sligar SG. Science. 2000; 287:1615. [PubMed: 10698731]
209. Nagano S, Poulos TL. J Biol Chem. 2005; 280:31659. [PubMed: 15994329]
210. Nagano S, Cupp-Vickery JR, Poulos TL. J Biol Chem. 2005; 280:22102. [PubMed: 15824115]
211. Davydov R, Makris TM, Kofman V, Werst DE, Sligar SG, Hoffman BM. J Am Chem Soc. 2001; 123:1403. [PubMed: 11456714]
212. Egawa T, Shimada H, Ishimura Y. Biochem Biophys Res Commun. 1994; 201:1464. [PubMed: 8024592]
213. Spolitak T, Dawson JH, Ballou DP. J Biol Chem. 2005; 280:20300. [PubMed: 15781454]
214. Kellner DG, Hung SC, Weiss KE, Sligar SG. J Biol Chem. 2002; 277:9641. [PubMed: 11799104]
215. Rittle J, Green MT. Science. 2010; 330:933. [PubMed: 21071661]
216. Rittle J, Younker JM, Green MT. Inorg Chem. 2010; 49:3610. [PubMed: 20380463]
217. Fedorov R, Ghosh DK, Schlichting I. Arch Biochem Biophys. 2003; 409:25. [PubMed: 12464241]

218. Madrona Y, Tripathi S, Li H, Poulos TL. Biochemistry. 2012
219. Raag R, Martinis SA, Sligar SG, Poulos TL. Biochemistry. 1991; 30:11420. [PubMed: 1742281]
220. Martinis SA, Atkins WM, Stayton PS, Sligar SG. J Am Chem Soc. 1989; 20:9252.
221. Kimata Y, Shimada H, Hirose T, Ishimura Y. Biochem Biophys Res Commun. 1995; 208:96. [PubMed: 7887971]
222. Gerber NC, Sligar SG. J Biol Chem. 1994; 269:4260. [PubMed: 8307990]
223. Vidakovic M, Sligar SG, Li H, Poulos TL. Biochemistry. 1998; 37:9211. [PubMed: 9649301]
224. Benson DE, Suslick KS, Sligar SG. Biochemistry. 1997; 36:5104. [PubMed: 9136869]
225. Makris TM, von Koenig K, Schlichting I, Sligar SG. Biochemistry. 2007; 46:14129. [PubMed: 18001135]
226. Lounnas V, Wade RC. Biochemistry. 1997; 36:5402. [PubMed: 9154922]
227. Stok JE, Yamada S, Farlow AJ, Slessor KE, De Voss JJ. Biochim Biophys Acta. 2013
228. Zheng J, Wang D, Thiel W, Shaik S. J Am Chem Soc. 2006; 128:13204. [PubMed: 17017800]
229. Groves JT, McClusky GA. J Am Chem Soc. 1976; 98:859.
230. Ortiz de Monellano PR, Stearns RA. J Am Chem Soc. 1987; 109:3415.
231. Bowry VW, Ingold KU. J Am Chem Soc. 1991; 113:5699.
232. Newcomb M, Manek MB, Glenn AG. J Am Chem Soc. 1991; 113:949.
233. Ortiz de Montellano PR. Chem Rev. 2010; 110:932. [PubMed: 19769330]
234. Cryle MJ, Ortiz de Montellano PR, De Voss JJ. J Org Chem. 2005; 70:2455. [PubMed: 15787531]
235. Newcomb M, Shen R, Lu Y, Coon MJ, Hollenberg PF, Kopp DA, Lippard SJ. J Am Chem Soc. 2002; 124:6879. [PubMed: 12059209]
236. Newcomb M, Toy PH. Acc Chem Res. 2000; 33:449. [PubMed: 10913233]
237. Shaik S, de Visser SP, Ogliaro F, Schwarz H, Schröder D. Curr Opin Chem Biol. 2002; 6:556. [PubMed: 12413538]
238. Shaik S, Lai W, Chen H, Wang Y. Acc Chem Res. 2010; 43:1154. [PubMed: 20527755]
239. Daiber A, Shoun H, Ullrich V. J Inorg Biochem. 2005; 99:185. [PubMed: 15598501]
240. Shoun H, Sudo Y, Seto Y, Beppu T. J Biochem. 1983; 94:1219. [PubMed: 6654854]
241. Shoun H, Suyama W, Yasui T. FEBS Lett. 1989; 244:11. [PubMed: 2924900]
242. Shoun H, Tanimoto T. J Biol Chem. 1991; 266:11078. [PubMed: 2040619]
243. Shimizu H, Park SY, Shiro Y, Adachi S. Acta Crystallogr D Biol Crystallogr. 2002; 58:81. [PubMed: 11752781]
244. Lee DS, Yamada A, Sugimoto H, Matsunaga I, Ogura H, Ichihara K, Adachi S, Park SY, Shiro Y. J Biol Chem. 2003; 278:9761. [PubMed: 12519760]
245. Moncada S, Gryglewski R, Bunting S, Vane JR. Nature. 1976; 263:663. [PubMed: 802670]
246. Chiang CW, Yeh HC, Wang LH, Chan NL. J Mol Biol. 2006; 364:266. [PubMed: 17020766]
247. Li YC, Chiang CW, Yeh HC, Hsu PY, Whitby FG, Wang LH, Chan NL. J Biol Chem. 2008; 283:2917. [PubMed: 18032380]
248. Brash AR. Phytochemistry. 2009; 70:1522. [PubMed: 19747698]
249. Song WC, Brash AR. Science. 1991; 253:781. [PubMed: 1876834]
250. Lee DS, Nioche P, Hamberg M, Raman CS. Nature. 2008; 455:363. [PubMed: 18716621]
251. Li L, Chang Z, Pan Z, Fu ZQ, Wang X. Proc Natl Acad Sci U S A. 2008; 105:13883. [PubMed: 18787124]
252. Grechkin AN, Hamberg M. Biochim Biophys Acta. 2004; 1636:47. [PubMed: 14984738]
253. Bredt DS, Snyder SH. Annu Rev Biochem. 1994; 63:175. [PubMed: 7526779]
254. Griffith OW, Stuehr DJ. Annu Rev Physiol. 1995; 57:707. [PubMed: 7539994]
255. Arnold WP, Mittal CK, Katsuki S, Murad F. Proc Natl Acad Sci U S A. 1977; 74:3203. [PubMed: 20623]
256. Bredt DS, Hwang PM, Glatt CE, Lowenstein C, Reed RR, Snyder SH. Nature. 1991; 351:714. [PubMed: 1712077]

257. McMillan K, Bredt DS, Hirsch DJ, Snyder SH, Clark JE, Masters BS. Proc Natl Acad Sci U S A. 1992; 89:11141. [PubMed: 1280819]
258. Stuehr DJ, Ikeda-Saito M. J Biol Chem. 1992; 267:20547. [PubMed: 1383204]
259. White KA, Marletta MA. Biochemistry. 1992; 31:6627. [PubMed: 1379068]
260. Abu-Soud HM, Stuehr DJ. Proc Natl Acad Sci U S A. 1993; 90:10769. [PubMed: 7504282]
261. Siddhanta U, Presta A, Fan B, Wolan D, Rousseau DL, Stuehr DJ. J Biol Chem. 1998; 273:18950. [PubMed: 9668073]
262. Tayeh MA, Marletta MA. J Biol Chem. 1989; 264:19654. [PubMed: 2584186]
263. Crane BR, Arvai AS, Ghosh DK, Wu C, Getzoff ED, Stuehr DJ, Tainer JA. Science. 1998; 279:2121. [PubMed: 9516116]
264. Fischmann TO, Hruza A, Niu XD, Fossetta JD, Lunn CA, Dolphin E, Prongay AJ, Reichert P, Lundell DJ, Narula SK, Weber PC. Nat Struct Biol. 1999; 6:233. [PubMed: 10074942]
265. Li H, Raman CS, Glaser CB, Blasko E, Young TA, Parkinson JF, Whitlow M, Poulos TL. J Biol Chem. 1999; 274:21276. [PubMed: 10409685]
266. Raman CS, Li H, Martasek P, Kral V, Masters BS, Poulos TL. Cell. 1998; 95:939. [PubMed: 9875848]
267. Hurshman AR, Krebs C, Edmondson DE, Huynh BH, Marletta MA. Biochemistry. 1999; 38:15689. [PubMed: 10625434]
268. Wei CC, Wang ZQ, Hemann C, Hille R, Stuehr DJ. J Biol Chem. 2003; 278:46668. [PubMed: 14504282]
269. Wei CC, Wang ZQ, Wang Q, Meade AL, Hemann C, Hille R, Stuehr DJ. J Biol Chem. 2001; 276:315. [PubMed: 11020389]
270. Stoll S, NejatyJahromy Y, Woodward JJ, Ozarowski A, Marletta MA, Britt RD. J Am Chem Soc. 2010; 132:11812. [PubMed: 20669954]
271. Huang H, Hah JM, Silverman RB. J Am Chem Soc. 2001; 123:2674. [PubMed: 11456942]
272. Pant K, Bilwes AM, Adak S, Stuehr DJ, Crane BR. Biochemistry. 2002; 41:11071. [PubMed: 12220171]
273. Doukov T, Li H, Soltis M, Poulos TL. Biochemistry. 2009; 48:10246. [PubMed: 19791770]
274. Tierney DL, Huang H, Martasek P, Masters BS, Silverman RB, Hoffman BM. Biochemistry. 1999; 38:3704. [PubMed: 10090758]
275. Davydov R, Ledbetter-Rogers A, Martasek P, Larukhin M, Sono M, Dawson JH, Masters BS, Hoffman BM. Biochemistry. 2002; 41:10375. [PubMed: 12173923]
276. Garcin ED, Bruns CM, Lloyd SJ, Hosfield DJ, Tiso M, Gachhui R, Stuehr DJ, Tainer JA, Getzoff ED. J Biol Chem. 2004; 279:37918. [PubMed: 15208315]
277. Xia C, Misra I, Iyanagi T, Kim JJ. J Biol Chem. 2009; 284:30708. [PubMed: 19737939]
278. Gachhui R, Presta A, Bentley DF, Abu-Soud HM, McArthur R, Brudvig G, Ghosh DK, Stuehr DJ. J Biol Chem. 1996; 271:20594. [PubMed: 8702805]
279. Narayanasami R, Nishimura JS, McMillan K, Roman LJ, Shea TM, Robida AM, Horowitz PM, Masters BS. Nitric Oxide. 1997; 1:39. [PubMed: 9701043]
280. Li H, Das A, Sibhatu H, Jamal J, Sligar SG, Poulos TL. J Biol Chem. 2008; 283:34762. [PubMed: 18852262]
281. Sevrioukova I, Shaffer C, Ballou DP, Peterson JA. Biochemistry. 1996; 35:7058. [PubMed: 8679531]
282. Salerno JC, Ray K, Poulos T, Li H, Ghosh DK. FEBS Lett. 2013; 587:44. [PubMed: 23159936]
283. Feng C. Coord Chem Rev. 2012; 256:393. [PubMed: 22523434]
284. Feng C, Tollin G, Holliday MA, Thomas C, Salerno JC, Enemark JH, Ghosh DK. Biochemistry. 2006; 45:6354. [PubMed: 16700546]
285. Feng C, Dupont AL, Nahm NJ, Spratt DE, Hazzard JT, Weinberg JB, Guillemette JG, Tollin G, Ghosh DK. J Biol Inorg Chem. 2009; 14:133. [PubMed: 18830722]
286. Astashkin AV, Elmore BO, Fan W, Guillemette JG, Feng C. J Am Chem Soc. 2010; 132:12059. [PubMed: 20695464]
287. Persechini A, Tran QK, Black DJ, Gogol EP. FEBS Lett. 2013; 587:297. [PubMed: 23266515]

288. Panda K, Haque MM, Garcin-Hosfield ED, Durra D, Getzoff ED, Stuehr DJ. J Biol Chem. 2006; 281:36819. [PubMed: 17001078]
289. Smith BC, Underbakke ES, Kulp DW, Schief WR, Marletta MA. Proc Natl Acad Sci U S A. 2013; 110:E3577. [PubMed: 24003111]
290. Hager LP, Morris DR, Brown FS, Eberwein H. J Biol Chem. 1966; 241:1769. [PubMed: 5945851]
291. Morris DR, Hager LP. J Biol Chem. 1966; 241:3582. [PubMed: 4162151]
292. Morris DR, Hager LP. J Biol Chem. 1966; 241:1763. [PubMed: 5949836]
293. Piontek K, Ullrich R, Liers C, Diederichs K, Plattner DA, Hofrichter M. Acta Crystallogr Sect F Struct Biol Cryst Commun. 2010; 66:693.
294. Thomas JA, Morris DR, Hager LP. J Biol Chem. 1970; 245:3129. [PubMed: 5432803]
295. Hager LP, Doubek DL, Silverstein RM, Hargis JH, Martin JC. J Am Chem Soc. 1972; 94:4364. [PubMed: 4338632]
296. Sundaramoorthy M, Terner J, Poulos TL. Chem Biol. 1998; 5:461. [PubMed: 9751642]
297. Wagenknecht HA, Woggon WD. Chem Biol. 1997; 4:367. [PubMed: 9195874]
298. Manjo, KM.; Hager, LP. Proc. 14th Intl. Cof. on Cytochromes P450; Dallas (Texas). 2005. p. 139
299. Hofrichter M, Ullrich R. Appl Microbiol Biotechnol. 2006; 71:276. [PubMed: 16628447]
300. Allain EJ, Hager LP, Deng L, Jacobsen EN. J Am Chem Soc. 1993; 115:4415.
301. Kuhnel K, Blankenfeldt W, Terner J, Schlichting I. J Biol Chem. 2006; 281:23990. [PubMed: 16790441]
302. Manoj KM, Hager LP. Biochemistry. 2008; 47:2997. [PubMed: 18220360]
303. Green MT, Dawson JH, Gray HB. Science. 2004; 304:1653. [PubMed: 15192224]
304. Groves JT. J Chem Ed. 1985; 62:928.
305. Groves JT. Proc Natl Acad Sci U S A. 2003; 100:3569. [PubMed: 12655056]
306. Bordwell FG, Cheng JP, Ji GZ, Satish V, Hange ZX. J Am Chem Soc. 1991; 113:9790.
307. Sitter AJ, Reczek CM, Terner J. J Biol Chem. 1985; 260:7515. [PubMed: 3997887]
308. Dawson JH, Holm RH, Trudell JR, Barth G, Linder RE, Bunnenberg E, Djerassi C, Tang SC. J Am Chem Soc. 1976; 98:3707. [PubMed: 1270706]
309. Sigman JA, Pond AE, Dawson JH, Lu Y. Biochemistry. 1999; 38:11122. [PubMed: 10460168]
310. Antony J, Grodzicki M, Trautwien AX. J Pys Chem A. 1997; 101:2692.
311. Green MT. J Am Chem Soc. 1999; 121:7939.
312. Schoneboom JC, Lin H, Reuter N, Thiel W, Cohen S, Ogliaro F, Shaik S. J Am Chem Soc. 2002; 124:8142. [PubMed: 12095360]
313. Ogliaro F, de Visser SP, Shaik S. J Inorg Biochem. 2002; 91:554. [PubMed: 12237222]
314. Kikuchi G, Yoshida T. Mol Cell Biochem. 1983; 53–54:163.
315. Maines MD. Faseb J. 1988; 2:2557. [PubMed: 3290025]
316. Tenhunen R, Marver HS, Schmid R. Proc Natl Acad Sci U S A. 1968; 61:748. [PubMed: 4386763]
317. Tenhunen R, Marver HS, Schmid R. J Biol Chem. 1969; 244:6388. [PubMed: 4390967]
318. Farombi EO, Surh YJ. J Biochem Mol Biol. 2006; 39:479. [PubMed: 17002867]
319. Maines MD. Annu Rev Pharmacol Toxicol. 1997; 37:517. [PubMed: 9131263]
320. Maines MD. Antioxid Redox Signal. 2005; 7:1761. [PubMed: 16356137]
321. Williams SE, Wootton P, Mason HS, Bould J, Iles DE, Riccardi D, Peers C, Kemp PJ. Science. 2004; 306:2093. [PubMed: 15528406]
322. Yoshida T, Ishikawa K, Sato M. Eur J Biochem. 1991; 199:729. [PubMed: 1651244]
323. Wilks A, Black SM, Miller WL, Ortiz de Montellano PR. Biochemistry. 1995; 34:4421. [PubMed: 7703255]
324. Ratliff M, Zhu W, Deshmukh R, Wilks A, Stojiljkovic I. J Bacteriol. 2001; 183:6394. [PubMed: 11591684]
325. Schmitt MP. J Bacteriol. 1997; 179:838. [PubMed: 9006041]

326. Zhu W, Wilks A, Stojiljkovic I. J Bacteriol. 2000; 182:6783. [PubMed: 11073924]
327. Schuller DJ, Wilks A, Ortiz de Montellano PR, Poulos TL. Nat Struct Biol. 1999; 6:860. [PubMed: 10467099]
328. Friedman J, Lad L, Li H, Wilks A, Poulos TL. Biochemistry. 2004; 43:5239. [PubMed: 15122889]
329. Hirotsu S, Chu GC, Unno M, Lee DS, Yoshida T, Park SY, Shiro Y, Ikeda-Saito M. J Biol Chem. 2004; 279:11937. [PubMed: 14645223]
330. Schuller DJ, Zhu W, Stojiljkovic I, Wilks A, Poulos TL. Biochemistry. 2001; 40:11552. [PubMed: 11560504]
331. Sugishima M, Omata Y, Kakuta Y, Sakamoto H, Noguchi M, Fukuyama K. FEBS Lett. 2000; 471:61. [PubMed: 10760513]
332. Bianchetti CM, Yi L, Ragsdale SW, Phillips GN Jr. J Biol Chem. 2007; 282:37624. [PubMed: 17965015]
333. Caignan GA, Deshmukh R, Wilks A, Zeng YH, Huang HW, Moenne-Loccoz P, Bunce RA, Eastman MA, Rivera M. J Am Chem Soc. 2002; 124:14879. [PubMed: 12475329]
334. Matsui T, Iwasaki M, Sugiyama R, Unno M, Ikeda-Saito M. Inorg Chem. 2010; 49:3602. [PubMed: 20380462]
335. Matsui T, Unno M, Ikeda-Saito M. Acc Chem Res. 2010; 43:240. [PubMed: 19827796]
336. Unno M, Matsui T, Ikeda-Saito M. Nat Prod Rep. 2007; 24:553. [PubMed: 17534530]
337. Wilks A, Ortiz de Montellano PR. J Biol Chem. 1993; 268:22357. [PubMed: 8226746]
338. Ortiz de Montellano PR. Acc Chem Res. 1998; 31:543.
339. Wilks A, Torpey J, Ortiz de Montellano PR. J Biol Chem. 1994; 269:29553. [PubMed: 7961940]
340. Matsui T, Kim SH, Jin H, Hoffman BM, Ikeda-Saito M. J Am Chem Soc. 2006; 128:1090. [PubMed: 16433521]
341. Unno M, Matsui T, Chu GC, Couture M, Yoshida T, Rousseau DL, Olson JS, Ikeda-Saito M. J Biol Chem. 2004; 279:21055. [PubMed: 14966119]
342. Davydov RM, Yoshida T, Ikeda-Saito M, Hoffman BM. J Am Chem Soc. 1999; 121:10656.
343. Denisov IG, Ikeda-Saito M, Yoshida T, Sligar SG. Febs Lett. 2002; 532:203. [PubMed: 12459490]
344. Garcia-Serres R, Davydov RM, Matsui T, Ikeda-Saito M, Hoffman BM, Huynh BH. J Am Chem Soc. 2007; 129:1402. [PubMed: 17263425]
345. Davydov R, Matsui T, Fujii H, Ikeda-Saito M, Hoffman BM. J Am Chem Soc. 2003; 125:16208. [PubMed: 14692760]
346. Kumar D, de Visser SP, Shaik S. J Am Chem Soc. 2005; 127:8204. [PubMed: 15926850]
347. Sharma PK, Kevorkiants R, de Visser SP, Kumar D, Shaik S. Angew Chem Int Ed Engl. 2004; 43:1129. [PubMed: 14983454]
348. Matera KM, Takahashi S, Fujii H, Zhou H, Ishikawa K, Yoshimura T, Rousseau DL, Yoshida T, Ikeda-Saito M. J Biol Chem. 1996; 271:6618. [PubMed: 8636077]
349. Migita CT, Fujii H, Mansfield Matera K, Takahashi S, Zhou H, Yoshida T. Biochim Biophys Acta. 1999; 1432:203. [PubMed: 10407142]
350. Ortiz de Montellano PR. J Am Chem Soc. 1997; 31:543.
351. Liu Y, Moenne-Loccoz P, Loehr TM, Ortiz de Montellano PR. J Biol Chem. 1997; 272:6909. [PubMed: 9054378]
352. Morishima I, Fujii H, Shiro Y, Sano S. Inorg Chem. 1995; 34
353. Docherty JC, Schacter BA, Firneisz GD, Brown SB. J Biol Chem. 1984; 259:13066. [PubMed: 6436242]
354. Lai W, Chen H, Matsui T, Omori K, Unno M, Ikeda-Saito M, Shaik S. J Am Chem Soc. 2010; 132:12960. [PubMed: 20806922]
355. Kotake Y, Masayama T. Z Physiol Chem. 1936; 243:237.
356. Knox WE, Mehler AH. J Biol Chem. 1950; 187:419. [PubMed: 14794727]
357. Tanaka T, Knox WE. J Biol Chem. 1959; 234:1162. [PubMed: 13654338]
358. Yamamoto S, Hayaishi O. J Biol Chem. 1967; 242:5260. [PubMed: 6065097]

359. Platten M, Wick W, Van den Eynde BJ. Cancer Res. 2012; 72:5435. [PubMed: 23090118]
360. Munn DH, Zhou M, Attwood JT, Bondarev I, Conway SJ, Marshall B, Brown C, Mellor AL. Science. 1998; 281:1191. [PubMed: 9712583]
361. Sono M, Roach MP, Coulter ED, Dawson JH. Chem Rev. 1996; 96:2841. [PubMed: 11848843]
362. Efimov I, Basran J, Thackray SJ, Handa S, Mowat CG, Raven EL. Biochemistry. 2011; 50:2717. [PubMed: 21361337]
363. Sugimoto H, Oda S, Otsuki T, Hino T, Yoshida T, Shiro Y. Proc Natl Acad Sci U S A. 2006; 103:2611. [PubMed: 16477023]
364. Forouhar F, Anderson JL, Mowat CG, Vorobiev SM, Hussain A, Abashidze M, Bruckmann C, Thackray SJ, Seetharaman J, Tucker T, Xiao R, Ma LC, Zhao L, Acton TB, Montelione GT, Chapman SK, Tong L. Proc Natl Acad Sci U S A. 2007; 104:473. [PubMed: 17197414]
365. Zhang Y, Kang SA, Mukherjee T, Bale S, Crane BR, Begley TP, Ealick SE. Biochemistry. 2007; 46:145. [PubMed: 17198384]
366. Shimizu T, Nomiyama S, Hirata F, Hayaishi O. J Biol Chem. 1978; 253:4700. [PubMed: 26687]
367. Hamilton GA. Adv Enzymol Relat Areas Mol Biol. 1969; 32:55. [PubMed: 4978050]
368. Cady SG, Sono M. Arch Biochem Biophys. 1991; 291:326. [PubMed: 1952947]
369. Batabyal D, Yeh SR. J Am Chem Soc. 2009; 131:3260. [PubMed: 19209904]
370. Chauhan N, Basran J, Rafice SA, Efimov I, Millett ES, Mowat CG, Moody PC, Handa S, Raven EL. Febs J. 2012; 279:4501. [PubMed: 23083473]
371. Terentis AC, Thomas SR, Takikawa O, Littlejohn TK, Truscott RJ, Armstrong RS, Yeh SR, Stocker R. J Biol Chem. 2002; 277:15788. [PubMed: 11867636]
372. Chung LW, Li X, Sugimoto H, Shiro Y, Morokuma K. J Am Chem Soc. 2008; 130
373. Chauhan N, Thackray SJ, Rafice SA, Eaton G, Lee M, Efimov I, Basran J, Jenkins PR, Mowat CG, Chapman SK, Raven EL. J Am Chem Soc. 2009; 131:4186. [PubMed: 19275153]
374. Lewis-Ballester A, Batabyal D, Egawa T, Lu C, Lin Y, Marti MA, Capece L, Estrin DA, Yeh S-R. Proc Natl Acad Sci U S A. 2009; 106
375. Basran J, Efimov I, Chauhan N, Thackray SJ, Krupa JL, Eaton G, Griffith GA, Mowat CG, Handa S, Raven EL. J Am Chem Soc. 2011; 133:16251. [PubMed: 21892828]
376. Capece L, Lewis-Ballester A, Yeh S-R, Estrin DA, Marti MA. J Phys Chem B. 2012; 116
377. McIntire WS, Wemmer DE, Chistoserdov A, Lidstrom ME. Science. 1991; 252:817. [PubMed: 2028257]
378. Wilmot CM, Yukl ET. Dalton Trans. 2013; 42:3127. [PubMed: 23086017]
379. Davidson VL, Wilmot CM. Annu Rev Biochem. 2013; 82:531. [PubMed: 23746262]
380. Jensen LM, Sanishvili R, Davidson VL, Wilmot CM. Science. 2010; 327:1392. [PubMed: 20223990]
381. Li X, Fu R, Liu A, Davidson VL. Biochemistry. 2008; 47:2908. [PubMed: 18220357]
382. Li X, Fu R, Lee S, Krebs C, Davidson VL, Liu A. Proc Natl Acad Sci U S A. 2008; 105:8597. [PubMed: 18562294]
383. Li X, Feng M, Wang Y, Tachikawa H, Davidson VL. Biochemistry. 2006; 45:821. [PubMed: 16411758]
384. Tarboush NA, Jensen LM, Yukl ET, Geng J, Liu A, Wilmot CM, Davidson VL. Proc Natl Acad Sci U S A. 2011; 108:16956. [PubMed: 21969534]
385. Geng J, Dornevil K, Davidson VL, Liu A. Proc Natl Acad Sci U S A. 2013; 110:9639. [PubMed: 23720312]
386. Petsko GA. Genome Biol. 2007; 8:107. [PubMed: 17608958]
387. Lamb DC, Lei L, Warrilow AG, Lepesheva GI, Mullins JG, Waterman MR, Kelly SL. J Virol. 2009; 83:8266. [PubMed: 19515774]
388. Meharenna YT, Li H, Hawkes DB, Pearson AG, De Voss J, Poulos TL. Biochemistry. 2004; 43:9487. [PubMed: 15260491]
389. Hecker M, Ullrich V. J Biol Chem. 1989; 264:141. [PubMed: 2491846]
390. Grechkin AN, Bruhlmann F, Mukhtarova LS, Gogolev YV, Hamberg M. Biochim Biophys Acta. 2006; 1761:1419. [PubMed: 17049304]

Biography

Thomas L. Poulos was born in Monterey California on Feb., 1947. After graduation from Carmel High School he earned a B.A. degree in Zoology at the University of California, Santa Barbara in 1968 followed by a PhD in Biology in 1972 at the University of California at San Diego (UCSD). He then moved to the Chemistry Department at UCSD for postdoctoral work in the protein crystallography lab of Joe Kraut. While at UCSD he solved the first heme enzyme crystal structure, cytochrome c peroxidase, and initiated work on P450s. In 1983 he was recruited to Genex Corp. in Gaithersburg MD where he held the position of Principal Research Scientist and then Director of Protein Engineering. It was during this time that he solved the first cytochrome P450 structure. In 1987 he moved to the University of Maryland where he was a Professor of Chemistry and Director of the Center for Advanced Research in Biotechnology. In 1992 he moved to the Department of Molecular Biology and Biochemistry at UCI where he now holds the title of Chancellor's Professor and joint appointments in the Departments of Chemistry and Pharmaceutical Sciences. In 1991 he won the Presidential Meritorious Service Award from the University of Maryland, in 2004 the Brodie Award from the American Society of Experimental Pharmacology and Therapeutics, and in 2014 the Gordon Hammes Biochemistry ACS Lectureship. His primary research interests are in heme enzyme structure and function and structure-based drug design.

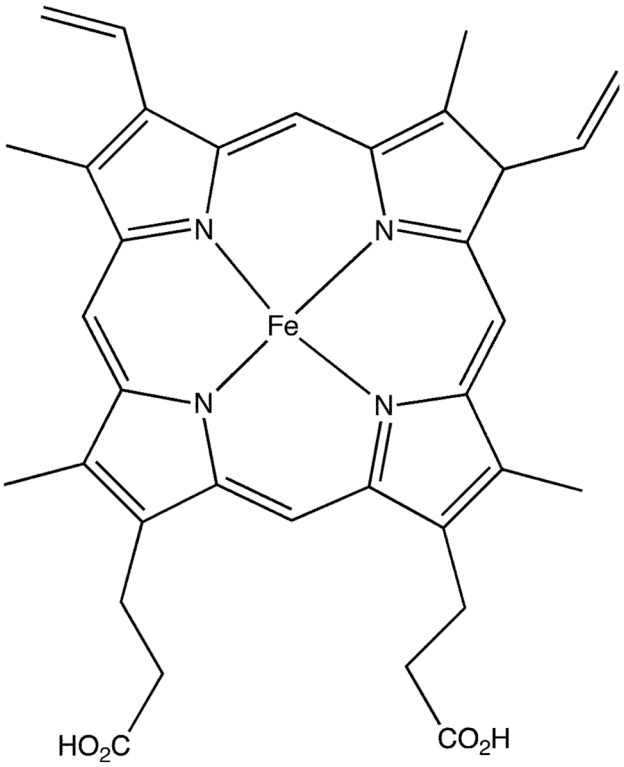

Figure 1.
Structure of iron protoporphyrin IX.

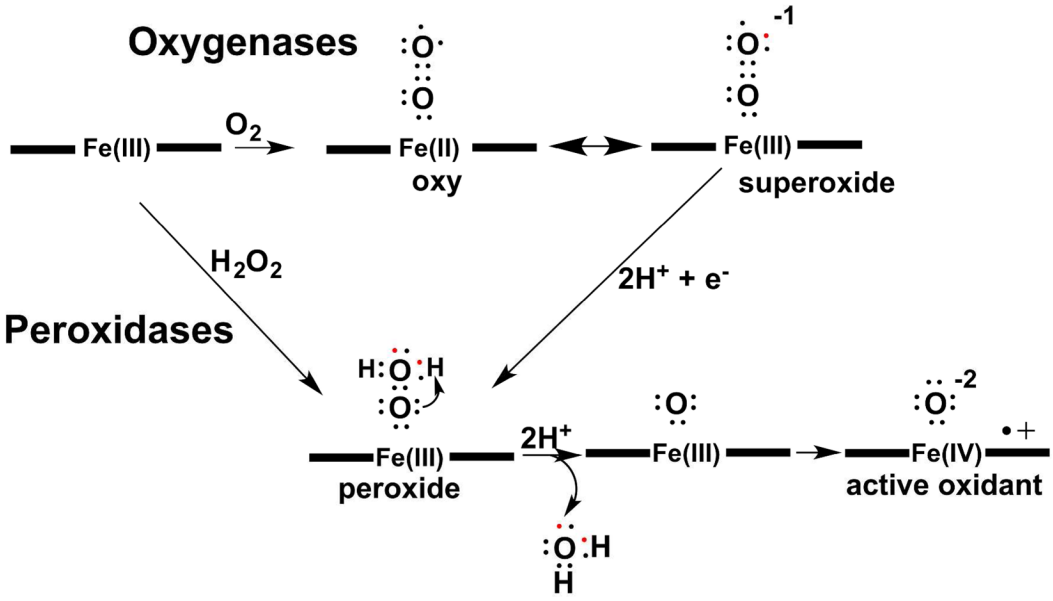

Figure 2.

Oxygen and peroxide activation by heme enzymes. Oxygenases like P450 must have the iron reduced to ferrous (Fe(II) or Fe^{2+}) before O_2 can bind. The oxy complex is best described as ferric-superoxide, Fe(III)-OO^{-}. A second electron transfer results in reduction of superoxide to the peroxide level. At this point the P450 and peroxidase mechanisms are similar. The distal O atom must be protonated to ensure heterolytic cleavage of the O-O bond resulting in the departure of water which leaves behind an O atom with only 6 valence electrons. A rearrangement of oxidizing equivalents results in the active oxidant often called Compound I.

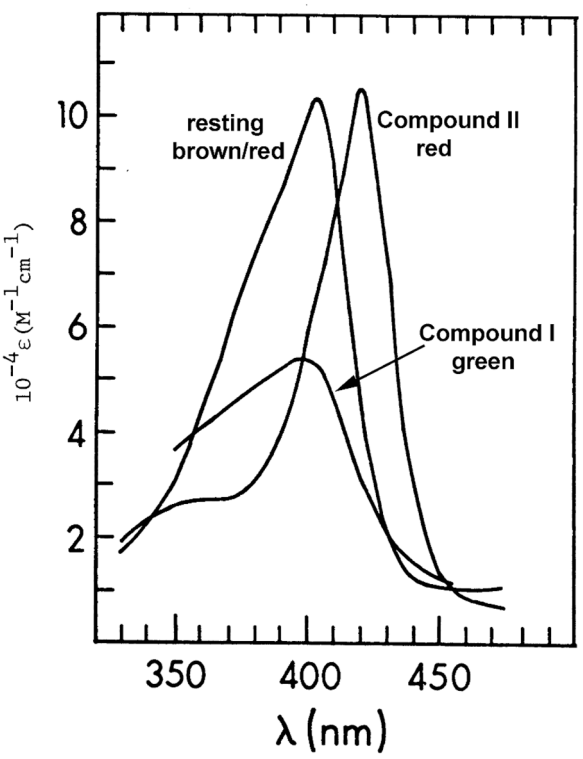

Figure 3.
Spectra of the various intermediates in HRP catalysis. This figure was adapted from Dunford.[10]

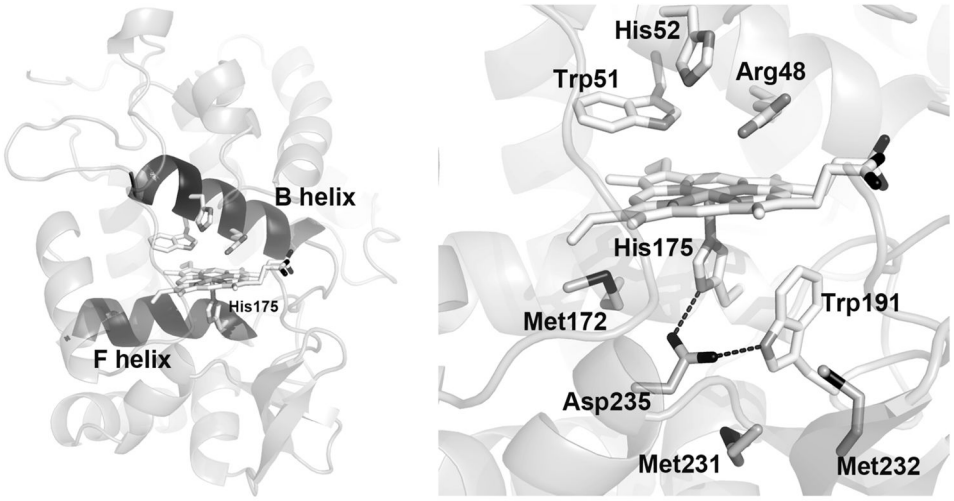

Figure 4.

Crystal structure of yeast cytochrome c peroxidase (CCP). The F helix contains the proximal His175 heme ligand which is H-bonded to the conserved Asp235. The B helix provides the His52 acid-base catalyst and Arg48 which helps to stabilize the ferryl center in Compound I. Trp191 forms a cation radical in Compound I.[15]

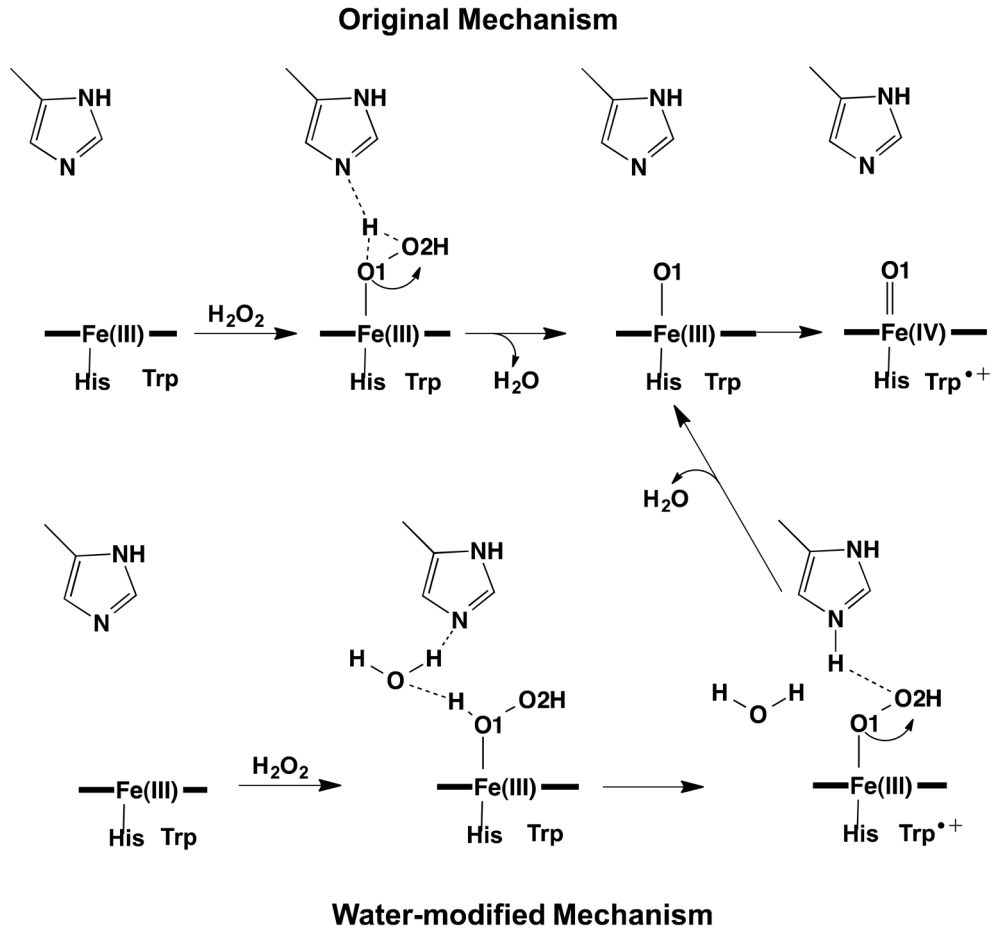

Figure 5.

Mechanism of peroxidase Compound I formation. In the original mechanism[32] the distal His shuttles the peroxide O1 proton to the O2 oxygen which promotes heterolysis of the O-O bond. However, the distal His is too far from O1 for direct H-bonding so in the modified mechanism,[39] a water molecule assists in the transfer of the O1 proton to O2.

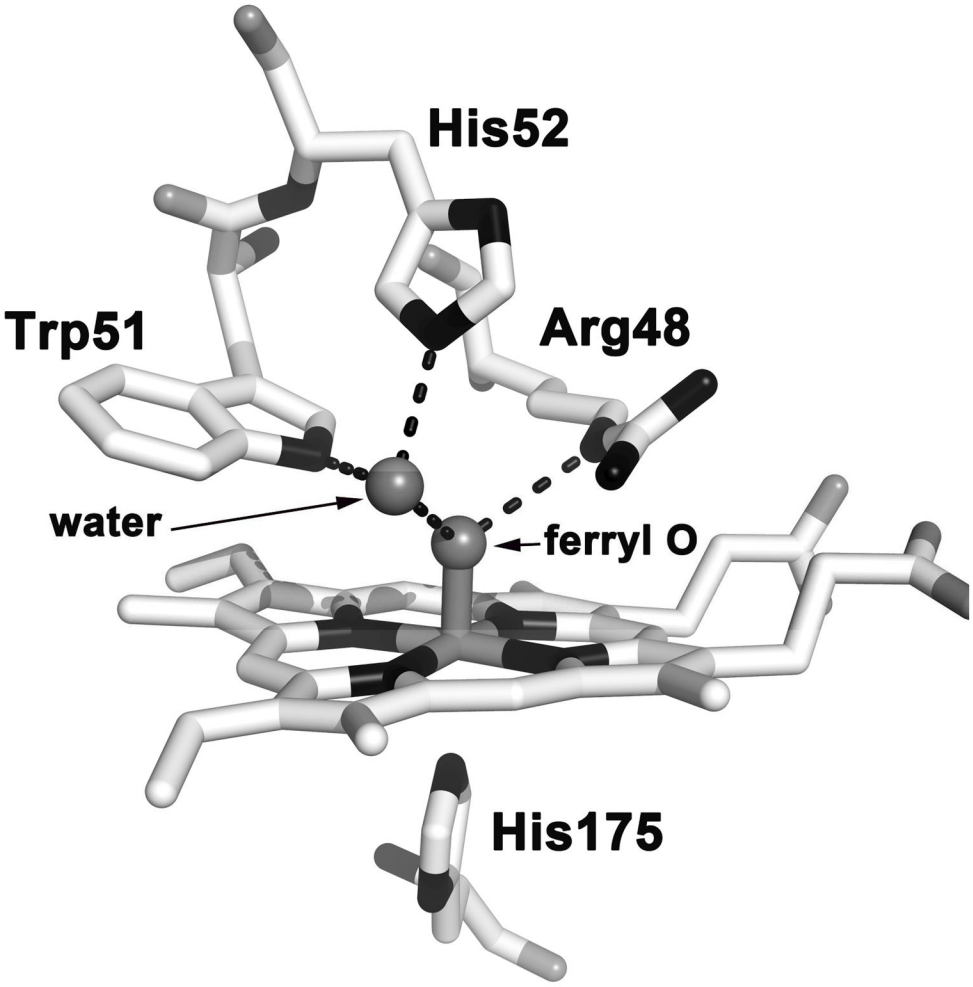

Figure 6.
Crystal structure of CCP Compound I[38] which is basically the same as the HRP Compound I structure.[37] The water molecule H-bonded to the ferryl O atom is ideally positioned to assist His52 in acid-base catalysis as suggested.[39]

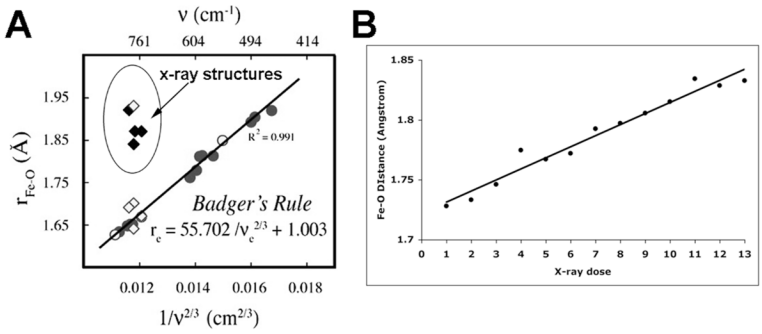

Figure 7.

A) Plot of computed stretching frequency vs. Fe-O bond distance (dark and clear circles, adapted from Green[50]). Clear diamonds are from resonance Raman or EXAFS, and the dark diamonds from x-ray crystal structures. A majority of the experimental determinations from EXAFS and resonance Raman fit well to the theoretical plot. The main outliers that overestimate the distance are derived from crystals structures. **B)** Plot of x-ray dose vs. the Fe-O bond distance in CCP Compound I adapted from Meharenna et al.[38]. This plot was based on the refinement of 13 crystal structures with increasing x-ray dose. The plot extrapolates back to a Fe-O bond distance of 1.72Å to be compared with 1.68Å obtained from resonance Raman data.[41]

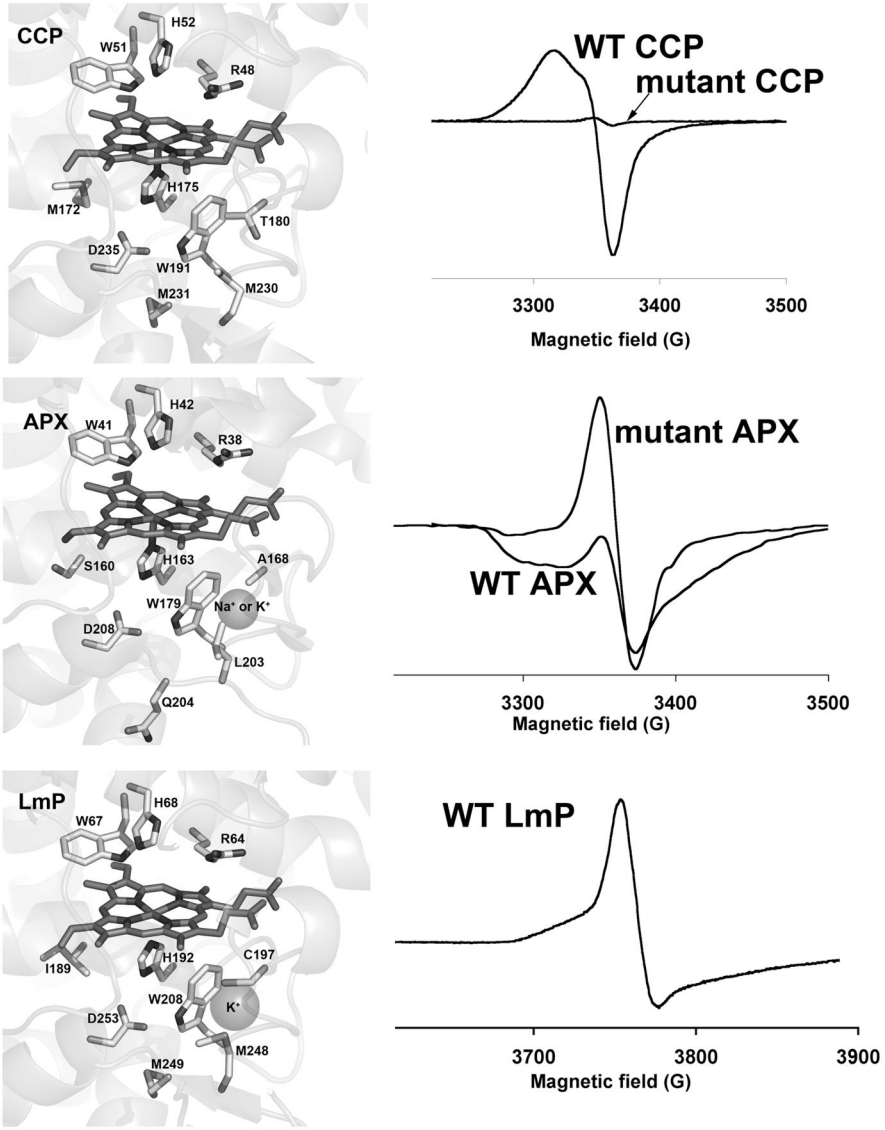

Figure 8.

Location of the monovalent cation in APX and LmP (water in CCP) that is about 8Å from the proximal pocket Trp. The EPR spectra are of the Trp radical in all three peroxidases for both wild type and mutant forms. In CCP the mutant spectrum was generated from a CCP where the APX K^+ site was introduced.[66,68] For the APX mutant the three Met residues important for stabilizing the Trp radical in CCP were introduced.[72] For wild type APX the radical is about 0.09 spin equivalents while for the mutant this increases to 0.24. These experiments illustrate that it is possible to turn on/off the Trp radical signal by modifying the local electrostatic environment.

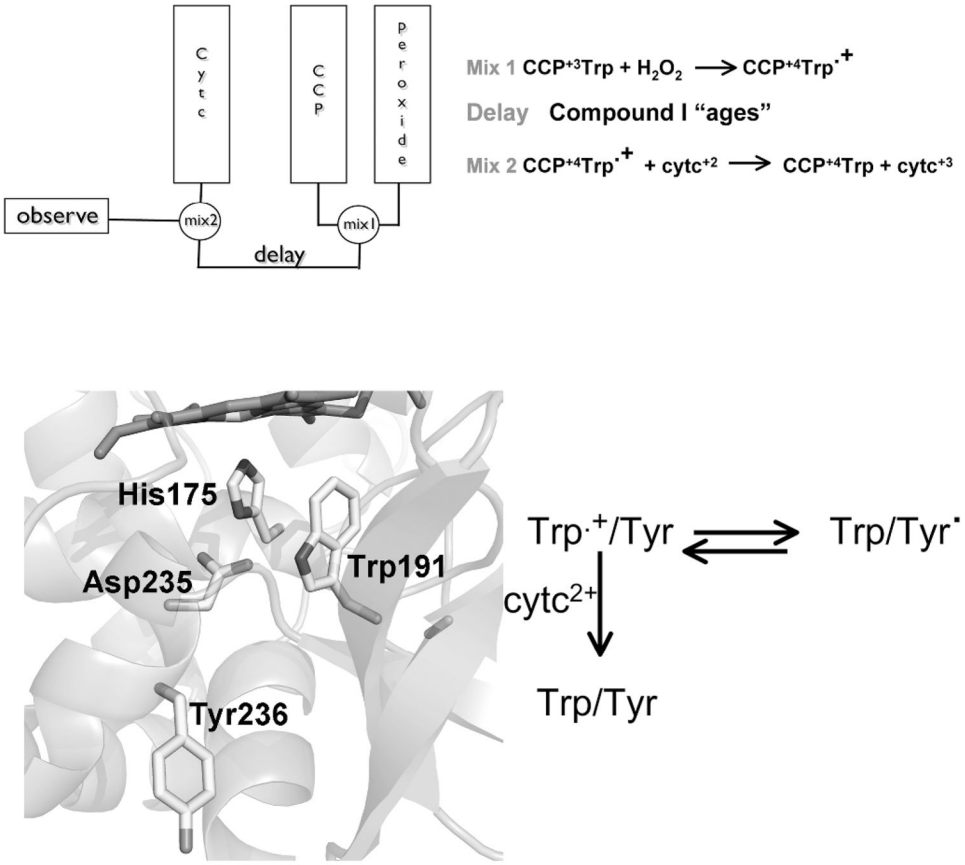

Figure 9.

Outline of the stopped flow method used to measure the life time of the Trp radical in various mutants of CCP. This approach centers on the fact that rapid electron transfer from Cyt c to CCP Compound I requires the Trp radical. In a double mix experiment, CCP Compound I is formed in the first mix, allowed to age for various delay times, and then in the second mix reduced Cyt c is added. As the Trp radical decays the rate and extent of Cyt c oxidation will decrease as the delay time is increased. Mutating Tyr236 to Phe increases the lifetime of the Trp191 radical even in the CCP mutants designed to have a destabilized Trp191 radical. The most likely reason is that the Trp191 radical has been kinetically trapped since the nearest Tyr residue capable of forming a relatively stable radical, Tyr236, has been changed to Phe.

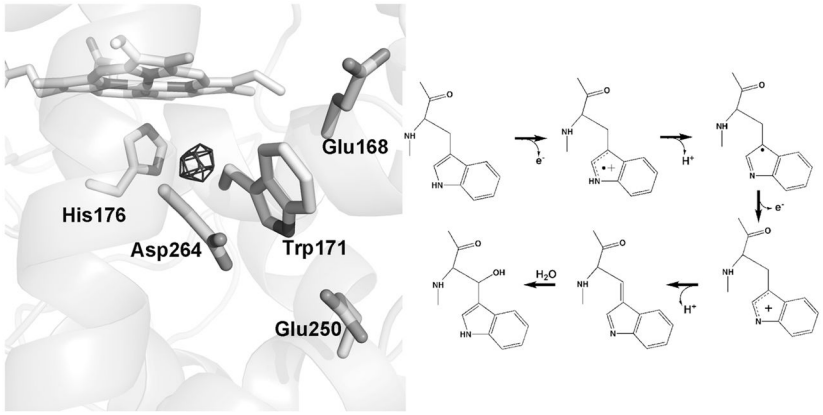

Figure 10.

An early unpublished Fo-Fc electron density map from our lab showing a large lobe of difference density about 1.5Å from the Cβ carbon of Trp171. The proposed mechanism involves oxidation of Trp171 by Compound I.[84]

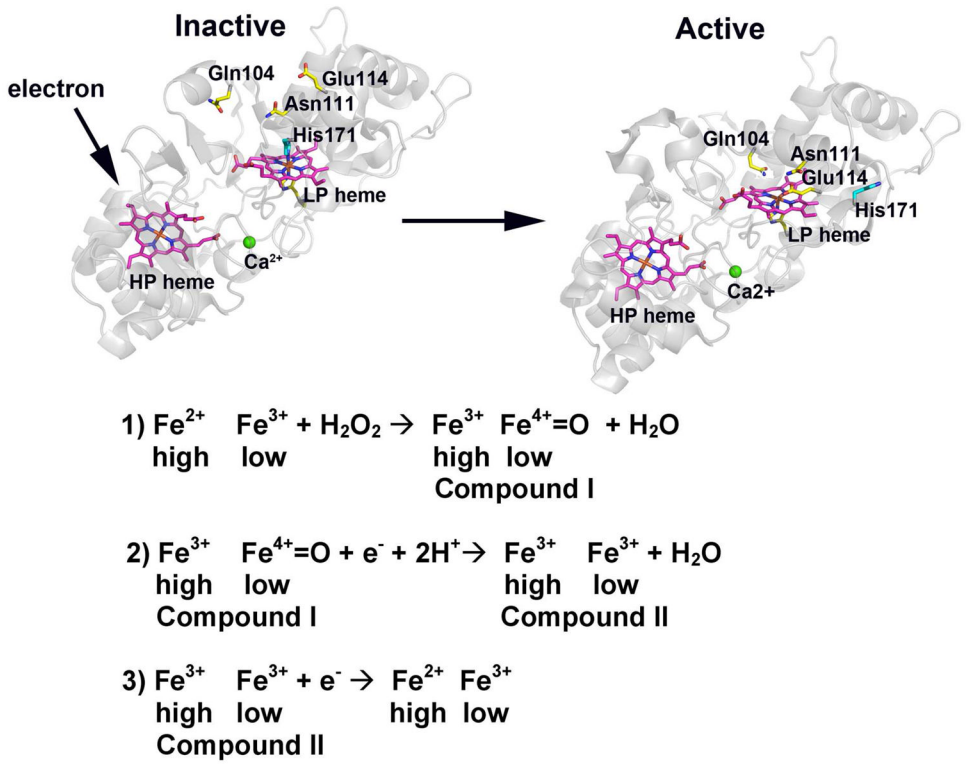

Figure 11.

Structure and mechanism of diheme bacterial cytochrome c peroxidases. In the inactive state both the LP (low potential) and HP (high potential) hemes are Fe^{3+} and low spin. Upon reduction of the HP heme, the His171 LP heme ligand is displaced and swings out to the surface which frees up one axial coordination position for peroxide binding. In addition Glu114 moves from the surface into the active site where it likely serves an acid-base catalytic role in Compound I formation. The overall mechanism is very similar to other peroxidases except a porphyrin or amino acid radical is not involved. Instead the second electron required for peroxide activation derives from the HP heme.

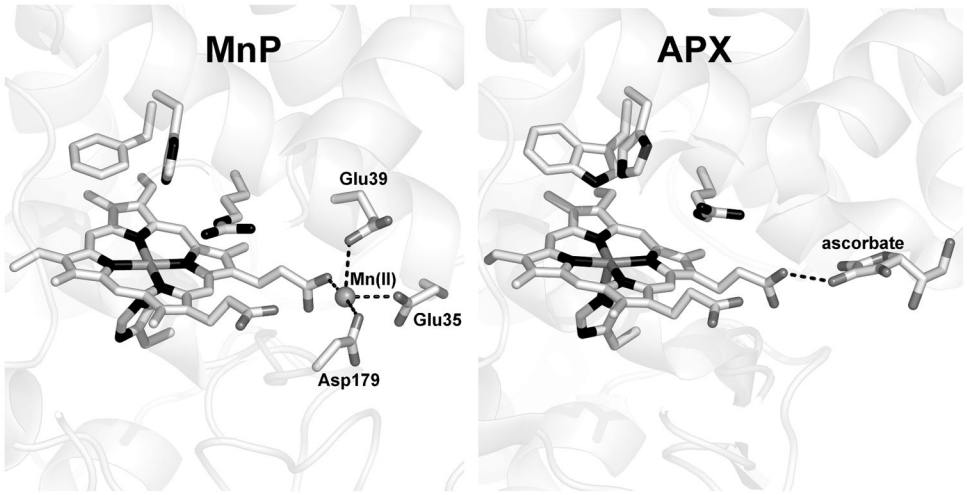

Figure 12.
Substrate binding sites in manganese (MnP)[109] and ascorbate (APX)[98] peroxidases. Both use one heme propionate for binding which provides a direct electron transfer path along the heme propionate to the porphryin radical and Fe(IV) center.

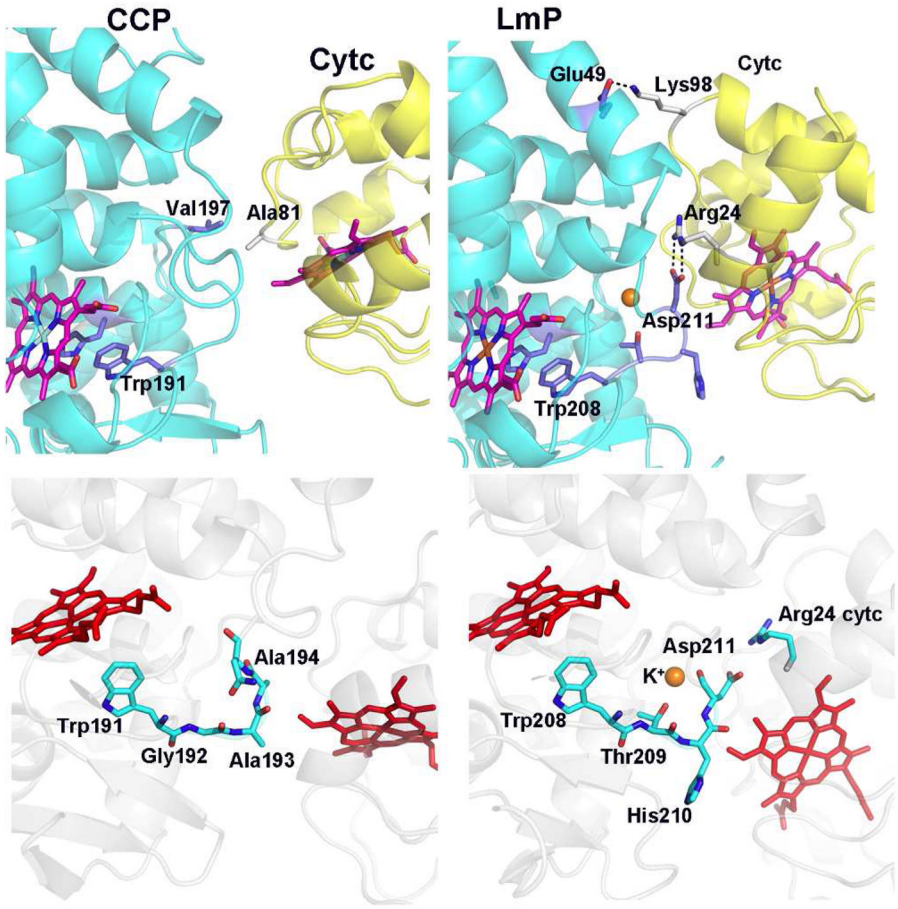

Figure 13.

Crystal structures of the CCP-Cyt c[119] and LmP-Cyt c[124] complexes. The peroxidases are oriented the same which shows that the cyt c, while binding to the same surface, is oriented quite differently. In the LmP-Cyt c complex one strong (Arg24-Asp211) and one weaker salt bridges (Lys98-Glu49) form while there are no ion pairs in the yeast CCP-Cyt c complex. Although the cyt cs differ in orientation, the heme edge of cyt c contacts the same section of polypeptide in both complexes so the ET distance is the same. However, the types of amino acids and local electrostatic environment along the ET path are substantially different.

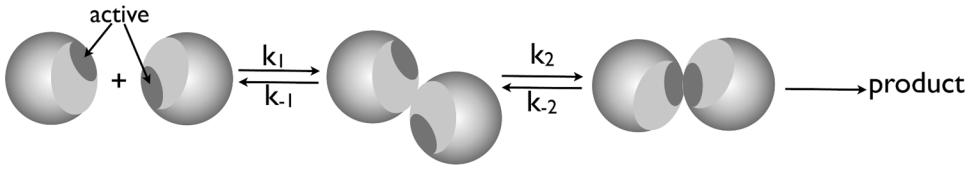

Figure 14.

A scheme showing the interaction between redox partners. The large complementary electrostatic surfaces (light gray) result in rapid formation of the initial inter-protein complex. The active interaction regions (dark gray) are much smaller so redox partners must sample each other's surfaces before the ET active orientation is reached which is governed by k_2. The actual ET event is fast so the rate limiting step under steady state conditions can be a complicated mix of the various rate constants which are heavily influenced by ionic strength.

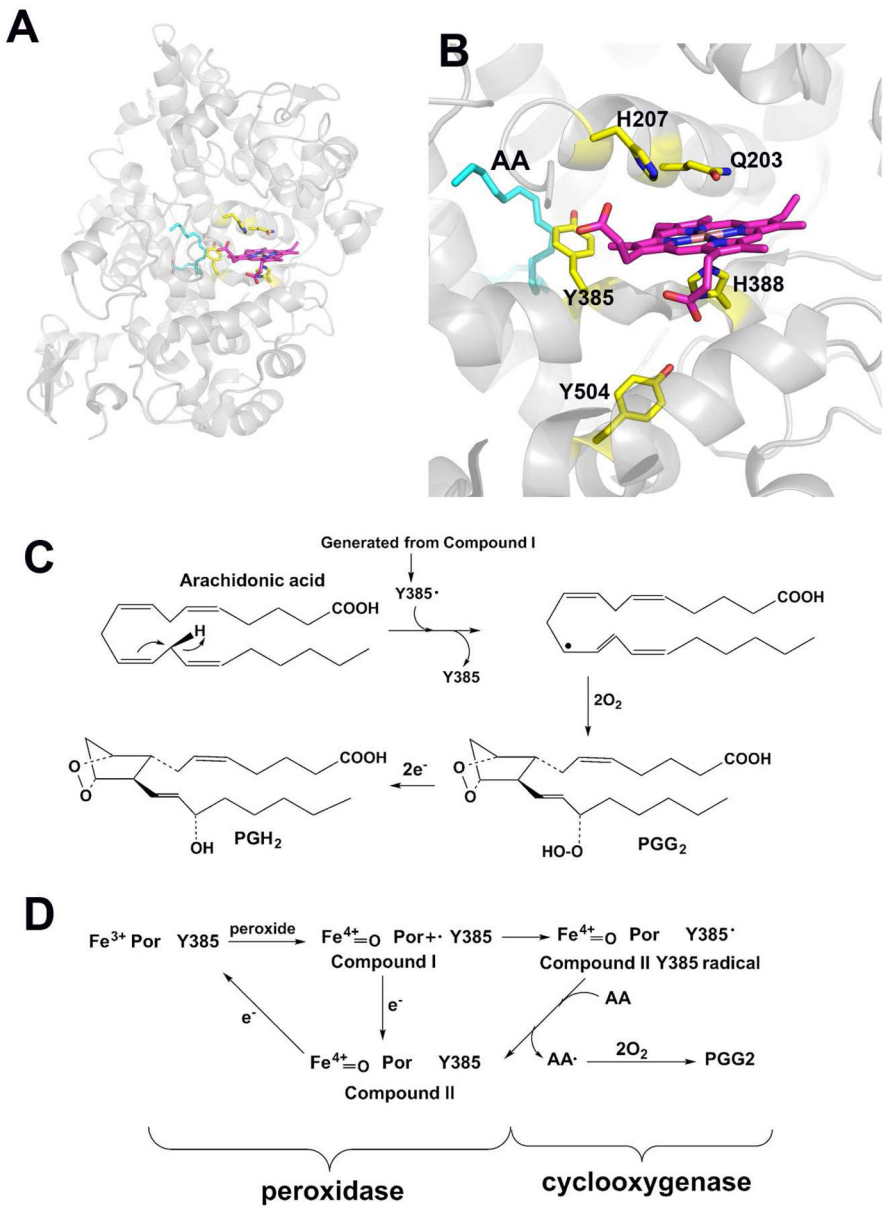

Figure 15.

Crystal structure and mechanism of prostaglandin H synthase. **A)** Overall view. **B)** Active site structure showing how arachidonic acid (cyan color labeled AA) binds. Tyr385 forms a radical upon oxidation with peroxide. The resulting Tyr385 abstracts an H atom from AA leading to subsequent reactions with oxygen to give the final products. **C)** Overall mechanism for the conversion of arachidonic acid to PGH_2. The Tyr385 radical abstracts an H atom from arachidonic acid and the resulting radical intermediate reacts with 2 O_2 molecules to give PGG_2. PGG_2 can be converted to PGH_2 by serving as the peroxide substrate in forming Compound I or PGG_2 is reduced by endogenous reductants to give PGH_2. **D)** Overall PGHS reaction cycle.[126] In the presence of a suitable reducing substrate the peroxidase part of the reaction functions independent of the cyclooxygenase reaction. However, the cyclooxygenase activity requires the Tyr385 radical which forms by reaction with Compound I generated by the peroxidase reaction.

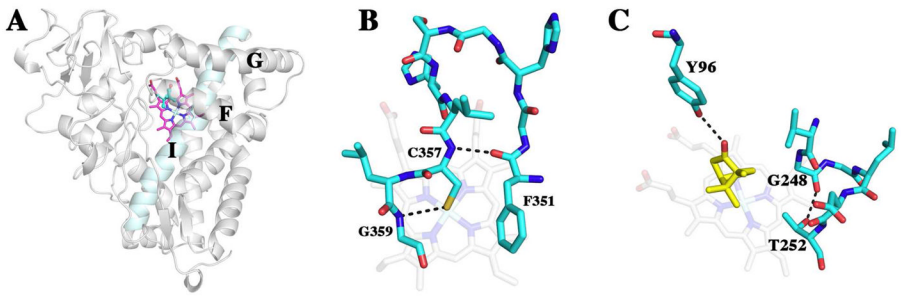

Figure 16.

Crystal structure of P450cam.[147] **A)** Overall structure viewed looking along the heme normal with the substrate binding site facing the viewer. The I helix runs directly over the heme and provides part of the O_2 binding pocket. **B)** Detailed structure around the Cys357 heme ligand. This structure is highly conserved in all P450s and forms a tight β-bulge structure. Note the H-bond between the Cys357 S atom and a peptide NH group which helps to modulate the heme iron redox potential. **C)** Close up of the I helix near the O_2 binding site. The local helical H-bonding pattern is disrupted and Gly248 no longer participates in an α–helical H-bond but instead accepts an H-bond from the highly conserved Thr252.

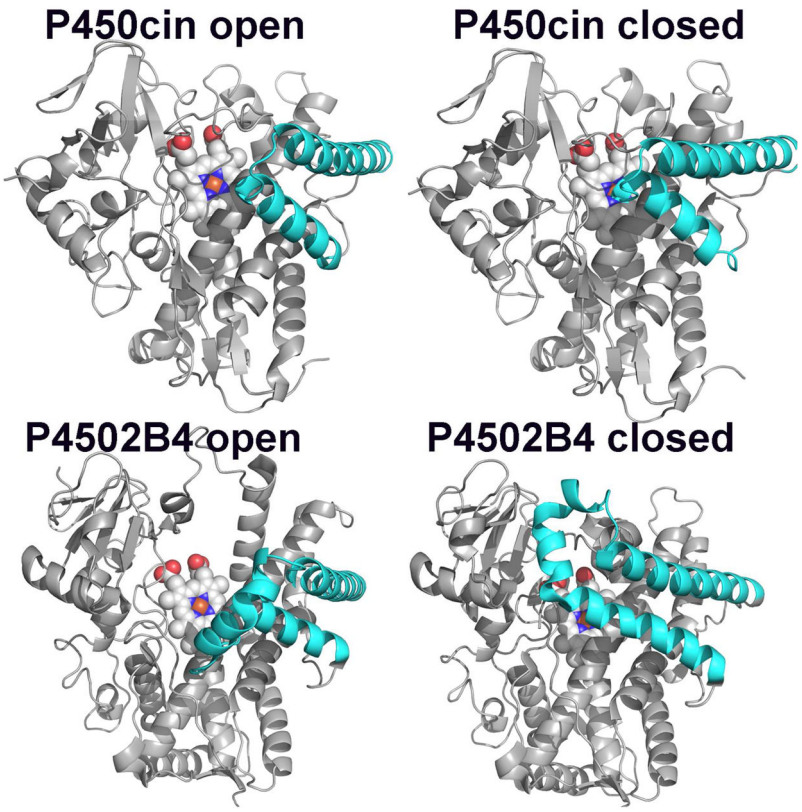

Figure 17.
Some examples of open and closed structures in bacterial P450cin[218,388] and mammalian P4502B4.[151,152] The F and G helices which experience the largest movement are in cyan.

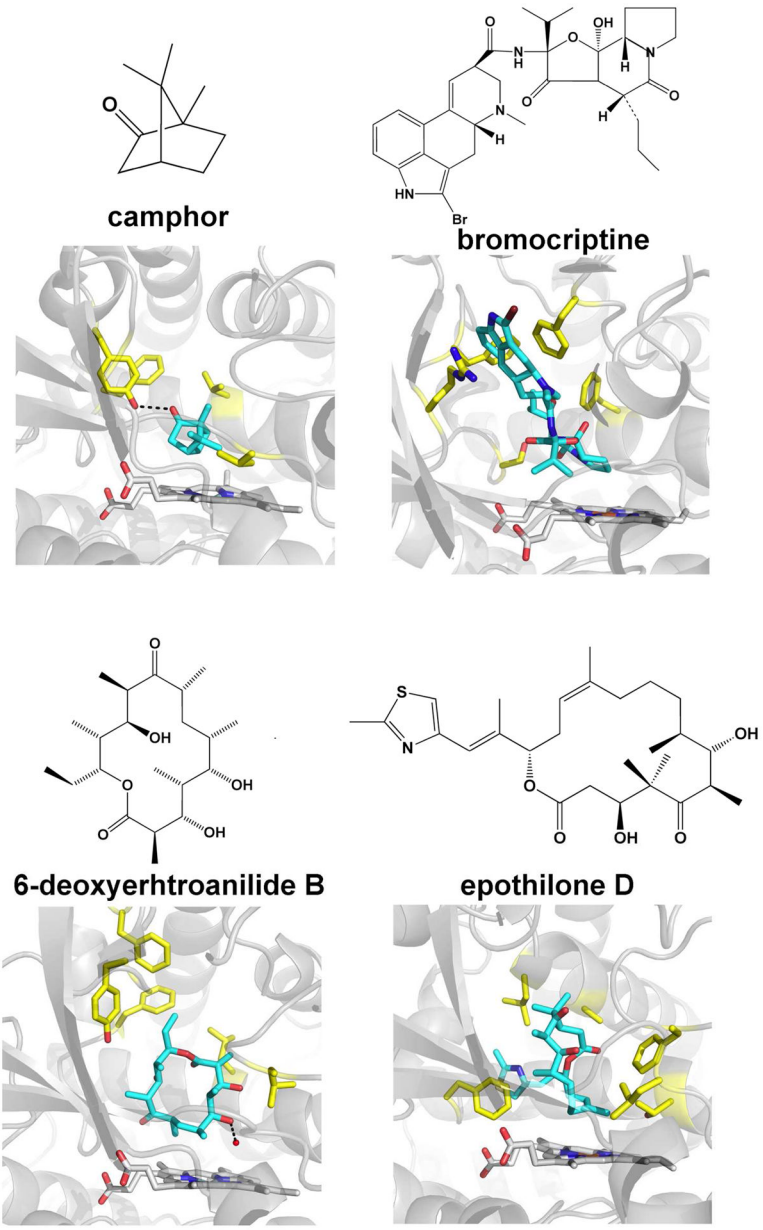

Figure 18.

Crystal structures solved in our lab of various P450-substrate complexes. They vary widely in size, shape, and polarity. In some cases, as in P450eryF, water participates directly in substrate binding by forming an H-bonding bridge between the substrate and protein. In all these and other examples, the atom to be hydroxylated is within 4–5Å to the iron and thus can directly interact with the Fe(IV)=O O atom.

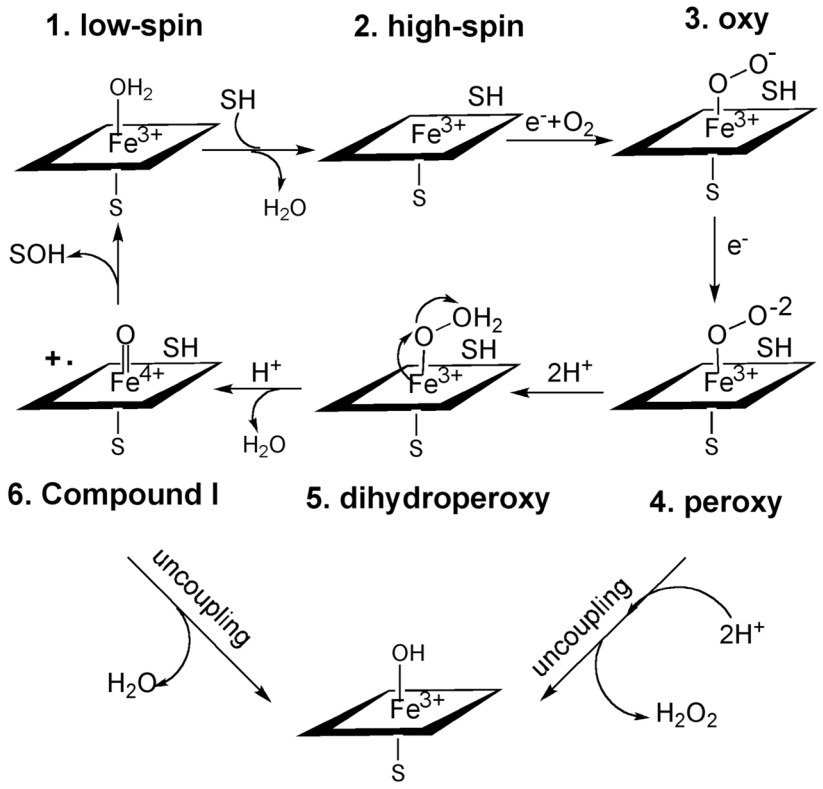

Figure 19.

P450 starts off as low-spin hexacoordinate and when substrate (SH) binds, the axial water ligand is displaced and the heme shifts to high spin and the redox potential increases. This enables electron transfer from the redox partner to proceed to give the oxy complex. This is followed by a second electron transfer step that ultimately generates the dihydroperoxy species which undergoes heterolytic cleavage to give Compound I.

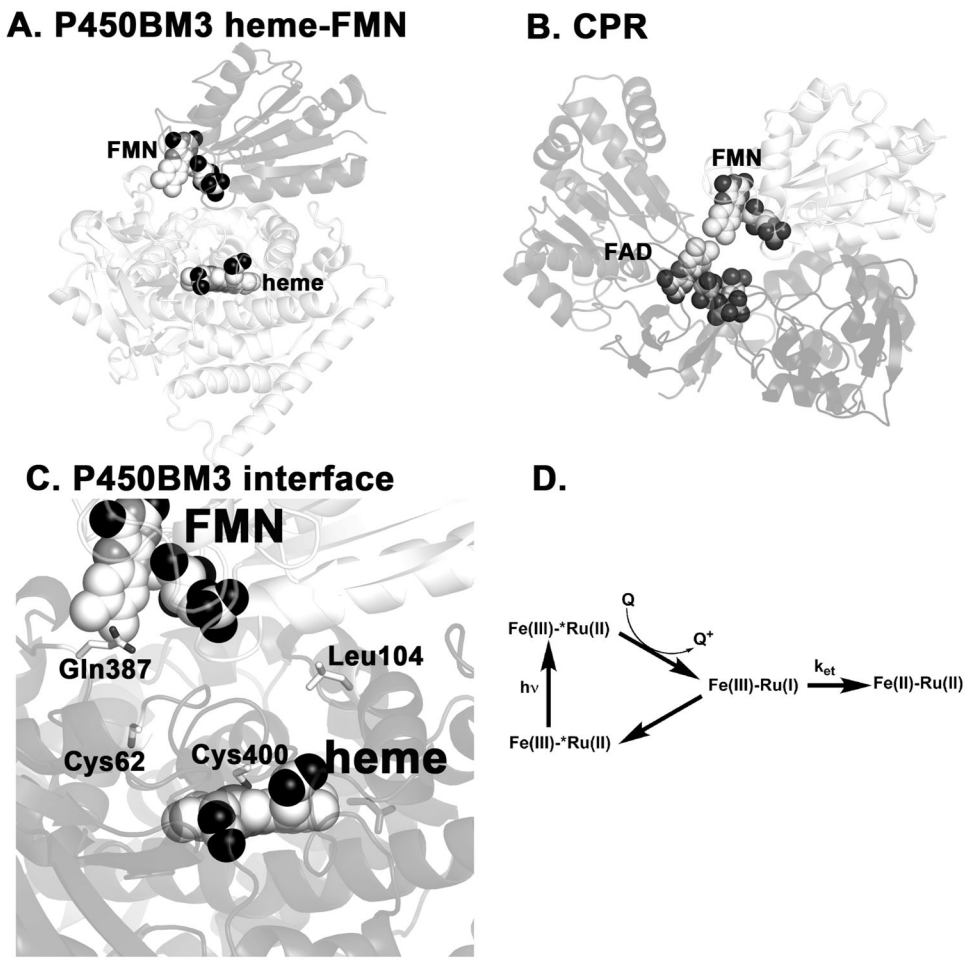

Figure 20.

A) Overall structure of P450BM3 complexed with its redox partner.[164] **B)** Structure of P450 reductase.[170] The FMN and FAD cofactors are in direct contact and it now is generally thought that the FMN module must dissociate and reorient in order for the FMN domain to properly dock to the P450. **C)** Close up view of the P450BM3-redox partner interface. Specific groups at the interface were chemically modified to probe the importance of these residues and these studies proved to be consistent with the crystal structure.[172] Glu387Cys and Cys62 were labeled with a Ru reagent to enable photo-induced electron transfer (panel **D**) to be measured.[173] ET from Cys387 proceeds rapidly but not from Cys62 despite the Cys-iron distance being about the same. This result indicates that ET along the polypeptide from the modified Gln387Cys to Cys400 is the preferred ET path.

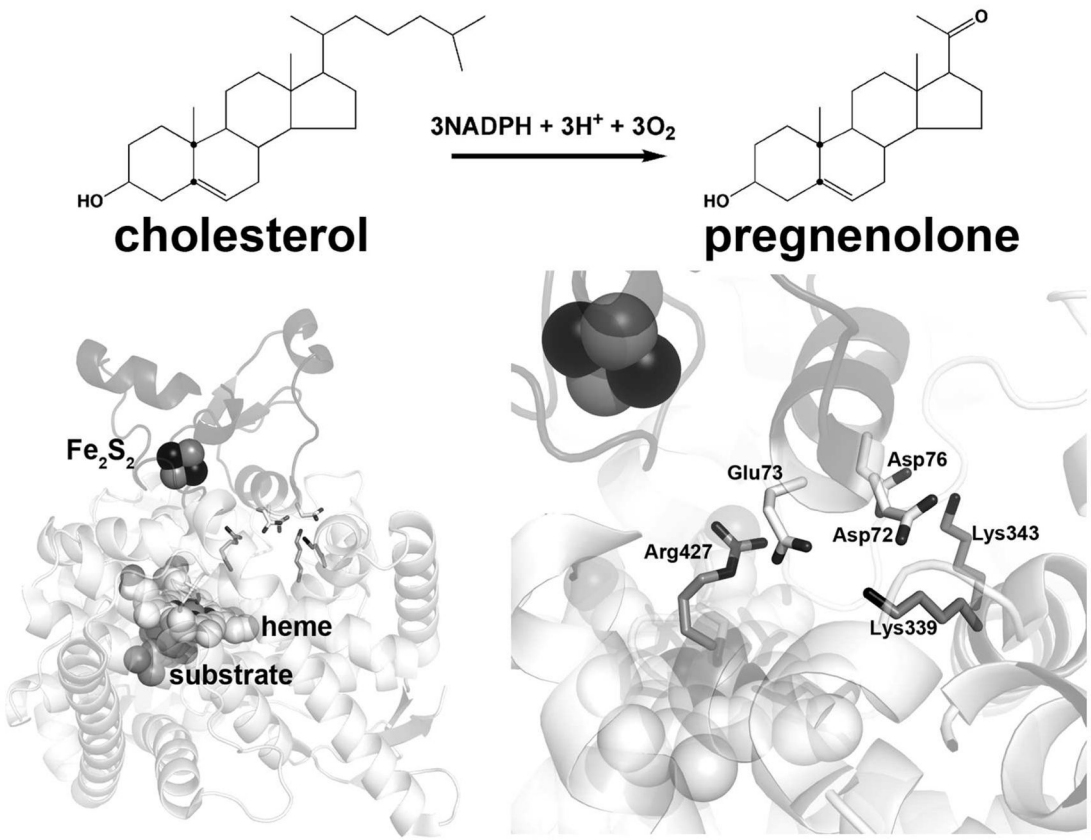

Figure 21.
Crystal structure of the complex formed between CYP11A and Fe_2S_2 redox partner, adrenodoxin.[165]

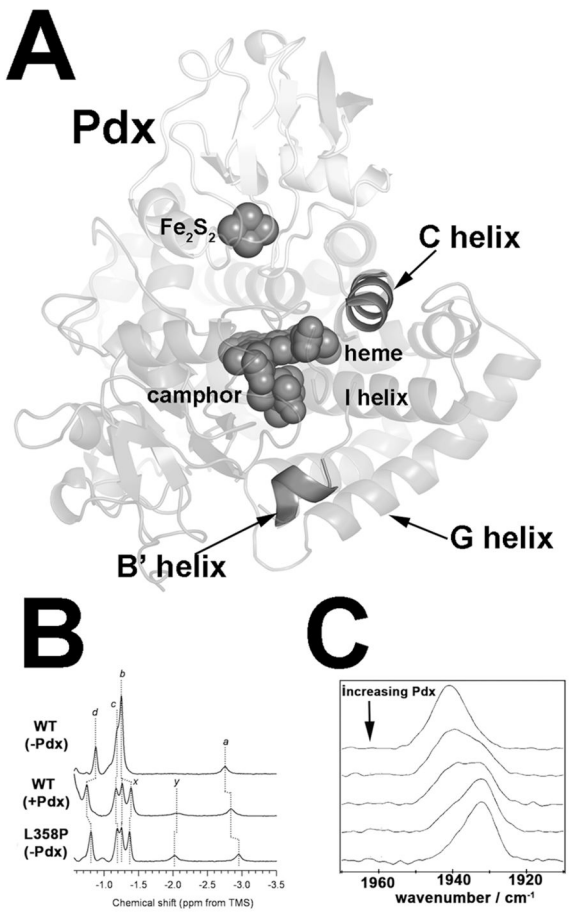

Figure 22.

A) Hypothetical model of the P450cam-Pdx complex.[184] Highlighted are the B′ and C helices that NMR studies show are the most perturbed by Pdx binding.[195] **B)** NMR spectra showing the effects of Pdx binding and the Leu358Pro mutant. a,d,x, and y have been assigned to the β-proton of the Cys357 ligand, the γ-methyl proton of Thr252, the 9-methyl group, and 5-*exo* proton of camphor, respectively. This figure was reproduced from reference 193. **C)** The effect of Pdx on the Infrared CO stretching frequency in CO-P450cam. This figure was reproduced from reference 191.

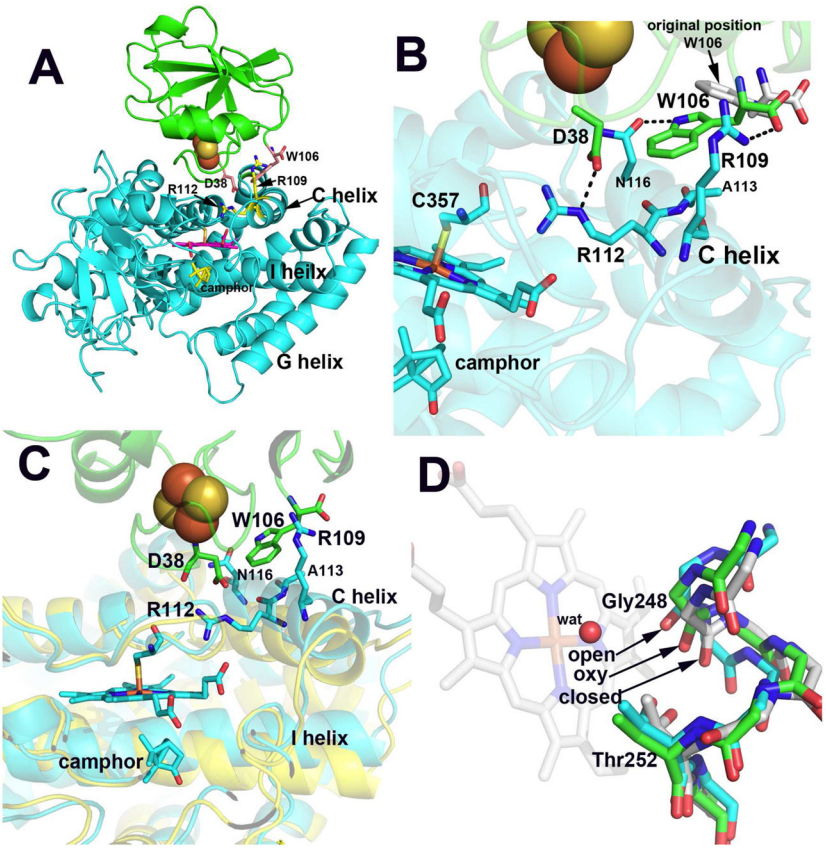

Figure 23.

A) Overall structure of the P450cam-Pdx complex. **B)** Close up of the interface. The only significant change in Pdx is that Pdx_{Trp106} adopts a new rotamer conformation in order to interact with P450cam. The ion pair formed between $P450cam_{Arg112}$ and Pdx_{Asp38} requires little movement but the interactions between Pdx_{Trp106} and P450cam require about a 2–3Å movement of the C helix up toward Pdx. **C)** The closed (yellow) P450cam structure superimposed on the open (cyan) structure. The C helix motion is coupled to changes in the I helix. **D)** The superposition of the I helix in the closed, oxy, and open P450cam structures. In the closed structure Thr252 forms a tight H-bond with the carbonyl O atom of Gly248. In the open conformation this H-bond is weakened which enables Gly248 to move closer to the axial heme water ligand for H-bonding interactions. The motion of the I helix when O_2 binds is midway between these two extremes. The widening of the I helix groove in the oxy complex allows key waters to move in to the active site to establish the proton relay network required for O_2 activation.

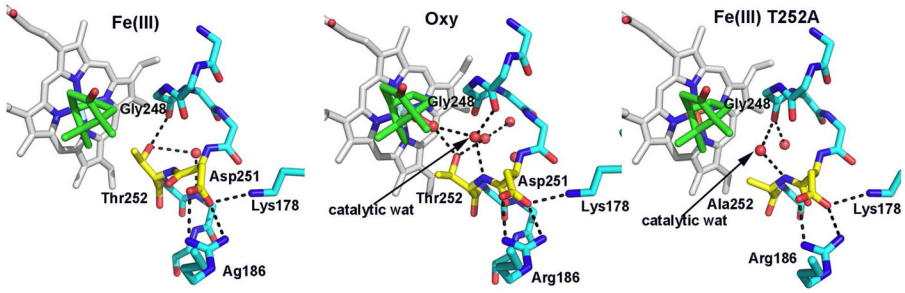

Figure 24.

Comparison of the I helix environment in the Fe(III), oxy, and T252A mutant of P450cam. When O_2 binds the H bond between Thr252 and Glu248 is broken and the I helix opens up. This provides additional room for water molecules to establish an H-bonding network that is generally considered to be important for promoting O-O bond heterolysis. The T242A mutant adopts the same open conformation.

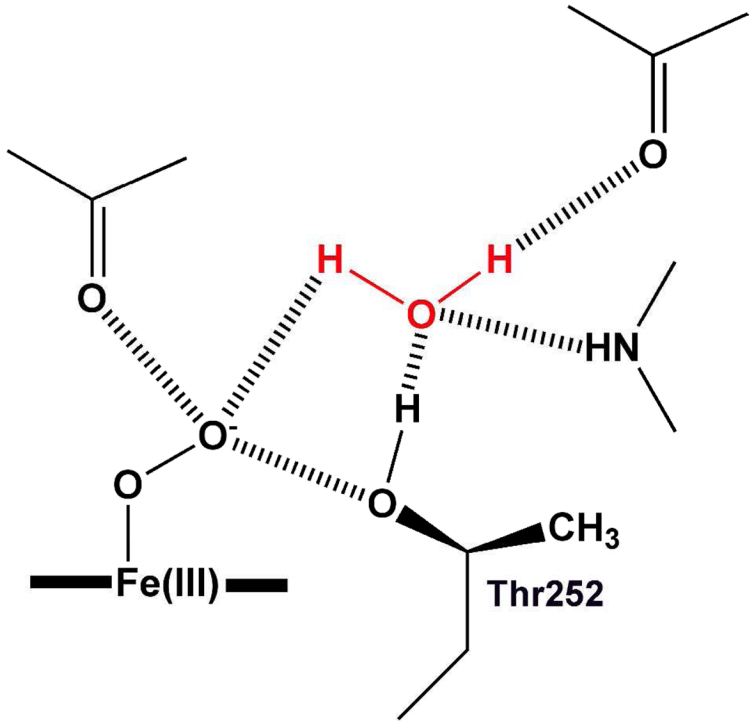

Figure 25.
The probable H-bonding arrangement in the oxy-P450cam complex. The distal O_2 oxygen atom is close to a peptide carbonyl and the Thr252 side chain oxygen atoms which is electrostatically unfavorable and will promote protonation of the distal O atom.

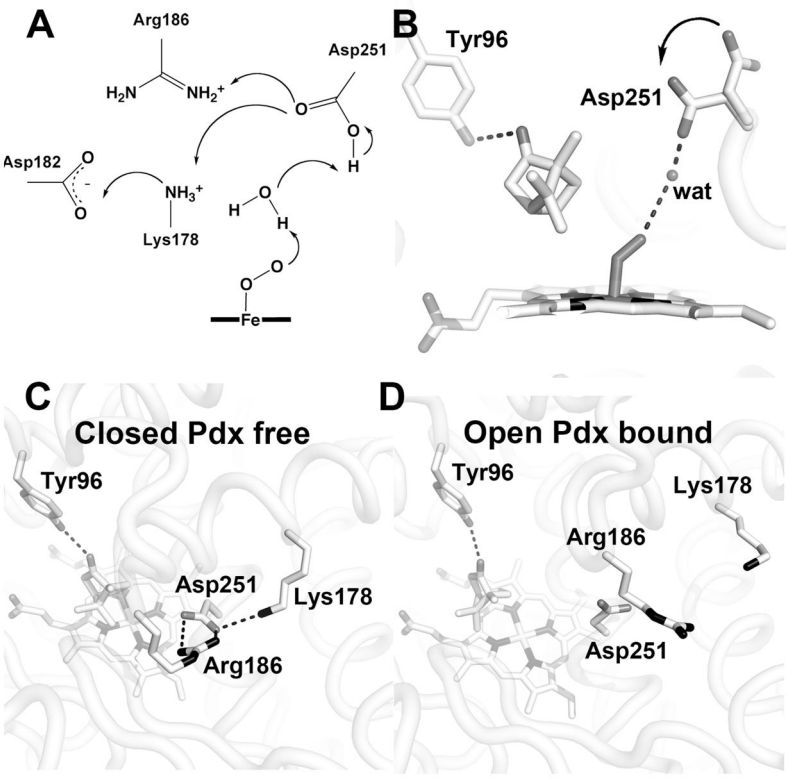

Figure 26.

A Initial mechanism for the role of Asp251 in O_2 activation.[222]. The arrows indicate the direction of proton flow. The main modification to the original proposal is the removal of Thr252 as a proton donor to O_2. The weight of the evidence favors Thr252 serving as an H bond acceptor. The most recent proposal based on the P450cam-Pdx structure removes Arg186 and Lys178 from the mechanism since the ion pairs with Asp251 are broken which frees Asp251 to pick up protons from bulk solvent and then rotate into the active site to deliver protons to dioxygen. **B)** The oxy-P450cam structure was superimposed on to the P450cam-Pdx structure so the dioxygen and water molecule shown are from the oxy-P450cam structure and the rest is from the P405cam-Pdx structure. One of the favored rotamers of Asp251 places Asp251 in an ideal position to interact with the active site water found in the oxy-P450cam structure. **C)** The Asp251 ion pairs found in the closed ferric substrate bound P450cam structure. **D)** The environment of Asp251 when Pdx binds. The ion pairs are broken and the active site opens up which frees Asp251 to shuttle protons from bulk solvent to the active site.

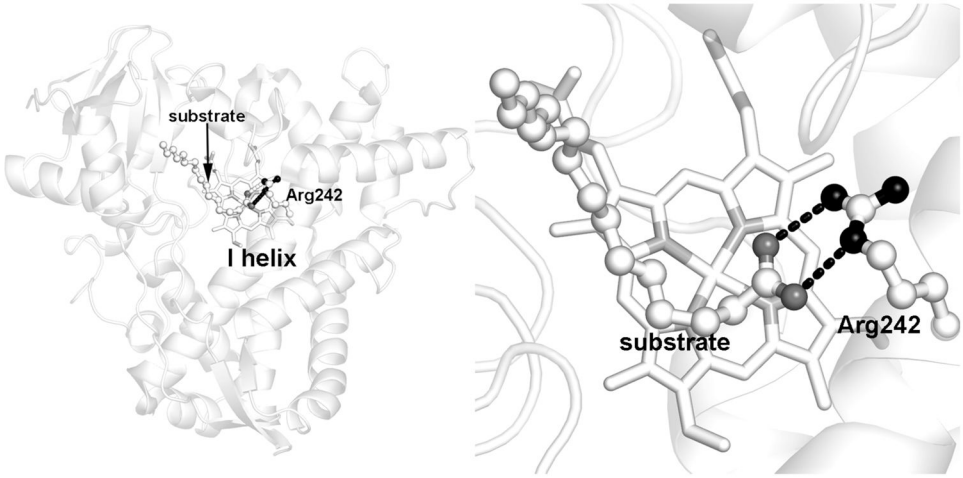

Figure 27.
The structure of P450BSβ [244] The I helix has an Arg that interacts with the fatty acid substrate carboxyl group. This places the carboxyl group in position to serve a similar acid/base catalytic function as the distal His in more traditional peroxidases.

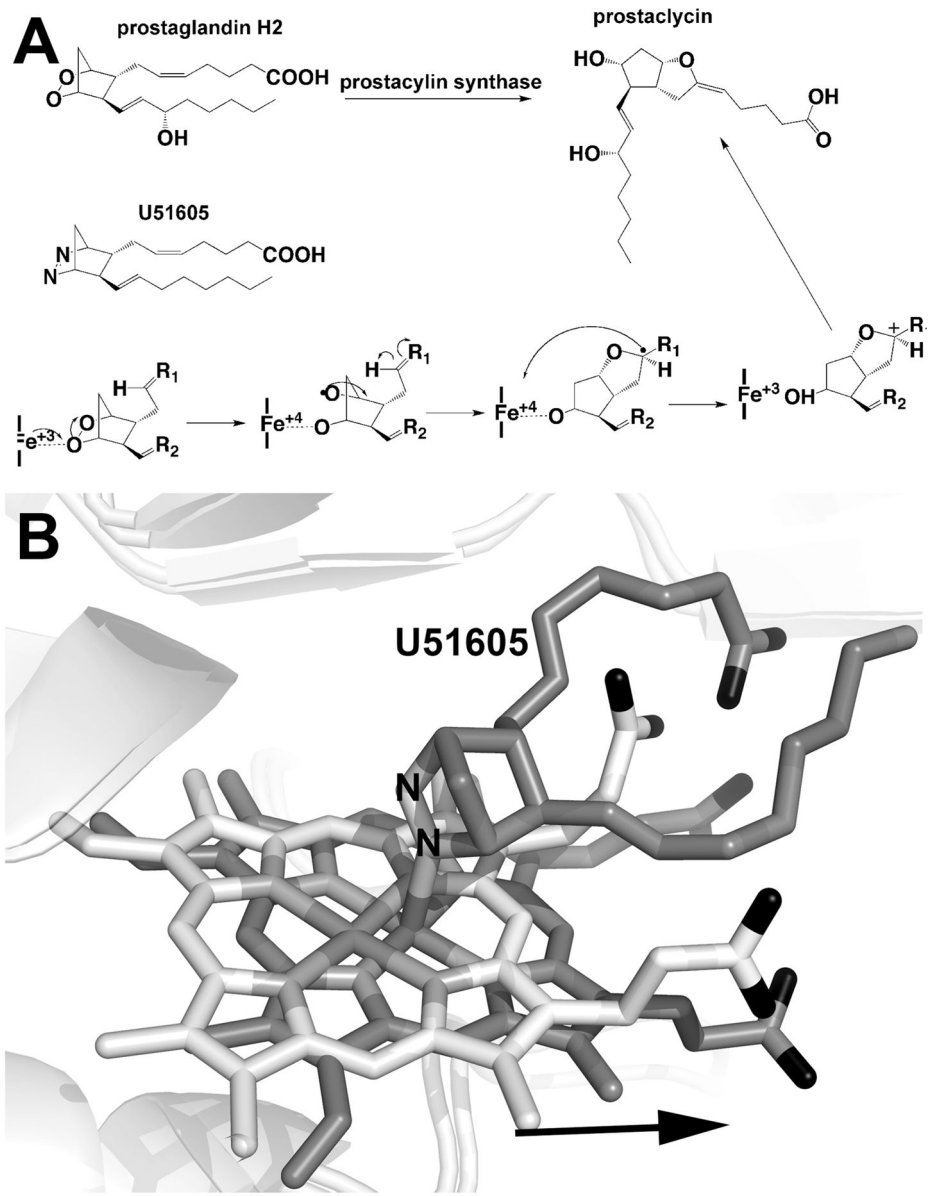

Figure 28.

A) Mechanism proposed for prostacylcin synthase.[389] B) The substrate-free (white) and substrate analog-bound (gray) structures of zebra fish PGIS.[247] The arrow shows the direction of heme movement when substrate binds. The movement is required to enable the U51605 N atom to coordinate with the heme iron. In the substrate-free state the iron thus is "protected" from non-specific interactions with other potential ligands.

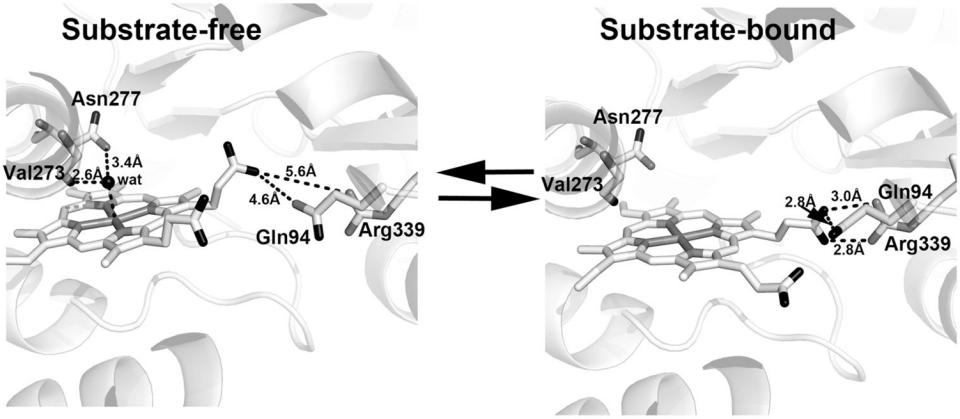

Figure 29.

The substrate-free and -bound forms of zebra fish PGIS.[247] For clarity the substrate analog in the bound state is not shown. As the heme slides from the free to bound state, H-bonds are lost between the axial water ligand and surrounding protein groups but new ones are made between the heme propionate and Arg339 and Gln94.

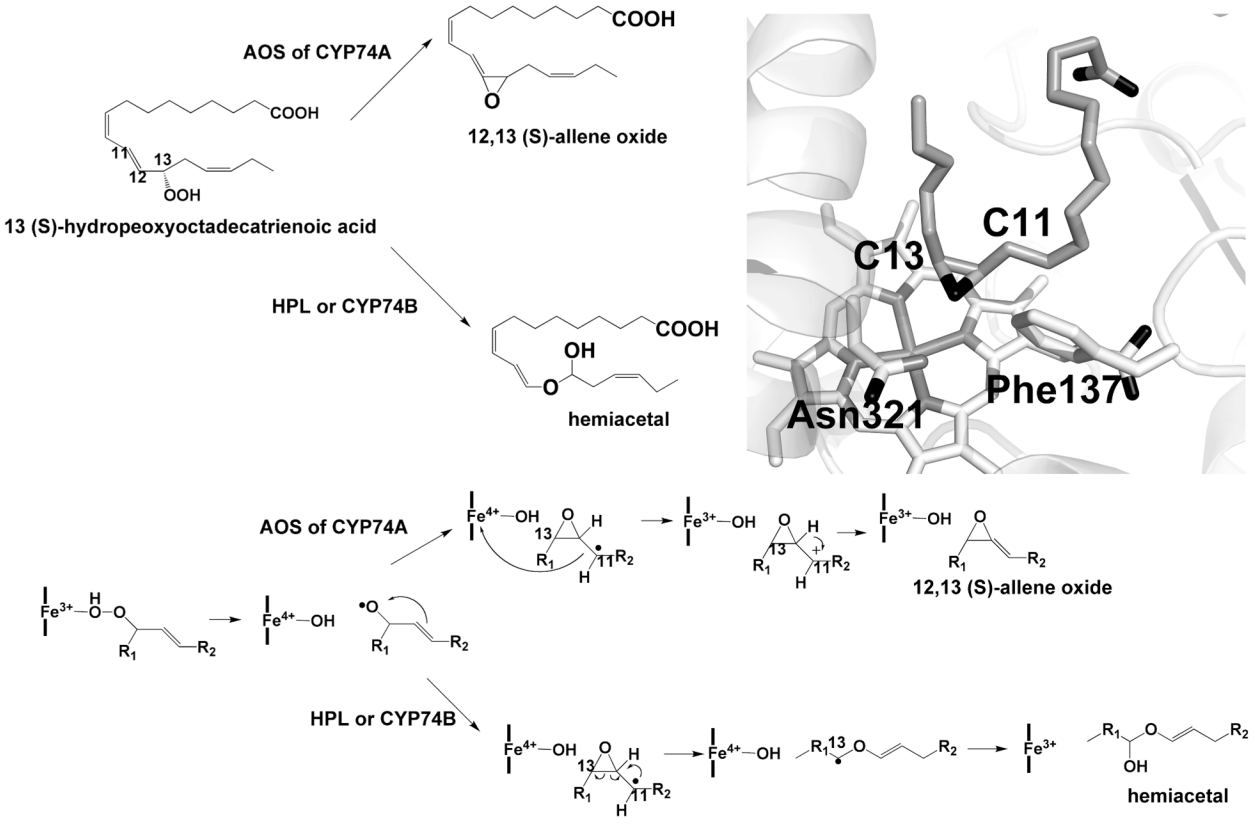

Figure 30.

Possible mechanisms for Cyp74A and Cyp74B.[248,250–252,390]. The proposed mechanisms are not limited to those shown but are consistent with the crystal structures and especially the mutagenesis work where the replacement of Phe137 converts AOS (Cys74A) into CYP74B.[250] Given the close proximity of C11 to Phe137, the Phe ring stabilizes the radical and carbocation on C11 thus favoring formation of allene oxide. In Cyp74B, however, Phe137 is replaced with Leu. Therefore, radical formation on C13 is favored and given the close proximity of C13 to the ferryl O atom, radical rebound gives the final hemiacetal product.

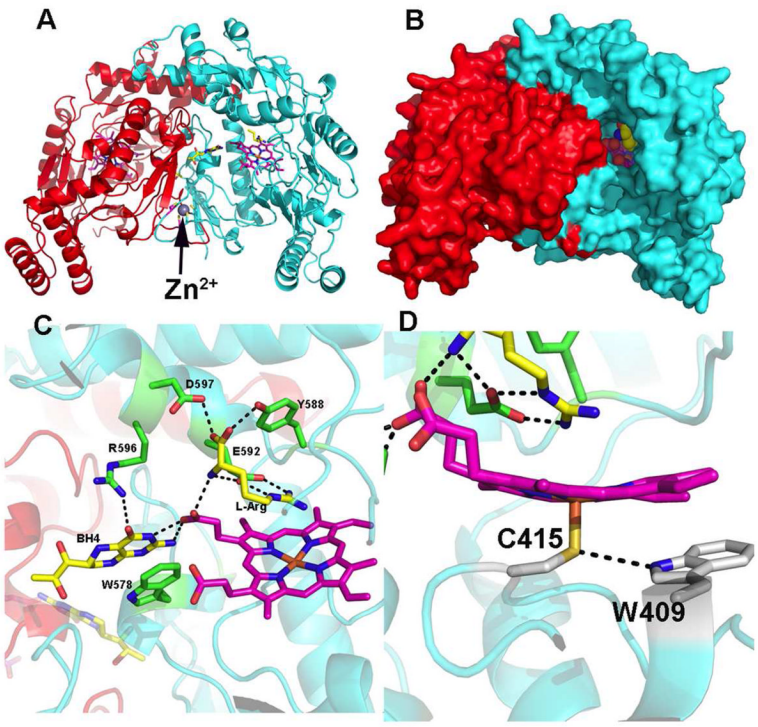

Figure 31.

Structure of rat nNOS. A) Ribbon diagram of the nNOS dimer. A single Zn^{2+} ion is tetrahedrally coordinated to pairs of symmetry related Cys residues exactly along the dimer axis. B) Surface diagram showing the exposure of the heme active site pocket. C) Close-up view of the active site showing the interactions between the substrate, L-Arg, and surrounding protein groups. The cofactor, BH4, is bound in a pocket at the dimer interface where it H-bonds with the same heme propionate as the substrate. D) The Cys ligand environment showing the H-bond between the Cys and Trp409.

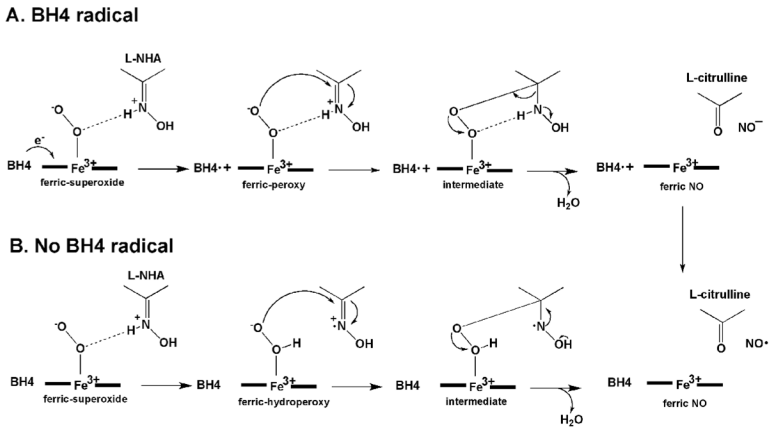

Figure 32.

Two possible mechanisms for the oxidation of N^{ω}-L-hydroxyarginine (L-NHA) by NOS. In the BH4 radical mechanism BH4 reduces the oxy complex to the peroxy species which then forms the cyclic intermediate. This collapses to give L-citrulline and NO^{-}. The BH4 radical then is reduced by NO^{-} to give nitric oxide. In the no BH4 radical mechanism the source of the electron is the substrate itself rather than BH4 which gives the ferric-peroxy species. The cyclic intermediate then collapses to give the final products.

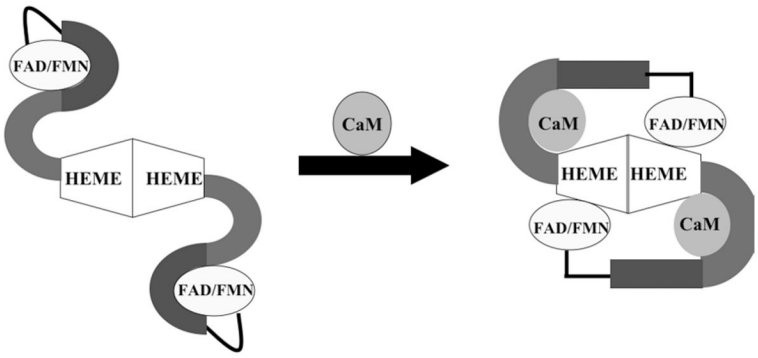

Figure 33.

Cartoon representation of the how NOS is regulated by calmodulin (CaM). All mammalian NOS isoforms dimerize through the heme domain. The binding of CaM to the linker results in a structural change that enable the FMN of molecule A in the dimer to transfer electrons to the heme of molecule B.

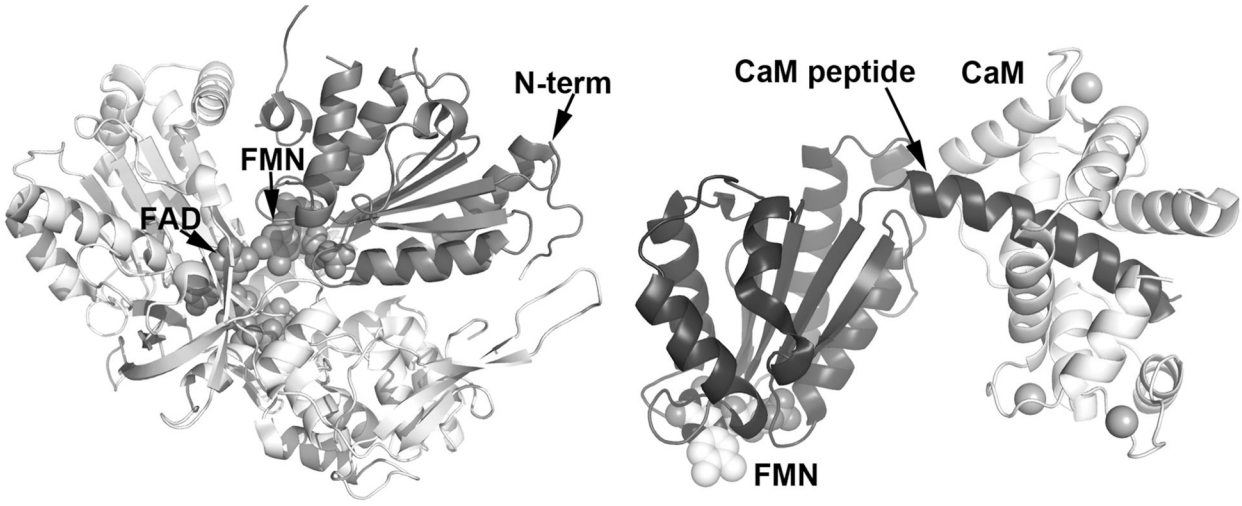

Figure 34.

A) The nNOS reductase structure.[276] The reductase domain of NOS is very similar to P450 reductase. In both structures the FMN and FAD are in close proximity and form direct non-bonded contacts. **B)** Crystal structure of the iNOS FMN domain complexed with calmodulin.[277] The grey spheres in CaM represent Ca^{2+} ions.

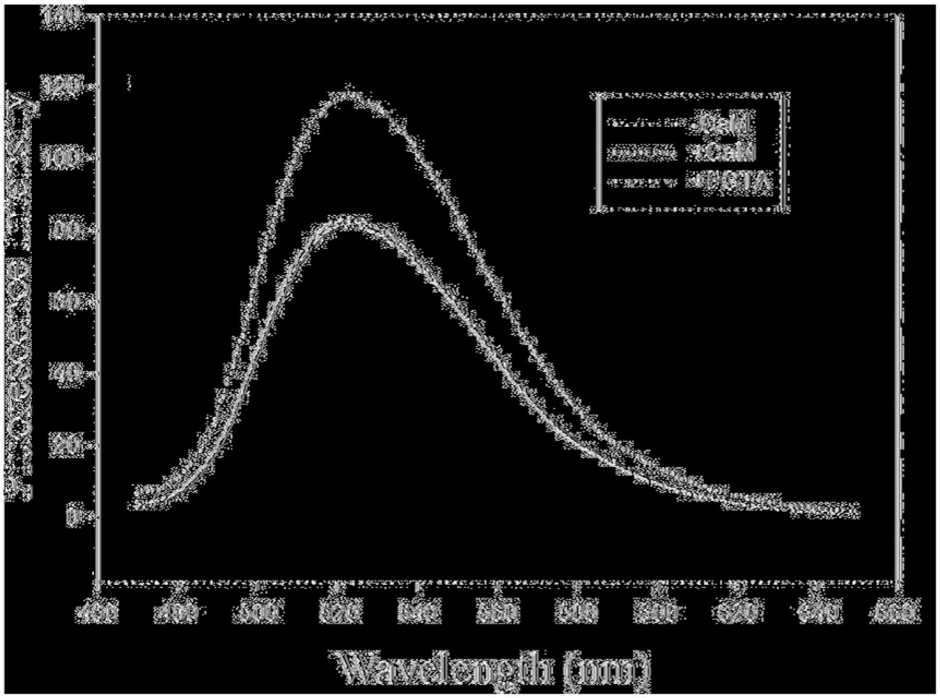

Figure 35.
Fluorescence emission spectra of nNOS ±CaM adapted from.[280]

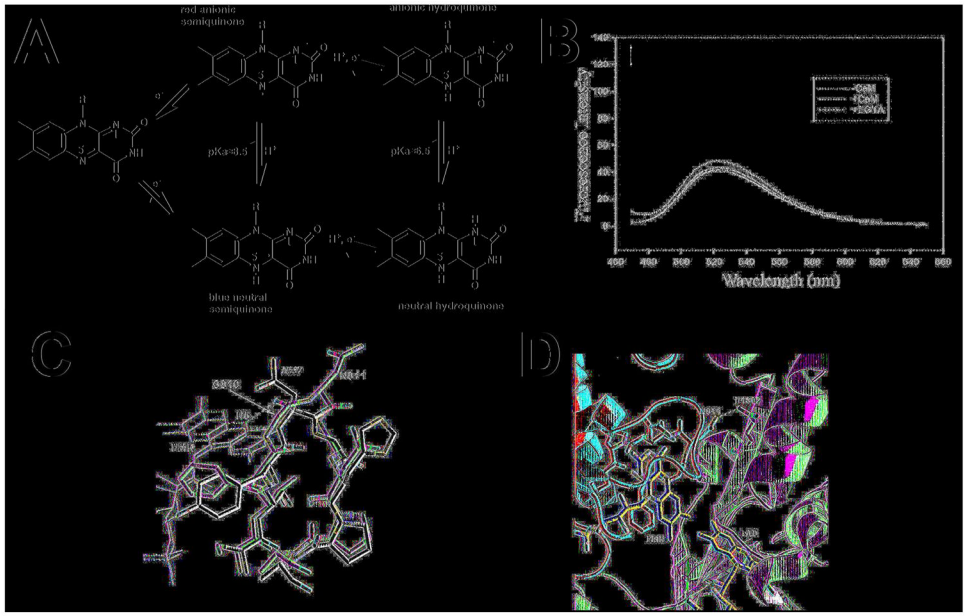

Figure 36.

A) Various redox states available to FMN. **B)** Fluorescence emission spectra of the ΔGy810 nNOS mutant showing that CaM has little effect. **C)** Comparison of the FMN loop region in nNOS (green) and P450BM3 (white). **D)** Close-up view at the FMN-FAD interface showing the Asn811-Glu1392 H-bond which is most likely lost int he ΔGly810 mutant. This could loosen the FMN-FAD interaction thus accounting for the lack of any significant change in fluorescence when CaM is bound. These figures were adapted from.[280]

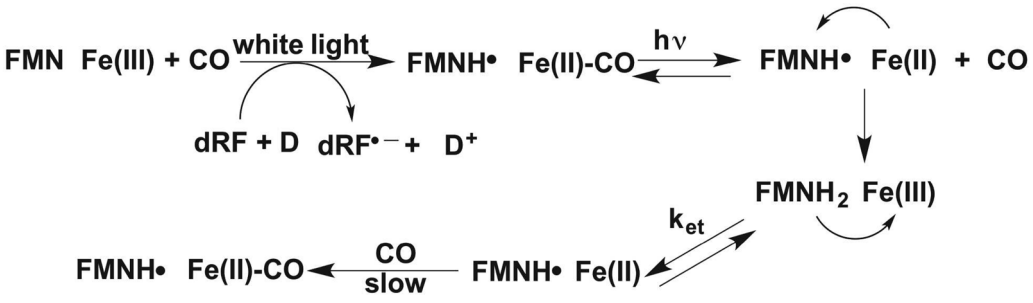

Figure 37.

Procedure developed by Feng et al.[283] to measure electron transfer from the NOS $FMNH_2$ hydroquinone to Fe(III). Deazariboflavin (dRF) is photo-reduced using a sacrificial electron donor (D) like semicarbazide. This reduces both FMN and iron which, in the presence of CO, forms Fe(II)-CO. Flashing off the CO generates Fe(II) which reduces the flavin semquinone to the hydroquinone, $FMNH_2$, which enables the $FMNH_2$-to-Fe(III) ET rate to be measured. This procedure isolates the key CaM-dependent ET reaction.

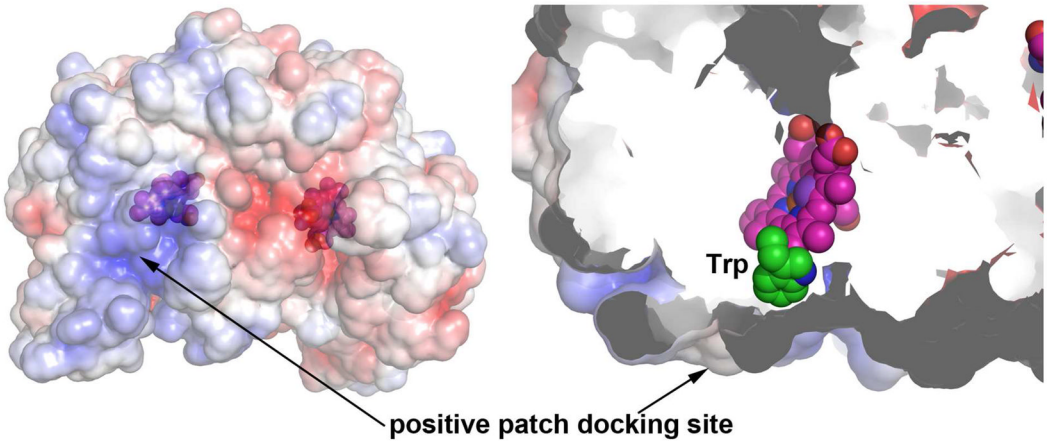

Figure 38.
Two views of the nNOS dimer showing the patch of positive electrostatic potential that could serve as the FMN docking site. A conserved Trp residue is positioned on the backside of the heme near the surface and could possibly serve as a conduit for electron transfer from FMN.

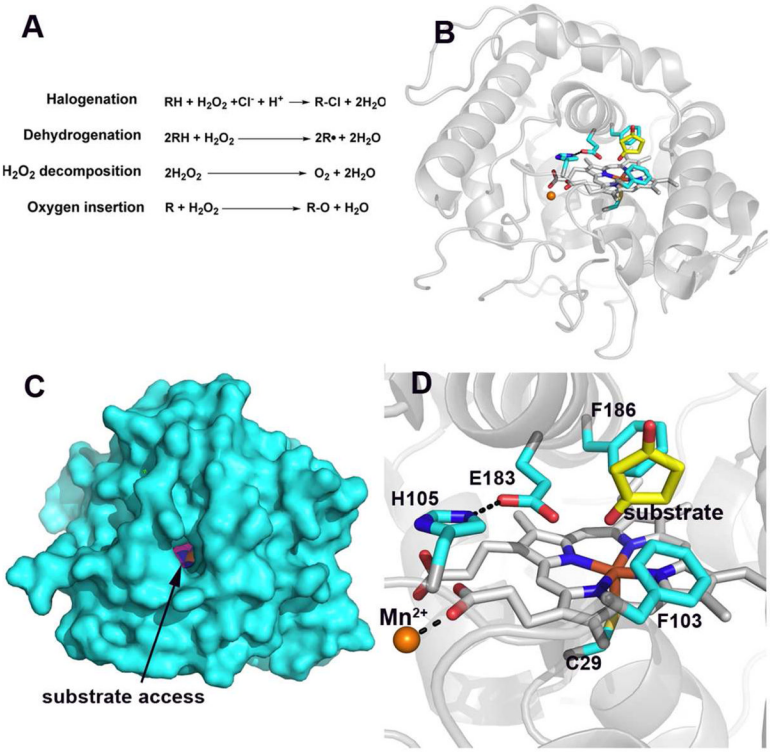

Figure 39.

A) Reactions catalyzed by CPO. **B)** Crystal structure of CPO in a complex with itsxsubstrate cyclopentanedione (yellow).[301] **C)** A surface diagram of CPO showing the small opening just above the heme that provides the most likely route of substrates into the active site. **D)** Close-up view of the CPO active site.

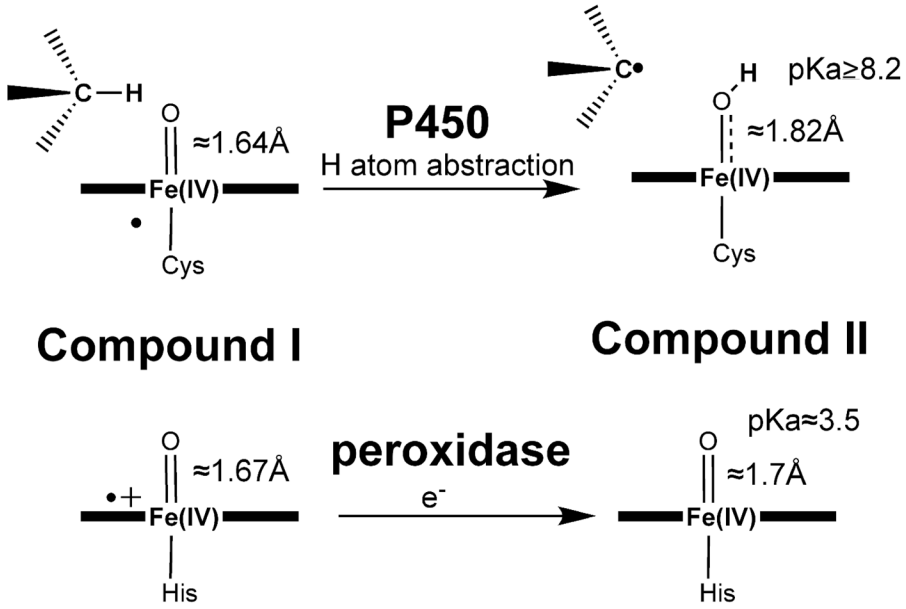

Figure 40.

The difference between the oxyferryl center in P450 and peroxidase. The distances shown are taken from the EXAFS data of Green et al.[303] The radical in P450 Compound I is depicted as being shared by the sulfur and porphyrin as depicted by Green et al.[303] although QM/MM calculations indicate the local protein electrostatic environment favors a porphyrin radical.[312] The ferryl center is similar for both in Compound I while in P450 the radical is most likely delocalized between the porphyrin and sulfur ligand while in peroxidase the porphyrin πcation radical dominates. After H atom abstraction in P450 to give Compound II the Fe-O bond increases giving a high pKa ferryl O atom that favors H atom abstraction from the substrate. In peroxidase Compound II the Fe-O bond remains short with a low pKa and as a result peroxidases are poor at H atom abstraction.

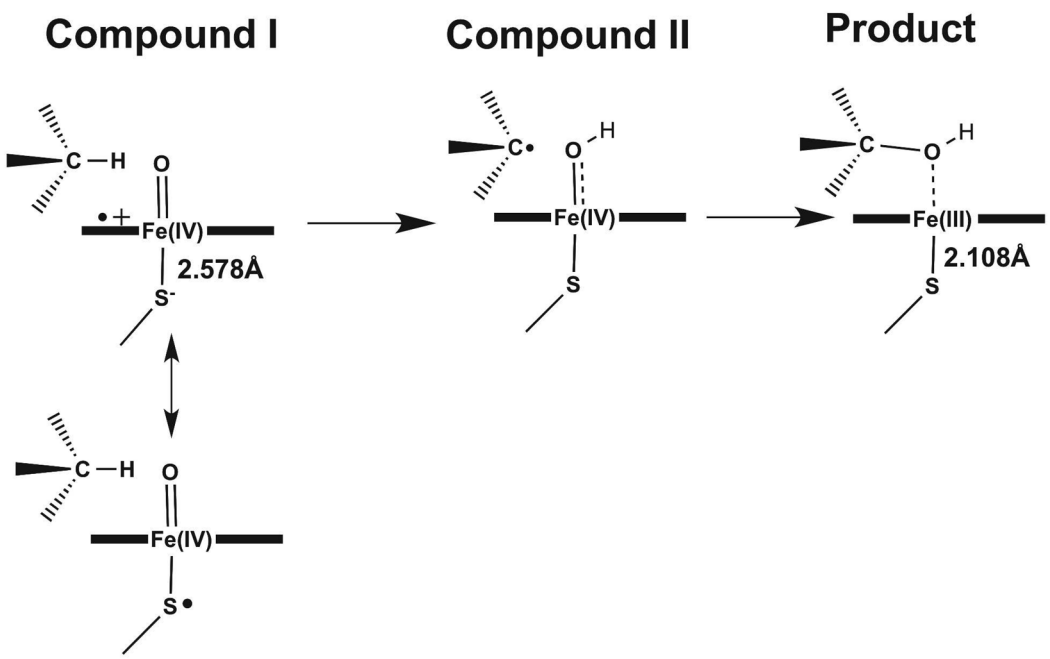

Figure 41.
QM/MM[313] calculations indicate that Compound I is a mix of near isoenergetic radical states with the radical localized on either the porphyrin or sulfur with the porphyrin radical being the reactive species. Hydroxylation results in a shortening of the S-Fe bond.

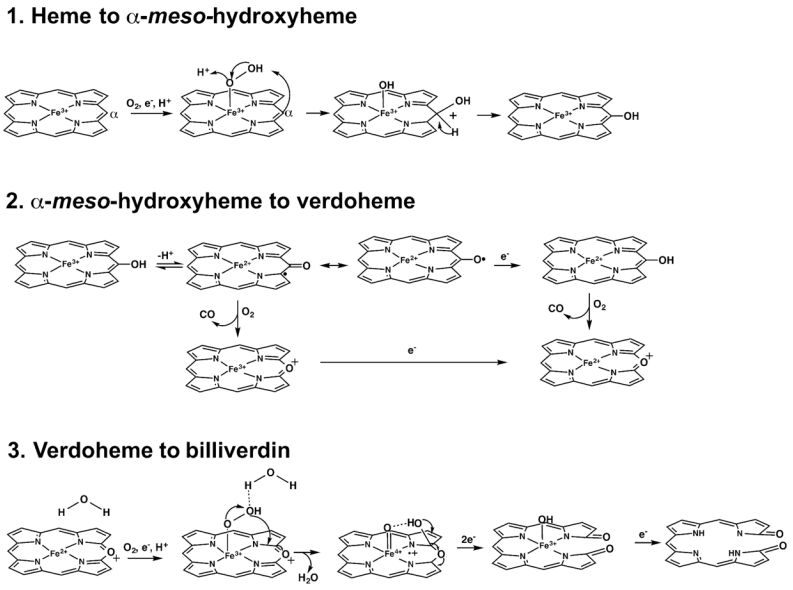

Figure 42.
Mechanism of heme degradation to billiverdin.

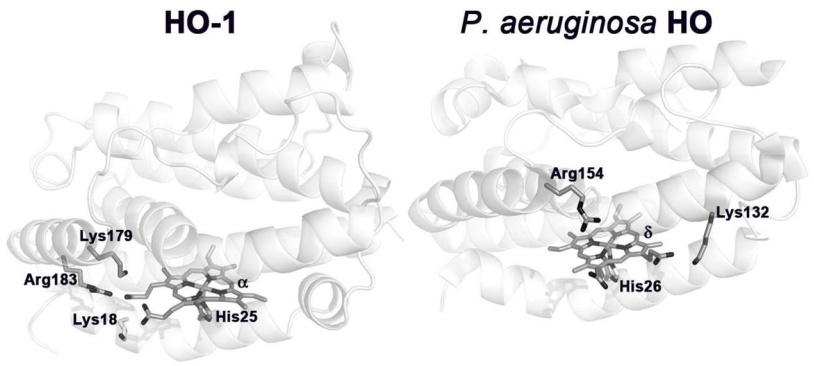

Figure 43.

Comparison of the human HO-1[327] and the HO from *P. aerugionosa*.[328] The structures share the same helical fold but in the bacterial enzyme the heme is rotated relative to the human enzyme. This places the δ-meso heme carbon at the same position as the α-meso heme carbon in HO-1. The orientation is controlled in part by the cluster of basic side chains that interact with the heme propionates.

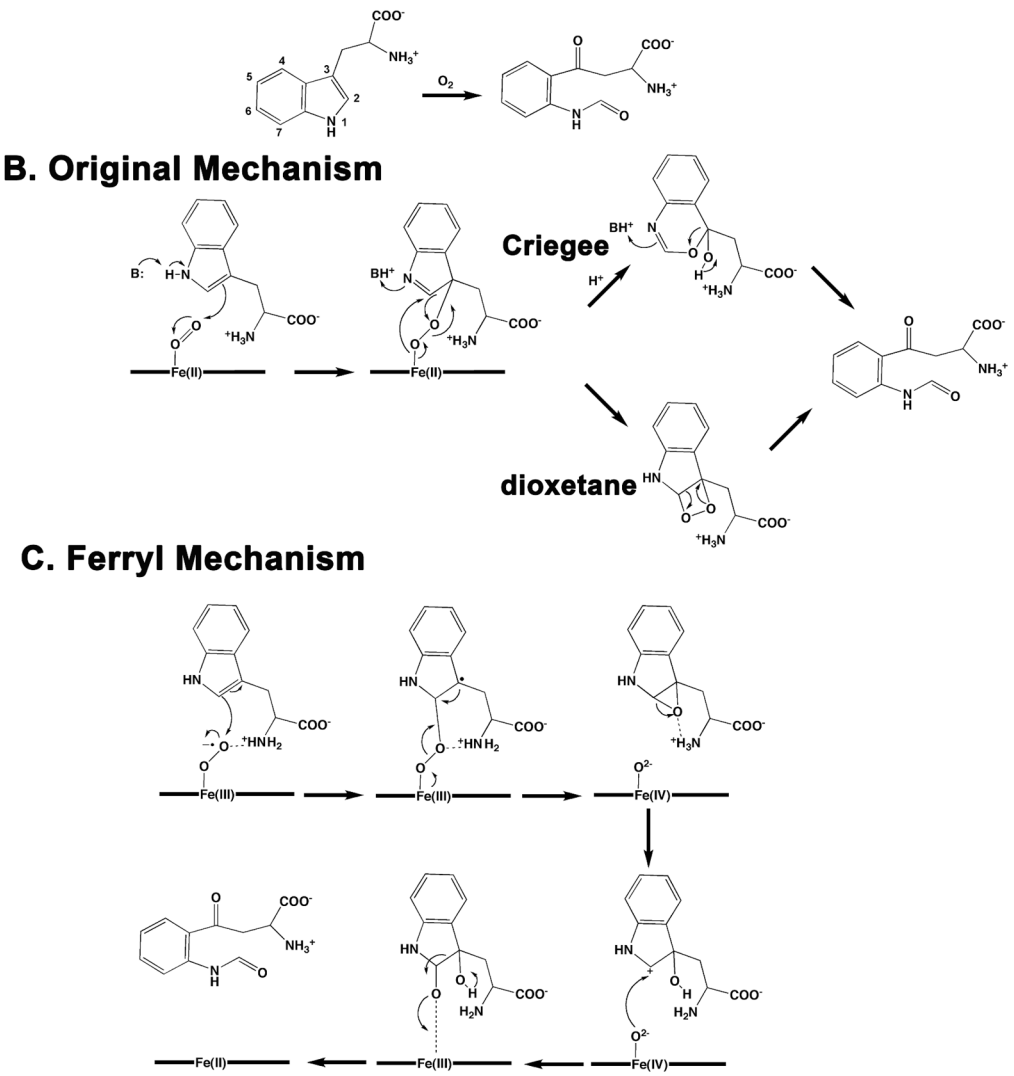

Figure 44.

A) Overall reaction catalyzed by TDO. **B)** Original mechanism proposed for TDO where a protein base abstracts the substrate indole proton. **C)** Sequential addition of O atoms into the substrate *via* a ferryl intermediate.

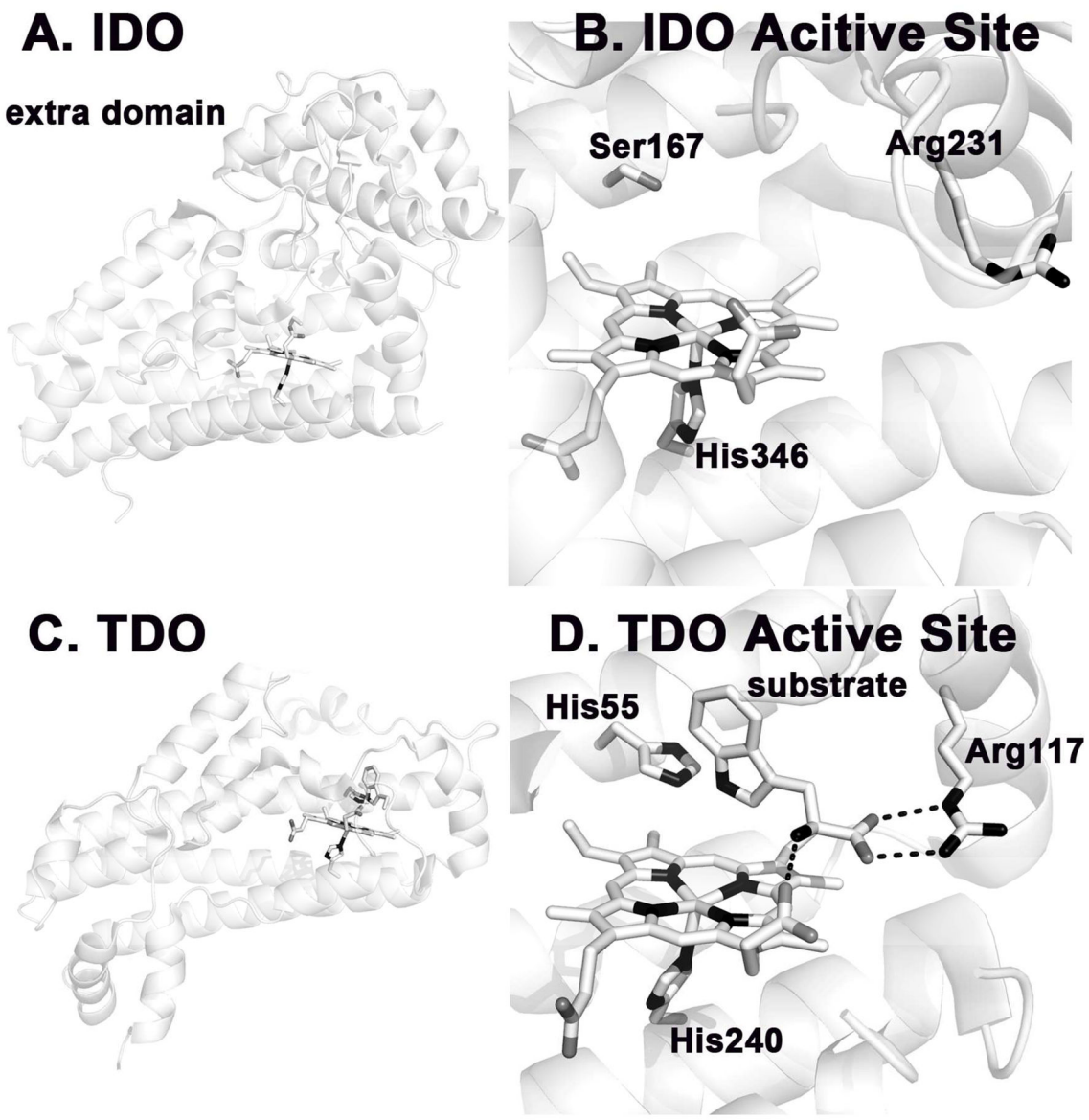

Figure 45.
IDO and TDO crystal structures. A) The structure of human IDO[363] has an extra domain not found in the bacterial enzyme. B) IDO active site. C) Bacterial TDO structure.[364] D) Active site of bacterial TDO in a complex with the substrate, L-tryptophan.

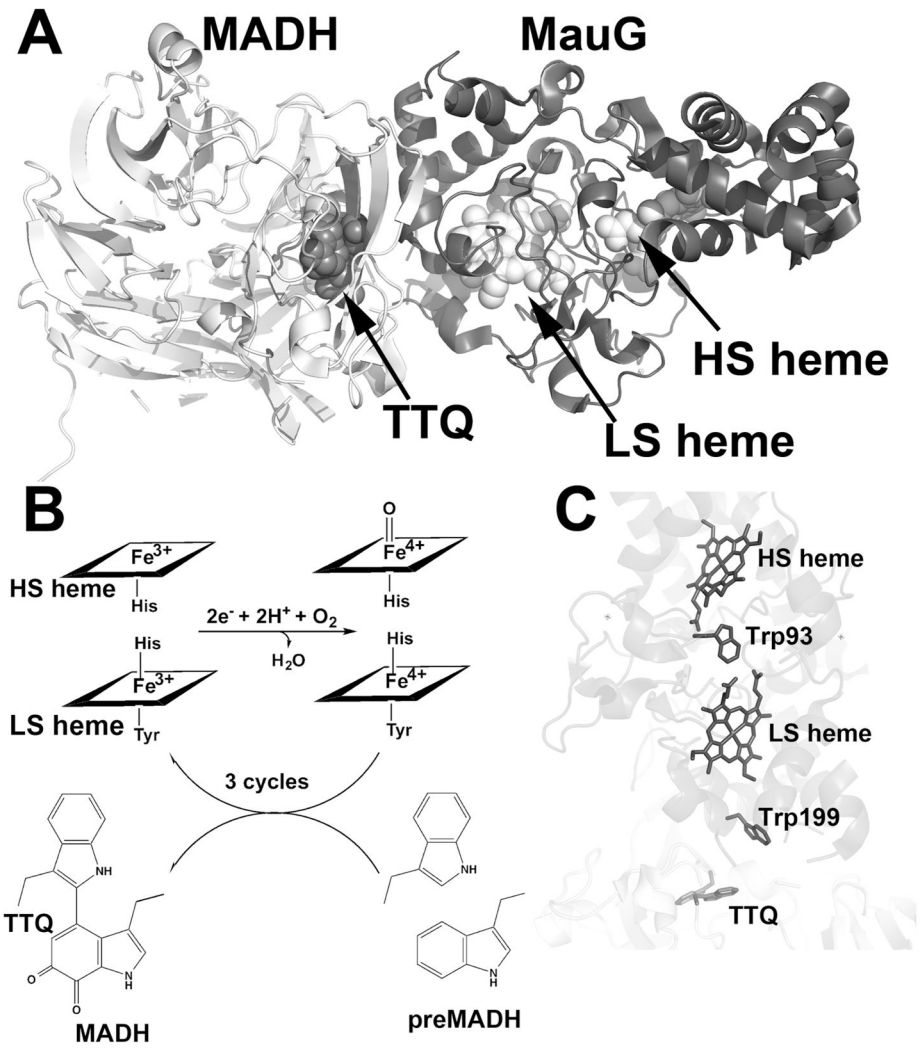

Figure 46.

A) Crystal structure of the MauG-MADH complex.[380] B) The overall reaction of MauG catalyzed formation of TTQ. This is a 6 electron oxidation reaction and thus requires 3 cycles of O_2 activation and electron transfer. D) A close up view of the MauG-MADH interface and key Trp residues. Trp93 provides the electronic couple between the two heme such as both hemes behave as a single redox unit.[385] Trp199 is thought to play a key role in electron transfer from the Trp residues destined to become TQQ and the low potential MauG heme[384].

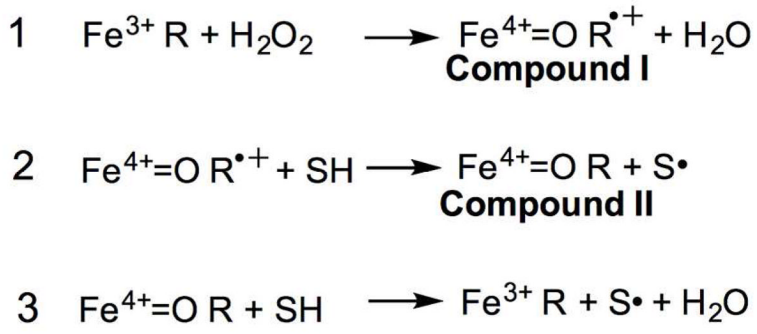

Scheme 1.

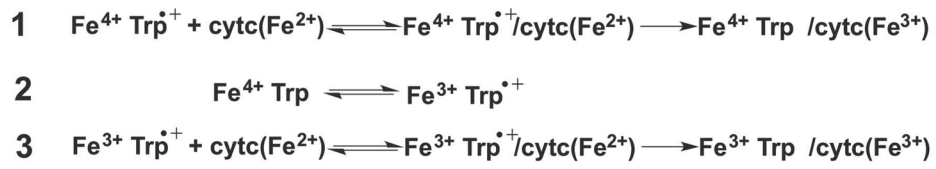

Scheme 2.

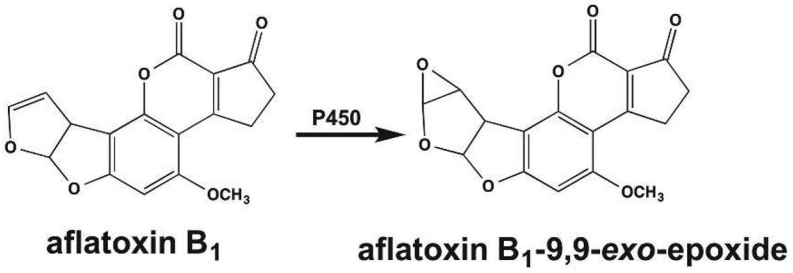

aflatoxin B_1 aflatoxin B_1-9,9-*exo*-epoxide

Scheme 3.

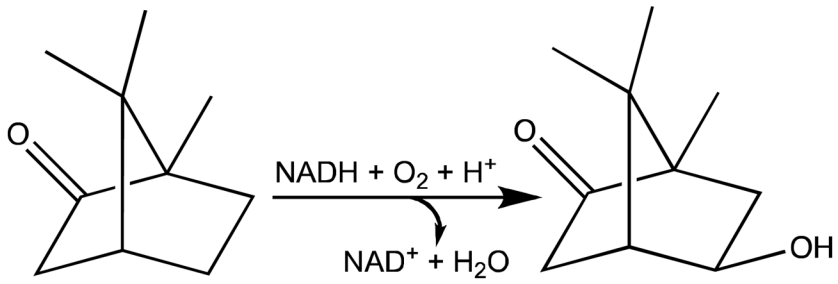

Scheme 4.

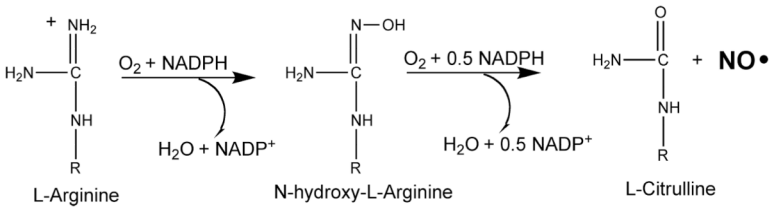

Scheme 5.

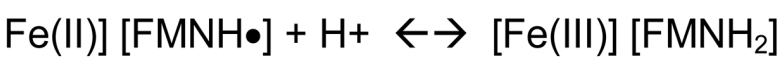

Scheme 6.